Final report dated 15.12.2021
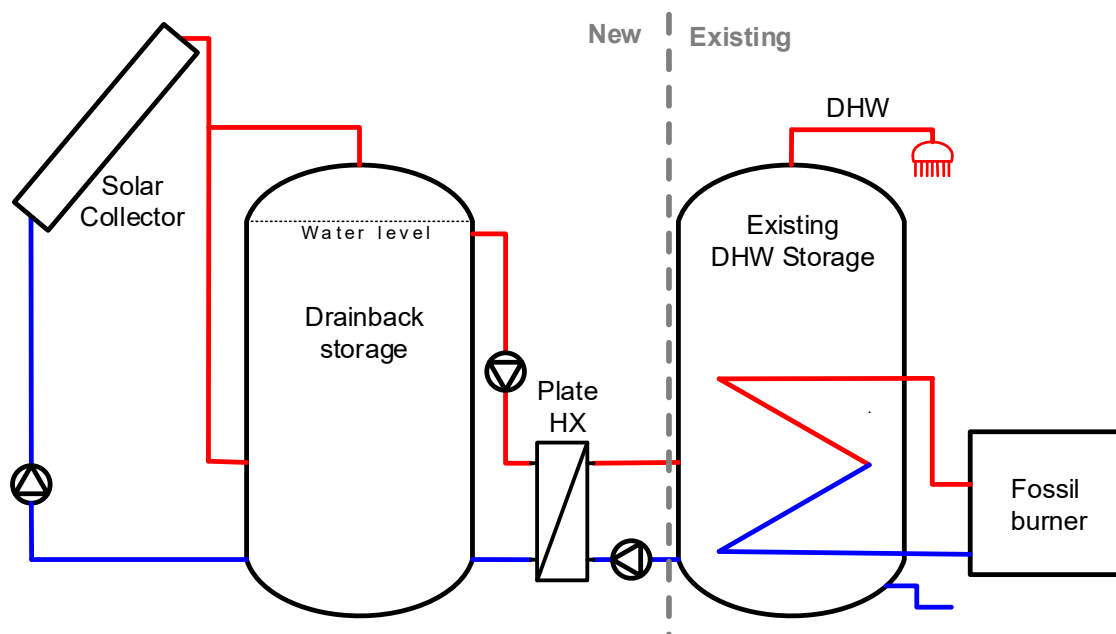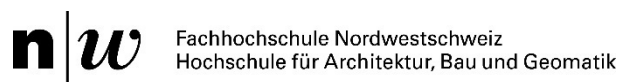
SimplyDrain

Simplest solar drainback systems as add-on for DHW preparation in multifamily houses

Authors:
Daniel Philippen, SPF, daniel.philippen@spf.ch
Severin Kundert, SPF, severin.kundert@spf.ch
Sara Eicher, Lesbat, sara.eicher@heig-vd.ch
Martin Guillaume, Lesbat, martin.guillaume@heig-vd.ch
Ralph Eismann, INEB, ralph.eismann@fhnw.ch
Andreas Genkinger, INEB, andreas.genkinger@fhnw.ch

The authors bear the entire responsibility for the content of this report and for the conclusions drawn therefrom.

Zusammenfassung

Verschiedene Varianten eines kostengünstigen solarthermischen Drainback-Systems wurden konzipiert. Dieses kann als Zusatz zur konventionellen Warmwasserbereitung in Mehrfamilienhäusern (MFH) eingesetzt werden. Mit Experten-Interviews wurden die wichtigsten Erneuerungssituationen in MFH ermittelt, in denen das Drainback-System eingesetzt werden kann. Der Vergleich der Energieträgervermeidungskosten (LCoH) von vier untersuchten solarthermischen Drainback-Systemen (DBS) mit einem konventionellen solarthermischen System zeigt relevante Kostensenkungen für die DBS von bis zu 33 %. Im Labor wurde ein Demonstrations-DBS installiert, bei dem der Transfer der Solarwärme über das Kaltwasseranschlussrohr des Warmwasserspeichers des bestehenden Warmwassersystems realisiert wurde. Dieses System wurde mit Hilfe von thermohydraulischen Simulationen (THS) ausgelegt. Mit Hilfe der THS wurden auch Auslegeschritte für kleine DBS mit einer Kollektorreihe formuliert, die von Herstellern zur Auslegung von DBS mit hoher Betriebssicherheit eingesetzt werden können.

Résumé

Plusieurs variantes d'un système solaire thermique économique de type drainback destinés à complémenter un système de chauffage d'eau chaude sanitaire conventionnel pour l'habitat collectif ont été conçus. Les principaux scénarii de rénovation d'habitat collectif pour lesquelles un tel système Drainback peut être mis en œuvre ont été déterminés aux cours d'entrevues avec des experts. Le comparatif des diminutions de coûts liés à la source d'énergie de quatre systèmes solaires thermiques de type drainback montre une réduction des coûts significatifs allant jusqu'à 33% pour les systèmes drainback. Un tel système a été installé en laboratoire à des fins de démonstration. Le transfert de la chaleur solaire s'effectue au niveau du tuyau d'alimentation en eau froide du réservoir de stockage du dispositif de production d'eau chaude sanitaire existant. Des simulations thermo-hydrauliques ont aidé à dimensionner le système. Grâce à ces simulations, des propositions de dimensionnement pour de petits systèmes drainback ont été formulées, permettant aux fabricants de dimensionner de tels systèmes avec une grande sécurité de fonctionnement.

Summary

Different variants of a cost-effective solar thermal drainback system were designed, which can be used as an add-on to conventional domestic hot water systems in multi-family houses (MFH). Expert interviews were conducted to identify the most important renovation situations in MFH in which the drainback system can be used. The comparison of levelized cost of heat (LCoH) of four investigated solar thermal drainback systems (DBS) with a conventional solar thermal system, shows relevant cost reductions for the DBS of up to 33 %. A demonstration DBS was installed in the laboratory, where the transfer of solar heat was implemented through the cold water connection pipe of the hot water storage tank of the existing DHW system. The system was designed using thermal hydraulic simulations (THS). THS was used to formulate design steps for small DBS with one row of collectors, which can be used by manufacturers to design DBS with high operational reliability.

Contents

Abbreviations

DB   Drainback

DBS   Drainback system

DHW   Domestic hot water

FSO   Swiss Federal Office of Statistics

GRP   Glass fibre reinforced plastic

HTF   Heat transfer fluid

LCoH   Levelized cost of heat

MFH   Multi-family housing

MoPEC /MuKEn   Mustervorschriften der Kantone im Energiebereich, a set of joint model cantonal provisions in the energy sector

O&M   Operation and maintenance

ST   Solar thermal

1 Introduction

1.1 Motivation

Although solar thermal heat is expected to play an important role for the supply of buildings with renewable heat, the yearly installed total area of solar thermal collectors in Switzerland is not increasing, as shown in the market figures of recent years [1]. Some studies have analysed the market situation in Switzerland for solar thermal and suggest measures to boost the solar thermal market on different levels such as technical, legal, incentive, and communication level [2] [3]. On the technical level, as addressed by the SimplyDrain project, the studies call for measures that lead to a general cost reduction of solar thermal systems. Ways to reduce the costs of solar thermal installations were extensively discussed and analysed in IEA SHC Task 54 [4]. This Task highlighted various strategies to reduce investment cost and the cost of avoiding fossil fuel by solar thermal systems. Most important strategies are overheating prevention in the systems, use of polymeric components, reduction of maintenance costs, "easy to install" components, standardisation, and performance increase. All these strategies are covered by project SimplyDrain, which deals with cost-effective solar thermal drainback systems (DBS).

Solar thermal drainback systems have been known for decades. Most of these systems are small [5]. Especially in the Netherlands, also large systems have been built and operated successfully [6]. While the functional principle is generally known, the specific knowledge of dimensioning and commissioning has been almost exclusively anchored with the manufacturers of such systems. Drainback systems seem to be problem-free in principle. At a closer look, however, questions regarding operational safety arise. The effect of solubility of non-condensable atmospheric gases on the pressure in the system was first investigated by the experimental work of Rühling and Schabbach [7], which clearly showed the expected effects, even though, the system they investigated was operated using a water-glycol mixture: It has been shown that the gas pressure inside the system reduces over time due to the reaction of molecular oxygen with the glycol. Botpaev et al. [8] did experimental research on the filling and draining processes at the system start and shutdown.

In Switzerland, the market of domestic hot water (DHW) preparation in multi-family houses (MFH) is seen as an important market section by Swiss solar thermal companies [2]. Especially for this market section, costs of the solar thermal systems have to be reduced, as owners of MFH tent to be more cost-sensitive than owners of single family homes [9]. For MFH it can be expected that retrofitting of fossil burners used for DHW preparation or for room heating will be a relevant field of application for solar thermal systems. The reason for this is that the legal framework is changing in many Swiss Cantons with the implementation of MoPEC 2014 regulations [10]. According to an estimation of the city of Zürich [9], the regulations of MoPEC 2014, in particular Part F, may be of major importance for all renewables, as their use is one of the measures that have to be realised when retrofitting existing heating systems in MFH that have high thermal building losses. One of the measures accepted by MoPEC 2014 Part F is the installation of a solar thermal system which supports the DHW preparation. However, in the MoPEC regulations, solar thermal is only one of several solutions that can be adopted. Hence, solar thermal systems still must persist the competition with other renewables and efficiency measures. To foster the diffusion of solar thermal systems, the above-mentioned cost reduction measures should be implemented especially for MFH applications.

1.2 Objectives

The SimplyDrain project aims for cost reductions in solar thermal drainback systems (DBS) used as "add-on" for existing DHW systems in multifamily houses. Three variants of a very simple solar thermal drainback system concept were analysed in this project. The purpose was to keep system design,

installation, operation, and maintenance as simple and easy as possible. The solar thermal systems have been designed as drainback systems (DBS) with water as heat transfer fluid. The term "drainback" points out that the heat transfer fluid drains back from the collectors and the uppermost pipes of the solar loop into a vessel when the solar pump stops.[1] The narrow focus on DHW preparation in MFH helped to find concepts that allow for a high degree of concept standardisation of the DBS.

The most promising of the three variants was tested and demonstrated on lab scale. Being based on the analysis of market needs and the framework given by the market, the variants fit well to the expectations of the stakeholders and thus, have a high potential for acceptance. The developments were be oriented towards an application in the frame of the MuKEn regulations (existing fossil burner). However, it will also be possible to use the system concepts with heating systems other than fossil ones, e.g. heat pumps or pellet boilers.

The following objectives were defined:

1) Finding the boundary conditions, the DBS concepts have to fit in. A specific market survey by means of interviews of experts in the Swiss building sector will be conducted.
(**Chapter 2: Feasibility of Drainback Add-on Systems for DHW**)

2) Selection of optimal design and sizing of the three concept variants. This will be done by means of simulations of energy performance and of cost calculations. The technical practicability for the market and the levelized cost of heat (LCoH) will be the main indicators for choosing the most promising system out of the three variants.
(**Chapter 3: System design, Energy and Cost**)

3) The most promising variant will be built in the lab. As preparatory work, the components that are relevant for the drainback function will be sized by means of thermohydraulic simulations.
(**Chapter 4: Thermohydraulic simulations**)

4) A DBS will be built in the lab to give a proof-of-concept and to gain measurement data for the validation of the thermohydraulic simulations. A solar storage tank that includes the drainback volume will be further developed based on the outcome of project ReSoTech 2 [11]. Knowledge gains regarding safe operation of a water-based DBS will be derived.
(**Chapter 5: Drainback system: design and experiments**)

---

[1] In some hydraulic concepts for drainback systems, also a valve has to be activated to allow for draining.

2 Feasibility of Drainback Add-on Systems for DHW

The objective of the first work package was to investigate the suitability of integrating DBS concepts in the renovation of DHW systems in existing MFH. The main task here was the analysis of the market situation with the characterisation of the typical Swiss MFH, its technical room and its most common DHW system and storage type. Features such as the size of existing components, dominant hydraulic set-ups, availability of space for additional equipment, typical renovation strategies, legal obligations and possibility for ST were sought. This was performed by means of phone interviews, analysis of national statistical data and relevant energy regulations.

This work allowed for gathering essential information for the design of suitable DBS concepts for DHW systems retrofit. A DHW reference system for a typical MFH was also defined from the compiled data which was later used in WP2 for assessing the energy and cost advantages of the concepts.

2.1 Methods

Statistical data from the Swiss Federal Office of Statistics (FSO) and complementary information from scientific reports were used to identify relevant building features and to cross-check the results of the phone interviews. Energy regulations provided information on the current legal requirements related to the renovation and retrofit of heating system in buildings.

In order to define the characteristics of the typical Swiss MFH, qualitative interviews were conducted with representatives from three experienced companies active in the Swiss building sector. The interviewees differ in the type of experience they have towards renovation of MFH. PPLUS is an engineering office based in Neuchâtel, expert in establishing CECB, a national label that provides an overall assessment of the building energy demand. ENGIE is a company that is active in energy services, facility management and building technology throughout Switzerland, with a solid knowhow in improving energy efficiency in existing buildings. Losinger-Marazzi is a leading company in the field of intelligent construction technology, mainly new buildings but also in upgrading existing ones. The interviewees were identified through personal contacts and other project collaborations. The large and complementary experience of the interviewees have allowed to establish a broad overview of the most current Swiss MFH, their common renovation strategies and the challenges facing the adoption of ST technology.

The interviews followed a semi-structured approach where open-ended questions left participants the freedom to dwell deeper into issues. Yet the interviews were somehow structured to ensure all interviewees were asked the same questions. Interview guidelines were designed to ensure a good quality of the interview. It was made up of about thirty questions, classified under six categories, namely: background; building characteristics; technical room; DHW system; DHW storage and miscellaneous. The interviews were conducted via telephone in January 2020 and lasted less than an hour each. Extra care was required in noting down all the answers, to avoid misunderstandings, and to guarantee the flow of the interview.

The first section of the interview addressed the background information of the interviewees, their experience and current job position. The second section focused on the architectural characteristics of existing MFH pertinent for ST integration. This was followed by three sections related to the common characteristics of the technical room, DHW systems in place and DHW storages used in existing MFH. The interview guideline can be found in Annex A.

2.2 Statistical data – MFH stock

According to the FSO, there are approximately 0.5 million MFH in Switzerland, accounting for about 27% of the total number of residential buildings, see Figure 1.
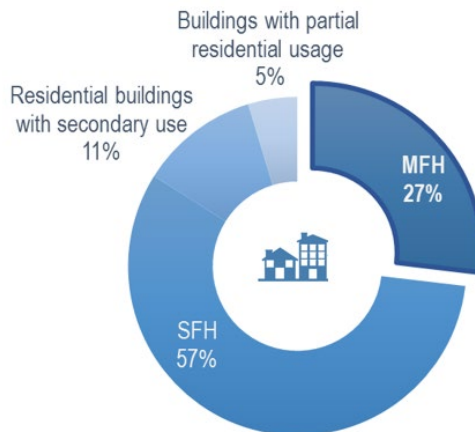
Figure 1: Distribution of residential buildings by building category [12].

Figure 2 illustrates that about two-thirds of MFH were built more than 40 years ago, before 1980 and are therefore relatively old. A sharp increase in MFH construction occurred from 1946-80, accounting for 35% of the entire existing MFH building stock. Among all MFH, two-thirds comprise less than four floors, the majority three floors (40%), a dominant characteristic of 1946-80 MFH. Pre-1980 MFH with 3 floors comprise 9 apartments on average, and the surface area per apartment ranges from 91 to 97 m^2. According to SIA 380/1 [13], occupation for MFH is about 40 m² per person.
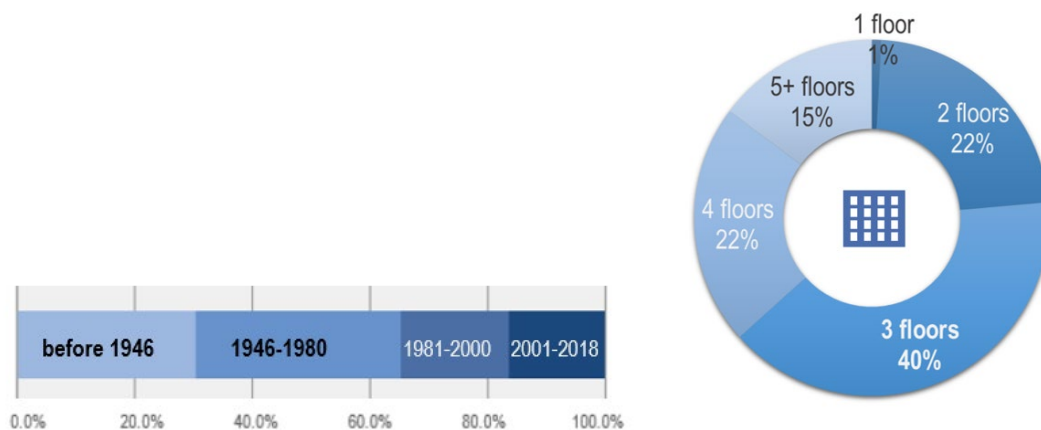
Figure 2: Distribution of MFH by period of construction and number of floors [12].

war from 1946 to 1960. The appearance of the first energy regulations defined the end of the fourth period: "pre-energy regulations from 1961-80".

Within the framework of this research project, the main architectural characteristics considered were the number of floors, the shape of the roof and its area availability for ST technology. The findings served to confirm the information collected in the interviews. A summary of results is given in Figure 3.
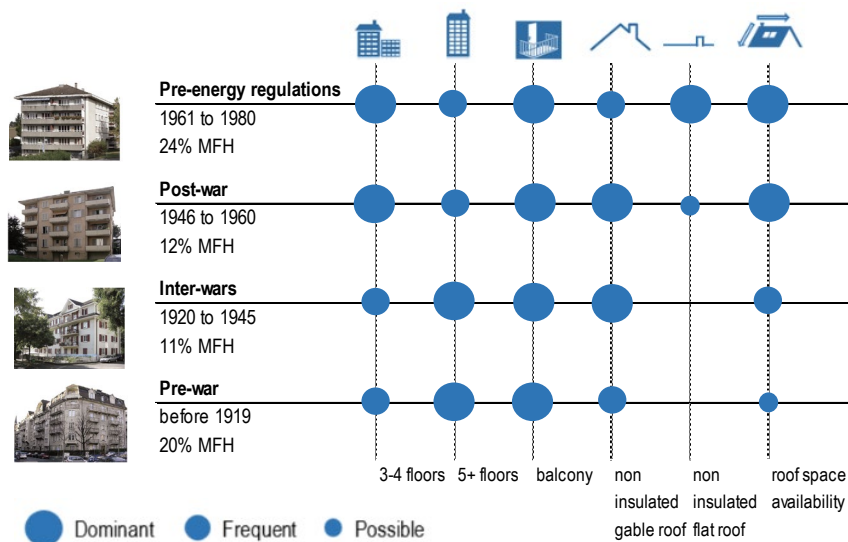
Figure 3: Summary of results for pre-1980 MFH [14].

In 2000, of all pre-1980 residential buildings, the renovation proportion over the previous 30 years was about 50% [15].[2] This rate varies widely from canton to canton. Typically, for MFH, values from 67% (JU) to 24% (GE) have been indicated (status in 2000). No up-to-date statistics for the rate of renovation of Swiss buildings was found. According to SIA 480 [16, p. 480], the average lifetime of a heating system is 35 years.

2.3 Statistical data - household energy figures

In Switzerland, 75% of pre-1980 MFH have a central heating system for the individual building [12, p. 201], which often means a centralised water storage for DHW distributing to the different points of use. Figure 4 shows the final energy used in Swiss households [17]. It can be seen that hot water supply is the second-largest consumer of final energy, accounting for over 14% of the total household consumption.

---

[2] Energy-related and non-energy-related renovations are counted here.
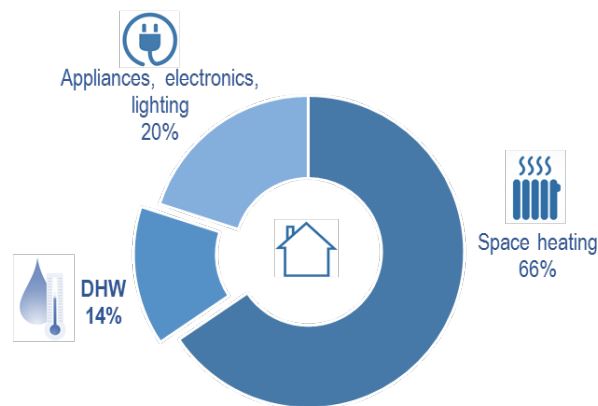
Figure 4: Final energy demand in Swiss households [17].

This equals the combined consumption of lighting (2%), electronics (3%) and some appliances (9%) such as refrigeration, cooking/dishwashing and washing/drying altogether. However, progress in building technology and more stringent high-quality building standards are increasingly leading to larger shares of the energy demand for hot water production, with values amounting to 60% of the energy consumption in a typical MINERGIE building [18].
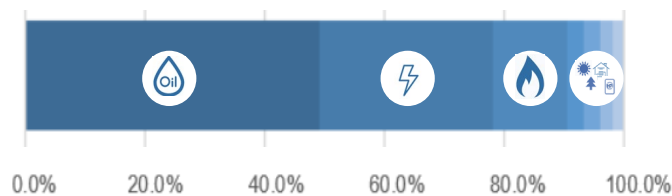
Figure 5: Main heat sources for DHW in MFH [12].

Main energy sources for hot water in Swiss MFH are still oil (49%), electricity (29%), and gas (12.5%), as shown in Figure 5. Only 8% are based on renewable energy such as wood and solar [12].

2.4 Energy regulations

In terms of energy regulations, the Swiss Federal Council pursues the implementation of the Energy Strategy 2050 that aims to gradually phase out nuclear power in Switzerland and increase the use of renewable energy sources. For residential buildings, this means to reduce final energy consumption, increase the use of renewable energies and thus contribute to a significant reduction in CO_2 emissions.

Following the 1998 Energy Law, cantons are primarily responsible for the regulation of the energy consumption in buildings [19]. Over time, cantons have developed completely different strategies from one another. To support and help cantons to achieve their energy targets in a more harmonised manner, the Conference of Cantonal Energy Directors (EnDK) created the Cantonal Energy Prescription Model (MoPEC), a set of energy regulations that defines the minimum standards for consumption of space heating and DHW, and also touches on-site electricity production. The modernisation of heating systems is one of the crucial aspects of the new MoPEC. The eleven "standard solutions" (SL) of the MoPEC 2014 define possible heating scenarios based on cantonal requirements for buildings that do not reach class D ranking.

Today, the implementation of the MoPEC in the Swiss cantons and their requirements for heating system replacement is shown in Figure 6.
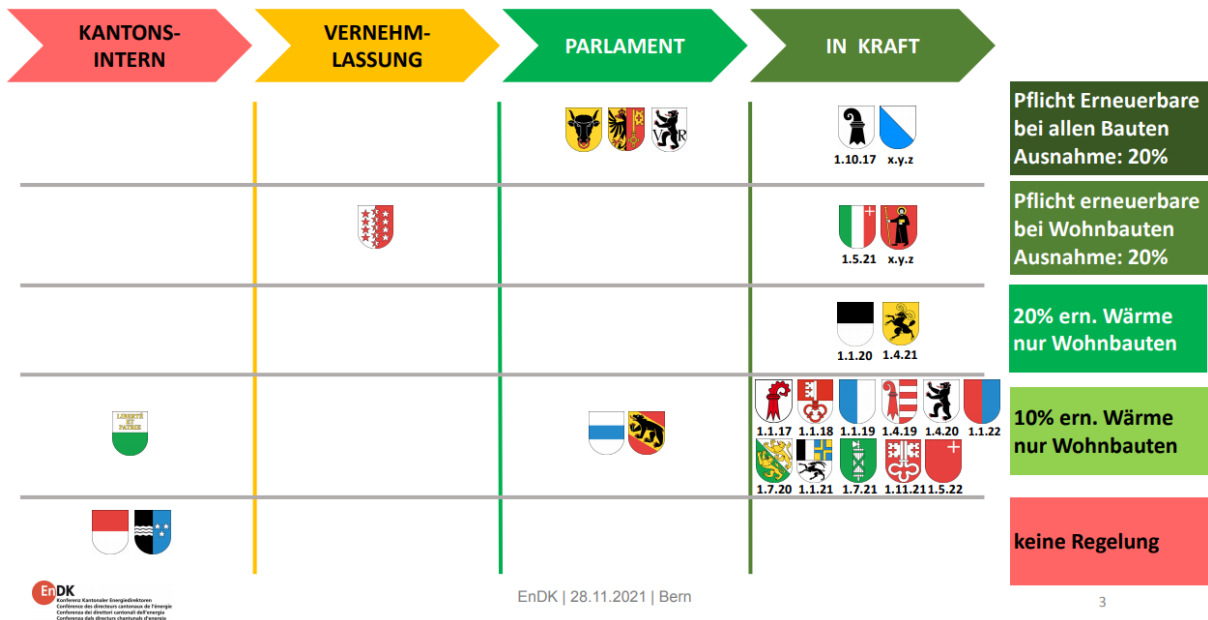
Figure 6: Status of MoPEC implementation in the Swiss cantons and their requirements for heating system replacement in Dec. 2021 [20].

By the end of 2021 MoPEC was in force in 117 cantons. One is undergoing consultation, and other five are in the parliament phase. Apart from the legal regulations, other key instruments of Swiss building policies are the CO_2 tax, funding programmes such as the Building Program[3] and other voluntary measures by EnergieSchweiz[4], in particular the new "Renewable Heating" programme[5]. All underline the importance and usefulness of switching from fossil fuels to indigenous renewable energies for heating through an incentive advice offer.

2.5 Interview results

All interviewees had their background in engineering with primary roles in building construction and use, including facility management and maintenance. Their experience and knowledge in energy renovation of existing MFH was very much alike, with tens to hundreds renovation projects conducted in Switzerland. In this analysis, only the features that bear an impact towards integration of DBS in an MFH renovation scenario are considered.

To infer the suitability of Swiss MFH to uptake DBS solutions within the framework of a DHW system renovation, it is crucial to first understand the typical MFH features. This part assesses what is perceived as the dominating building characteristics of MFH, see Table 1.

---

[3] www.dasgebaeudeprogramm.ch

[4] https://www.suisseenergie.ch

[5] https://erneuerbarheizen.ch

Table 1: Perceived MFH dominating characteristics.

DOMINATING MFH CHARACTERISTICS

CONSTRUCTION PERIOD	<1980
NUMBER OF FLOORS	3-4
ROOF TYPE	Gable, non-insulated
ROOF SPACE AVAILABILITY FOR ST	Yes

The interviewees unanimously agreed that the typical MFH is a building constructed before 1980 with three to four floors. It has a gable, non-insulated roof with enough space to accommodate ST technology. This is consistent with the statistical data presented earlier on.

For integration of DBS concepts in MFH renovation scenarios, information about the existing type of DHW system and its location plays a major role. The following part assesses the perceived features that dominate the technical room and characteristics of the DHW system and storage.

Table 2: Perceived dominating features of technical rooms in typical MFH.

DOMINATING FEATURES OF TECHNICAL ROOMS IN TYPICAL MFH

LOCATION	basement
SPACE AVAILABILITY FOR ADDITIONAL EQUIPMENT	yes
POSSIBILITY FOR SOLAR PIPE ROUTING	yes

According to interviewees, see Table 2, the typical technical room is situated at the basement, often with space available for additional equipment. Solar piping running down the building is quite often possible, due to existing pipe/cable passages in the building. In older buildings, unused chimneys, drain ducts, shafts and voids are seen as ideal for piping channels.

Table 3: Perceived dominating features of DHW systems in typical MFH.

DOMINATING FEATURES OF DHW SYSTEMS IN TYPICAL MFH

INSTALLATION TYPE	Separated boiler and DHW storage
ENERGY SOURCE	Oil and gas
INSTALLATION AGE	<30 years
REFURBISHMENT STRATEGY	Replacement by equivalent more modern system
RENEWABLES CONSIDERED	No, unless legal obligations
MOST COMMON REFURBISHMENT ACTION	Replacement of both boiler and storage

Table 3 indicates that the most common DHW system in a typical MFH is a separate boiler and DHW storage, no older than 30 years, mostly operated with oil or gas. The perceived installation age relates to the Energy 2000 action plan launched in 1990 by the Swiss Federal Office of Energy, aiming to promote the retrofitting of buildings by providing federal subsidies [21].

When the time has come for replacing the fossil fuel heating system, most often neither owners nor professionals consider renewable alternatives. The common approach is the replacement of the old fossil heating system with another equivalent, more modern, fossil heating system. This is because replacement happens usually after a sudden problem or failure and is carried out in a haste, particularly

if the breakdown occurs during winter. In this case, no time is left to envisage and implement other energy technology.

Nevertheless, current legal obligations such as the MoPEC 2014 now include mandatory targets, limiting the use of non-renewable energies or requiring a minimum of renewables for heating and hot water. Among the recommended SL for these applications, ST and HP technologies are considered. When asked what they observed as the preferred renewable technology heating solution for typical MFH, interviewees indicated ST over HP. The reason is that quite often the space heat distribution in these old MFH is still run with traditional high temperature radiators, which reduced the efficiency of heat pumps. Consequently, ST becomes often the preferred option, due to the impracticability of installing an underfloor heating system.

The typical features of existing DHW storages in MFH are presented in Table 4. It consists of one-single insulated DHW storage having a volume capacity of about 750 litre and standard hydraulic connections: auxiliary heating ports and DHW supply. According to interviewees, it is very complicated to integrate solar thermal in the existing DHW storages as everything is predefined and no additional extra ports exist. In addition, the combination of old and new systems is perceived as difficult since the control system will not be able to manage everything properly as the regulation of ST systems is seen to be quite limited. In any case, all interviewees see retrofitting of a DHW system in MFH as a very simple undertaking, where at the greatest problem to solve is the introduction of a storage tank into the technical room.

Table 4: Features of existing DHW storages in typical MFH.

FEATURES OF EXISTING DHW STORAGES IN TYPICAL MFH

NUMBER OF STORAGES	1
STORAGE VOLUME	750l
TYPE OF HYDRAULIC CONNECTIONS	Standard (no solar ports)
POSSIBILITY FOR ST INTEGRATION	no
COMBINATION OF OLD AND NEW SYSTEMS	difficult

Renovation costs also drive the decisions to adopt and use sustainable DHW production systems in the absence of legal obligations such as MoPEC. According to participants, integration of ST systems in existing MFH presents the most viable option for renewable DHW production. However, these are hardly considered, let alone adopted, because of the cost. This implies that cost is also a major barrier to the adoption of ST systems in energy renovations of MFH.

2.6 Reference MFH

Based on the interview evaluations and the frequency of the structural features from the official statistics, the dominating characteristics of the MFH to be used as reference in WP2 are the following:

Table 5: Reference MFH.

REFERENCE MFH

CONSTRUCTION PERIOD	<1980
NUMBER OF FLOORS	3
NUMBER OF APARTMENTS	9
AVERAGE SURFACE PER APARTMENT[6]	94 m^2
ROOF TYPE	gable, non-insulated

---

[6] Average surface value from statistics

TECHNICAL ROOM LOCATION	basement
NUMBER OF STORAGES	1
DHW STORAGE VOLUME	750 l

Other main findings regarding the feasibility of adding a solar thermal energy system to an existing MFH DHW system are the following:

- Roof space for solar collectors is often available

- Extra space for additional equipment in the technical room is often available

- Routes for the solar piping are often available

- The typical existing DHW-storage is a 750 litre tank with no spare/free connections for solar integration. However, these storages have normally an inspection flange that could be potentially used for solar connection. In refurbishing actions, it is common practice to replace the existing storage.

- The typical three floors MFH has about 21 inhabitants with a total DHW demand of about 16 MWh/a (taken equal to 18.5 kWh/m^{2}a according to SIA 385/2 [22].

2.7   Conclusion

The relevant boundary conditions that influence the integration of DBS in existing MFH were determined by means of interviews and analysis of available statistical data. Three representatives from companies of the building sector were interviewed, all of them with a large experience in assessing building energy issues in new and existing constructions and in current practices when retrofitting heating systems.

The relevant group of MFH has been identified belonging to the construction period pre-1980, representing approximately 40% of all MFH. According to statistics and interview results, these buildings typically present enough space on the roof and in the technical room to accommodate a DB add-on system with a solar storage. In addition, more than 75% of the pre-1980 MFH have a central heating system, and the vast majority have not yet been modernised in terms of heating systems.

The typical existing DHW-storage has a volume of 750 litre with no spare/free connections for solar integration. However, in refurbishing actions, it is common practice to replace the existing storage. When the storage is replaced, solar ports can be provided with the new storage, making the implementation of the solar part easier and the solar thermal system more efficient. Without replacing the DHW-storage, the integration point for a DB add-on system on an existing system could be at the level of the existing tank via the electrical rod flange and/or upstream of the existing tank to preheat the tapped water. These different variants are studied in chapter 3.

According to the interviewees, solar heat for DHW in MFH would be preferred over HPs, but there is little willingness to use renewable energy sources if there are no appropriate legal obligations. However, the tightening of regulations such as MoPEC is evolving in this direction. These features form the basis for the building model (reference MFH) for assessing the energy and cost advantages of different DBS concepts.

The findings regarding system size and DHW demand fit well to the assumptions made in the project ReSoTech [2]. Hence, the energy system simulation and cost of ReSoTech are in accordance with our findings and can be slightly adapted and used in this project.

3 System design, Energy and Cost

Simple and energy efficient add-on DBS concepts for existing DHW systems in MFH were drafted and analysed by means of energy performance simulations and cost calculations. The technical practicality for the market and the levelized cost of heat (LCoH) were the main evaluation indicators for selecting the most promising system among the investigated variants. For the proposed DBS solutions, the key objectives were to demonstrate:

- the energy and cost saving potential

- the technical feasibility and market acceptability

- the simplest integration approach

In the present study, the main focus was on the integration of add-on DBS into existing DHW systems of MFH. The simulation needed to consider the typical DHW demand of an MFH as well as the DHW system in place and overall MFH features pertinent to the integration of a solar thermal technology. Three DBS concepts are considered and compared to a classical no-DB solar thermal DHW system and a purely fossil DHW heating system to better seize the benefits of the developed concepts.

The simulation of the energy performance and the economic assessment (cost of useful heat and LCoH) are used to design and size suitable DBS. The cost calculation details as well as the simulation model are presented here.

3.1 Analysed system concepts

The focus was on a DBS variant that adds solar storage volume to an existing DHW storage (Variant A, Figure 7). The added solar storage volume does not contain drinking water (advantage for legionella safety) and the heat transfer to the existing boiler is done with an external plate heat exchanger. By adding solar storage volume, it is expected that high solar gains can be ensured at low cost.

Two additional variants of this main solution were analysed: Variant B (Figure 8) was designed for cases of limited space in the cellar. A compact solution of heat exchanger and solar storage volume was designed, such that it uses little volume and installation area. In Variant C (Figure 9), the new storage replaces an existing one. The new storage is used as a stand-alone storage with hot water preparation via a DHW heat exchanger (fresh water station). With this heat exchanger concept, storing of solar heat in drinking water at low temperature, which is sometimes seen as problematic because of possible growth of legionella, is avoided, just as with the two variants before. Variant C has the possibility to charge the upper section of the tank with auxiliary heat from burners (or heat pumps as well). This solution can be used for new buildings or when an existing DHW tank needs to be replaced.
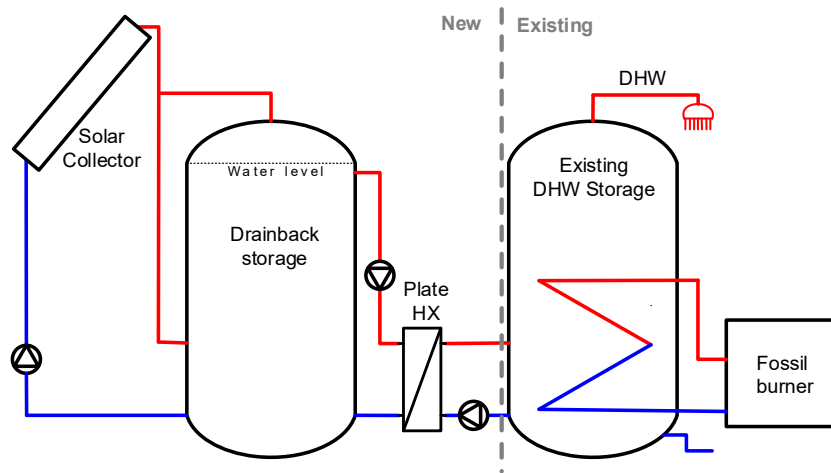
Figure 7: DBS A – a drainback system with large DB-storage which is coupled to an existing DHW storage tank via plate heat exchanger.
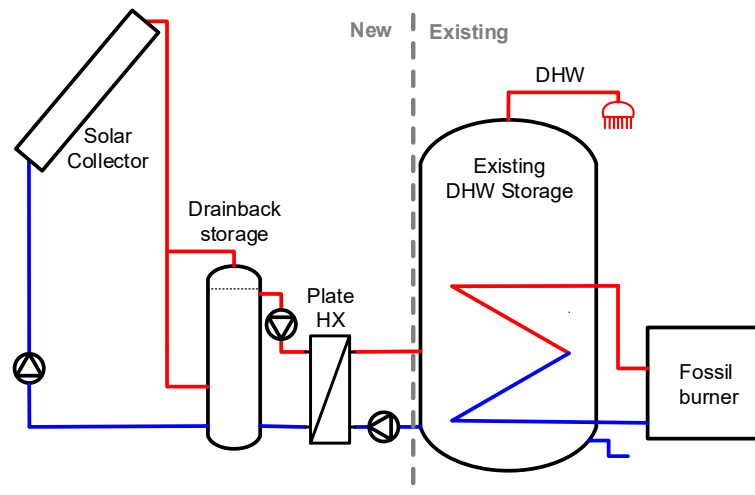
Figure 8: DBS B – a drainback system for reduced space with only small DB-storage which even might be only a drain back vessel, which is coupled to an existing DHW storage tank via plate heat exchanger.
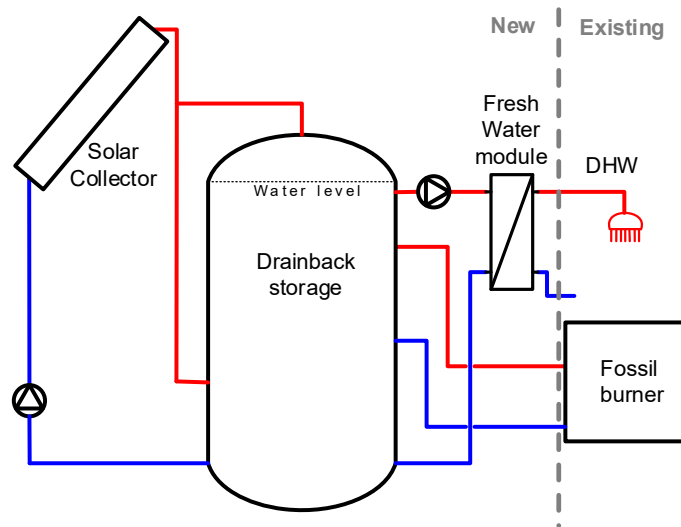
Figure 9: DBS C – a drainback system with large DB-storage which replaces the existing DHW storage tank. The DHW preparation is done with a fresh water module.

3.2 Methods

3.2.1 Cost of heat

The uptake of any new technology requires evidence of its advantages in terms of better cost-effectiveness than other alternatives on the market. In this way, the cost of the heat produced by the DBS concepts over their life time was calculated, and the result compared against that of two conventional systems: exclusively gas-fired and standard solar thermal, taken from the ReSoTech reference systems [2]. Two calculation methods were applied: cost of useful heat and LCoH.

The cost of useful heat considers all investment and operation and maintenance (O&M) costs for the overall system (existing part and the solar system addition). These costs were determined using quotes collected from two company experts in DBS in Switzerland who supported the project in an advisory board. In addition, cost data gathered in the ReSoTech project was also used. The advisory board companies were invited to submit offers for DBS concepts that kept the existing DHW storage, i.e. DBS A and DBS B.

The cost of the useful heat is calculated by dividing the annual costs by the useful heat consumed (Q_{use}) for hot water production:

$$\text{Cost of useful heat} = \frac{a.(I_0 - S_0) + C_t}{Q_{use}}$$

where:

a: annuity factor

I_0: initial investment in CHF

S_0: subsidies and incentives in CHF

C_t: operation and maintenance costs in CHF/a

Q_{use}: total energy consumed in kWh/a

The annuity factor is computed from the loan rate (LR) and loan term (t). These values were taken equal to those used in the ReSoTech study i.e. LR = 1 % and t = 30 a, this latter corresponding to the usual service lifetime of the system. Investment costs include the upfront expenses related to installation and commissioning of the system i.e. design, heat producer, heat distribution, storage, transport, installation and commissioning. O&M costs take into account all yearly expenses, including costs for maintenance of the existing parts and solar system addition and the cost for the used fossil fuel for the operation of the system. The overall O&M costs over the entire lifetime of the system is divided by t to obtain the yearly O&M expenses. The useful heat Q_{use} is computed from the simulations (chapter 3.2.2) and corresponds to the total energy consumed to provide the DHW demand for the defined case study (chapter 3.3.1).

Economic evaluation of the DBS concepts was also performed using the levelized cost of heat (LCoH) methodology developed within the framework of IEA-SHC Task54 [23]. This method allows for cost comparisons between different designs and technologies and is based on the saved final energy, i.e. the amount of final energy replaced by solar energy. The LCoH used in this project is defined by the following expression:

$$LCoH = \frac{I_0 - S_0 + \sum_{t=1}^{T} \frac{C_t}{(1+r)^t}}{\sum_{t=1}^{T} \frac{E_t}{(1+r)^t}}$$

where:

$LCoH$: levelized cost of heat in CHF/kWh

I_0: initial investment in CHF

S_0: subsidies and incentives in CHF

C_t: operation and maintenance costs (year t) in CHF

E_t: saved end energy (year t) in kWh

r: discount rate

T: period of analysis in year

It provides the quotient from the cost of the solar system part for DHW preparation over its service lifetime to the final gas consumption that is saved by the solar part of the system during this period.

This calculation requires the definition of a reference conventional fossil fuel system which would supply the same amount of energy for DHW preparation as the DBS but without solar assistance. A standard solar thermal system was also considered as reference to infer the advantages of the DBS concepts against the most common solar thermal systems in use. In the two cases, the gas consumption is compared with that of the auxiliary (backup) system used in the DBS concepts, which allows for the assessment of the benefits of these latter. Figure 10 presents a schematic representation of the reference systems considered. The reference systems and calculation assumptions were based on those of the project ReSoTech.
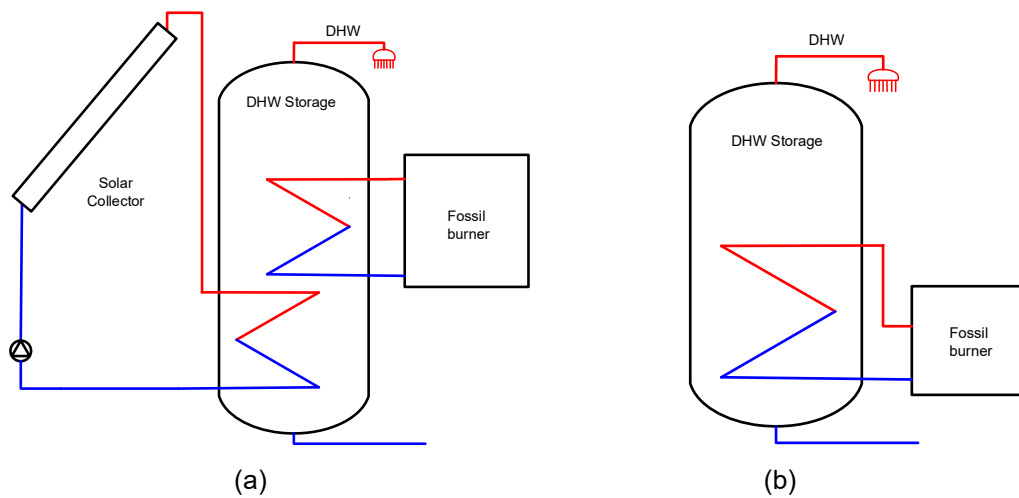
Figure 10: Reference systems – a) standard solar thermal and b) conventional gas-fired.

The initial investment (I_0) and O&M costs (C_t) are the same as for the cost of useful heat. Calculations with and without subsidies and other incentives (S_0) were considered. Subsidies were taken according to the ModEnHa 2015 [24] and incentives relate to cantonal tax-deductible measures. Municipal subsidies and tax reductions were excluded as these values vary widely within the country. The discount rate (r) and the period of analysis (T) are equivalent to the loan rate (LR) and loan term (t), respectively. The saved final energy (E_t) is computed from the simulations and corresponds to the difference between the gross final energy demand of the conventional fossil fuel system and the gross final auxiliary energy demand of the DBS concepts.

3.2.2   Simulation analysis

A simulation analysis was used to design and size the DBS concepts. It predicts the thermal performance of the system when supplying DHW for the MFH case study and provides comparisons against the performance of the reference cases described in section 3.2.1. The main elements of the simulated system are the solar thermals collectors, storage tank, heat exchangers and DHW profile. The final objective of the simulation was to identify the most suitable DBS concept and quantify its energy and economic advantages. Since the findings of chapter 2 regarding the system size and DHW demand fit well to the assumptions made in ReSoTech, the model developed under that project was slightly adapted and used in this project.

The simulations were performed using Polysun v.11.3 software with standard components and with validated, well-known third-party models. Useful heat consumed (Q_{use}), solar energy production (Q_{sol}) and fuel consumption (E_{aux}) were taken directly from simulation results and the annual energy savings as well as the solar coverage was calculated from these results.

The DHW demand was based on the SIA 385/2 [22], corresponding to 270 m³ of DHW at 60 °C per year (see chapter 3.3.1). The DHW tapping profile was taken from ReSoTech and corresponds to the VDI6002 for MFH. The distribution was simulated with a circulation loop that operates as indicated by the SIA 385/1 [13] with a temperature of 55 °C. The reference weather conditions are for the Rapperswil (SG) site.

The reference conventional fossil fuel system was a gas-fired and the size of the components were in line with the interview results. Characteristics of the components use in the Polysun model were the same as in the ReSoTech project and similar to those found in the market.

The standard solar thermal system model was also composed of standard components and derived from ReSoTech. The size of the solar collector field was defined from the MoPEC 2014

recommendations for MFH. Considering the 850 m² total energy reference area of the case study, the minimum size of the collector field according to the recommendations is 17 m². The storage tank used had 1500 litres of capacity with two internal heat exchangers (one for the solar in the lower part of the tank and another one for the auxiliary system in the upper part).

The size of the solar field for the DBS was 17 m². The size of the drainback storage for DBS A and C was defined with a capacity of 805 litres due to the technical manufacturing constraints and taking into account expansion and drain volumes (not included in the 805 litres). In the Polysun models, the DBS were connected to the existing tank via an external plate heat exchanger as described in chapter 3.1.

3.3 System Design

In chapter 2, the characteristics of the reference MFH and the main feasibility conditions for adding a solar thermal system to an existing MFH DHW system were defined. In here a description of the case study is presented and the technical considerations of the conceptual DBS designs are discussed.

3.3.1 Description of the case study

The case study defined for this project is an MFH building with three floors and three apartments per floor. The roof of the building is south oriented and gabled with 45° inclination. These features represent 40 % of the Swiss MFH market (chapter 2.2) and 100% of the answers received in the interviews. The total number of inhabitants in this building is 21. According to SIA 385/2, the domestic hot water consumption equivalent for this building is 270 m³ per year.

The size of the DHW production system includes a 15 kW modulating gas boiler and one 750 litre storage tank, components that agree with the interview results of chapter 2 and SIA 385/2 recommendations. Table 6 summarises the main features of the case study that was taken as a basis for the design and simulations of the solar thermal systems.

Table 6: Reference case study.

MFH CHARACTERISTICS [OFS]

Number of floors	3
Number of apartments	9
Average apartment surface	94 m^2
Total inhabitants of the building	21

DHW DEMAND [SIA 385]

Total DHW requirements	270 m³ per year
Building heat requirements for DHW (without losses in tank and pipes)	~16 MWh per year

EXISTING DHW SYSTEM

DHW storage capacity	750 litre
Auxiliary system	15 kW gas boiler

Based on the MoPEC 2014 Part F recommendations, the solar thermal collector field for hot water production must represent at least 2 % of the energy reference area of the building. In our case, the minimum solar collector area results in 17 m². This surface was considered as a reference for the comparison between the different solar thermal systems and was also considered as a minimum for the size optimisation. As previously described (chapter 3.2.2), the storage tank of the standard solar thermal system has 1500 litres of capacity, including the solar storage capacity and the auxiliary boiler capacity.

3.3.2   Technical considerations for the DBS concepts

Integration of solar thermal energy in the proposed concepts requires technical considerations to correctly define suitable embedding possibilities. Due to the different conceptual designs, the analysis of systems with add-on part, i.e. DBS A and DBS B, is separated from that of DBS C.

DBS A and DBS B integration

DBS A is made of a solar storage with integrated drainback volume. The solar storage is connected to an existing DHW storage. DBS B is a compact version for cases with limited space in the technical room, combining a small external drainback volume connected to the existing DHW system. In both cases, the add-on part is the component that allows for the connection of the new solar thermal system to the existing DHW storage, i.e. an all-in-one prefabricated unit composed of one heat exchanger, two circulation pumps, and the necessary piping.

According to the interview results, the typical existing DHW storage presents no spare/free connections for an additional energy source integration. To overcome this problem, four variants for connecting the solar part to the existing DHW storage tank via a plate heat exchanger (left from the pump in the figure) were proposed, see Figure 11:

a) If existing, use free connections for the flow and return pipe,

b) Integration of transfer flow via T-piece in the return pipe of the DHW circulation and integration of the transfer return pipe via T-piece at the fresh water inlet (stratification device inside the DHW tank might be needed)

c) Integration of two pipes (flow and return) via a flange with different heights inside the storage,

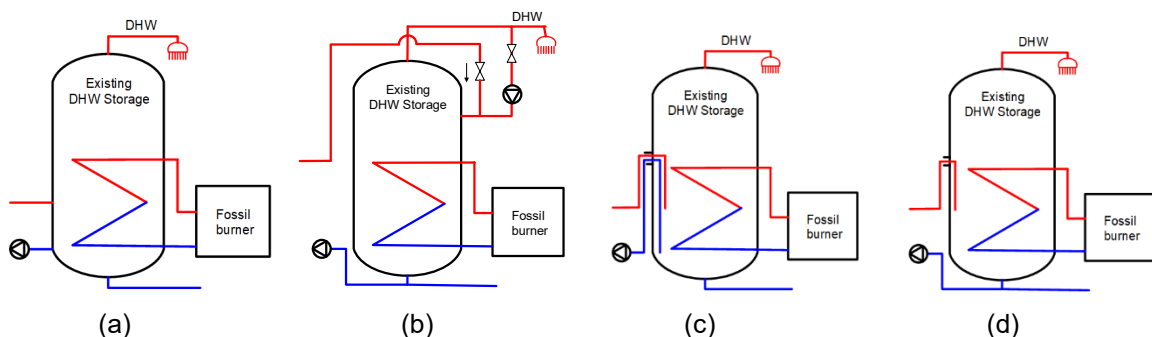d) Integration of the flow pipe via flange and of the return pipe via T-piece at the fresh water inlet,

Figure 11: Add-on part system integration possibilities for DBS A and DBS B, with four variants a - d to connect the secondary side of the transfer plate heat exchanger to the existing DHW storage (explanations see text).

DBS C integration

The DBS C concept uses the solar storage as a stand-alone tank to provide DHW through a fresh water module. The two main technical considerations here are (a) the integration of the fossil burner only for DHW and (b) in the case the fossil burner is also required for space heating, to use a separated space heating loop without tank (Figure 12).
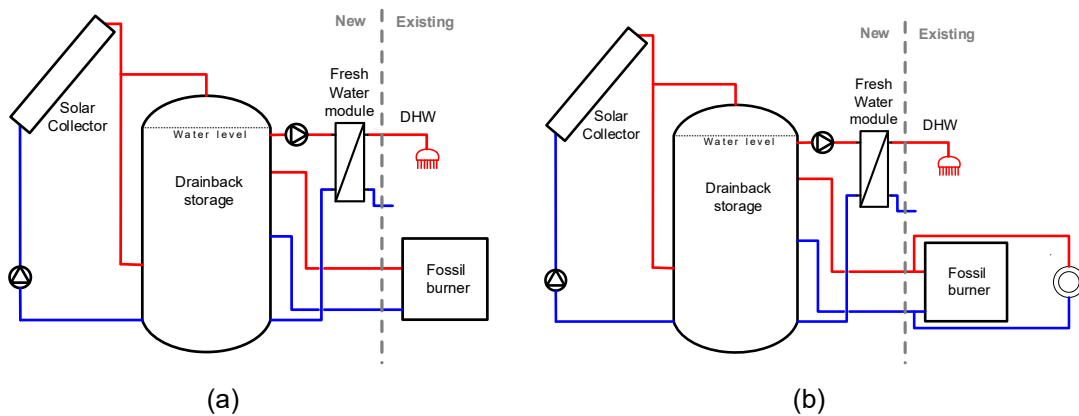
Figure 12: System integration possibilities for DBS C, a) without and b) with integration of space heating.

With a DHW demand of 16 MWh/a, the 805 litres storage volume of DBS C turns out to be slightly too small (SIA 385/2, 2015), which could potentially lead to a too large number of charging cycles per day by the burner. Consequently, for DBS C, two variants, C1 and C2, with different storage volumes are analysed. DBS C1 keeps the original 805 l, while DBS C2 storage is twice as large.

3.4 Cost of the hot water production systems

Here, the resulting costs of the different hot water systems considered are presented, including the standard solar thermal and the conventional gas-fired system. This latter was taken as the base reference cost and all other system costs were given in relation to the reference component costs to finally obtain the cost of the additional part of each of the other systems. Excluding the conventional gas-fired system, the maintenance costs for all systems correspond to the total amount over the whole lifetime of the system.

As far as the operation costs are concerned, these are system specific and include the gas consumption estimated in the simulations for each system which directly relates to the gas price, see assumptions in Table 7. These assumptions are conservative as the prices for natural gas were rising considerably during the project duration.

Table 7: Operation cost calculation assumptions.

OPERATION COSTS		
Energy price - Gas	0.093	CHF/kWh
Annual price increase for the energy	0	%

3.4.1 Conventional gas-fired system

The breakdown of costs for the conventional 15 kW gas-fired system for hot water production is shown in Table 8. According to chapter 2 this corresponds to the most common system in place in MFH.

It can be seen that the investment costs of the conventional gas-fired system amount to CHF 17'250 with a yearly maintenance cost of CHF 345.

Table 8: Cost breakdown of the conventional gas-fired system for hot water production for the MFH case study (supplier quote).

INVESTMENT COSTS			
Design	3%	550	CHF
Heat producer (15 kW gas burner+accessory set)	46%	8000	CHF
Heat distribution (device/piping+regulation)	11%	1850	CHF
Boiler (750l DHW tank+accessories)	17%	2850	CHF
Transport, installation and commissioning	23%	4000	CHF
Total Investment		**17250**	**CHF**
MAINTENANCE COSTS			
Factor of yearly maintenance costs		2	%
Total Maintenance		**345**	**CHF/year**

3.4.2 Standard solar thermal system

The cost of the standard solar thermal system for hot water production for the reference case with 17 m^2 collector field was obtained by calculating the cost of the additional solar part with regards to the conventional gas-fired installation components, see Table 9. It includes costs related to glycol changes and other miscellaneous costs related to replacement of small parts during the lifetime of the system. The investment cost without the conventional gas-fired part and without subsidies results in CHF 24'808. The annual maintenance costs are CHF 142.

Table 9: Cost breakdown of the solar part of the standard solar system for hot water production for the MFH case study (ReSoTech data).

INVESTMENT COST			
Design	*3%*	*650*	*CHF*
Collector Field (collectors+accessories+mounting)	*27%*	*6726*	*CHF*
Storage (805l DHW tank+piping/devices+mounting)	*14%*	*3487*	*CHF*
Solar Circuit Roof (piping/devices+mounting)	*16%*	*3871*	*CHF*
Solar Circuit Building (piping/devices+mounting)	*17%*	*4288*	*CHF*
Further (regulation, brine, transport/installation/commissioning)	*23%*	*5786*	*CHF*
Total Investment		**24808**	**CHF**
MAINTENANCE COSTS			

Glycol Change		*2359*	*CHF*
Miscellaneous		*1295*	*CHF*
Total Maintenance		**3654**	**CHF**

3.4.3   DBS variants

Table 10 presents the cost of the components needed to connect the solar part of DBS A and DBS B with the existing DHW storage. The costs were obtained from catalogue prices and own estimations and refer to the additional heat exchanger, circulation pumps and piping components. The mounting cost is estimated to 10% of the component costs. The add-on part results in an additional cost of CHF 2'046.

Table 10: Cost of the add-on part of DBS A and DBS B for hot water production for the MFH case study (catalogue prices and own estimation).

INVESTMENT COST		
Device (heat exchanger + insulation, pump)	*1800*	*CHF*
Piping (plastic pipe on the solar side, stainless steel pipe on the DHW side)	*60*	*CHF*
Mounting	*186*	*CHF*
Total Investment	**2046**	**CHF**

<u>DBS A:</u>

For defining the cost of DBS A, the standard solar thermal system is used as basis. A reduction in the hydraulic circuit that includes the replacement of the glycol with water and the replacement of conventional pipes by plastic pipes (CHF -3'100) is considered. A low-cost storage made of glass fibre reinforced plastic based on assumptions of ReSoTech [11] was added plus the cost of the plate hx (Table 10). In addition, for all DBS concepts no costs are associated with glycol changes. The net investment cost amounts to CHF 21'965 with a maintenance cost of CHF 1'295, corresponding to an annual maintenance cost of CHF 50.

Table 11: Cost breakdown of DBS A for hot water production for the MFH case study.

INVESTMENT COST			
Design	*3%*	*650*	*CHF*
Collector Field (collectors+accessories+mounting)	*31%*	*6726*	*CHF*
Storage (805l DB tank+piping/devices+mounting)	*10%*	*2211*	*CHF*
Add-on part (piping/devices+mounting)	*9%*	*2046*	*CHF*
Solar Circuit Roof (piping/devices+mounting)	*13%*	*2846*	*CHF*
Solar Circuit Building (piping/devices+mounting)	*10%*	*2279*	*CHF*
Further (regulation, transport/installation/commissioning)	*24%*	*5207*	*CHF*
Total Investment		**21965**	**CHF**

MAINTENANCE COSTS		
Miscellaneous	*1295*	*CHF*
Total Maintenance	**1295**	**CHF**

DBS B

The cost of DBS B is similar to the one computed for DBS A but integrates the replacement of the plastic drainback storage by a small drainback vessel. The cost of this latter was provided by the industrial partners. The resulting investment cost is CHF 22'430 with no changes in the maintenance cost.

Table 12: Cost breakdown of DBS B for hot water production for the MFH case study.

INVESTMENT COST			
Design	*3%*	*650*	*CHF*
Collector Field (collectors+accessories+mounting)	*30%*	*6726*	*CHF*
Storage (drainback vessel+piping/devices+mounting)	*12%*	*2676*	*CHF*
Add-on part (piping/devices+mounting)	*9%*	*2046*	*CHF*
Solar Circuit Roof (piping/devices+mounting)	*13%*	*2846*	*CHF*
Solar Circuit Building (piping/devices+mounting)	*10%*	*2279*	*CHF*
Further (regulation, transport/installation/commissioning)	*23%*	*5207*	*CHF*
Total Investment		**22430**	**CHF**
MAINTENANCE COSTS			
Miscellaneous		*1295*	*CHF*
Total Maintenance		**1295**	**CHF**

DBS C

The cost of DBS C is similar to the one computed for DBS A but excludes the add-on part while including a fresh water station taken from a product catalogue with costs for mounting (CHF +2'786). This results in CHF 22'705 of investment costs with, again, no changes in the maintenance cost.

Table 13: Cost breakdown for DBS C for hot water production for the MFH case study.

INVESTMENT COST			
Design	*3%*	*650*	*CHF*
Collector Field (collectors+accessories+mounting)	*30%*	*6726*	*CHF*
Storage (805l DB tank + fresh water station+piping/devices+mounting)	*22%*	*4997*	*CHF*
Solar Circuit Roof (piping/devices+mounting)	*13%*	*2846*	*CHF*
Solar Circuit Building (piping/devices+mounting)	*10%*	*2279*	*CHF*

Further (regulation, transport/installation/commissioning)	*23%*	*5207*	*CHF*
Total Investment		**22705**	**CHF**
MAINTENANCE COSTS			
Miscellaneous		*1295*	*CHF*
Total Maintenance		**1295**	**CHF**

The cost of the variant C2 adds the additional cost of the large storage (1610 litres) so that the total investment cost reaches CHF 24'605 with no additional maintenance costs.

3.5 Energy and heat cost

The simulation of the hot water supply for the defined case study was carried out with the parameters defined in 3.2.2. One indicator is used to determine the energy efficiency of the proposed DBS concepts, the fractional energy savings f_{sav}, that according to EN 12977 [25] is given by the following equation:

$$fsav = \frac{E_t}{E_{aux}^{ref}}$$

where E_t is the energy saved defined as the difference between the final energy consumption by the conventional gas-fired system E_{aux}^{ref} and the final energy consumption of the auxiliary in the standard solar thermal system E_{aux}^{sol}:

$$E_t = E_{aux}^{ref} - E_{aux}^{sol}$$

The fractional energy savings is the ratio of the energy saved E_t to the input energy by the conventional gas-fired system E^{ref}. The higher the fractional energy savings, the better. Table 14 presents a summary of the energy simulation and cost results for the case study conditions without any subsidies or incentives considerations.

Table 14: Summary of the energy simulations results and cost calculations for 17 m^2 collector area (no subsidies).

	Standard solar thermal system	DBS A	DBS B	DBS C1 (case: 805 L storage)	DBS C2 (case: 1610 L storage)
Investment cost (including only the costs for the solar system part)	24'808 CHF	21'965 CHF	22'430 CHF	22'705 CHF	24'605 CHF
O&M cost (including the gas cost and the maintenance costs for the conventional part and the solar part)	2'024 CHF/a	2'012 CHF/a	2'071 CHF/a	1'796 CHF/a	1'685 CHF/a
Energy saved (gas)	7'402 kWh/a	6'551 kWh/a	5'908 kWh/a	8'870 kWh/a	10'066 kWh/a
Fractional energy savings	31 %	27 %	25 %	37 %	42 %
LCoH	0.15 CHF/kWh	0.14 CHF/kWh	0.16 CHF/kWh	0.11 CHF/kWh	0.10 CHF/kWh

	Standard solar thermal system	DBS A	DBS B	DBS C1 (case: 805 L storage)	DBS C2 (case: 1610 L storage)
(relative to standard solar thermal thermal sys.)	(-)	(93 %)	(107 %)	(73 %)	(67 %)
Cost of useful heat of the overall system (conventional gas-fired system part and solar part)	0.22 CHF/kWh	0.21 CHF/kWh	0.21 CHF/kWh	0.20 CHF/kWh	0.20 CHF/kWh

It can be seen that all DBS concepts have lower investment costs than the standard solar thermal system with DBS C2 approaching the cost of this latter. For all DBS concepts the use of plastic components, despite the additional add-on part of DBS A and B and the fresh water station in DBS C cases, still results in an interesting cost saving. Not using a storage tank for DBS B has no concrete advantage in terms of investment costs because the drainback station, as currently sold commercially and considered for this system, is a more expensive solution than the cost estimated of the DB tank made of glass fibre reinforced plastic that was developed in this project.

As far as the O&M costs are concerned, the values are quite similar between the standard solar thermal system and DBS A and B. Despite the fact that the maintenance costs of DBS are lower than those of the standard solar system, the reduction in gas savings for the DBS A and DBS B means that O&M costs balance out. Gas consumption reductions lead to lower O&M expenses as show for DBS C1 and DBS C2.

Lower energy savings are obtained for DBS A and B in comparison to the standard solar thermal system and, consequently, lower fractional energy savings. The reasons are related to the small volume on the existing DHW storage that can be used for solar loading, a consequence of the integration design of the system that gets into conflict with the conventional gas-fired boiler. As a new integration strategy, the solar thermal system is connected to the cold water inlet upstream the existing DHW storage allowing solar heat to pre-heat the fresh water. This variant is investigated in chapter 3.6.3.

DBS A presents a lower LCoH and cost of useful heat than the standard solar thermal system while DBS B presents the highest LCoH of all systems as a consequence of the combined effect of lower energy savings and higher investment and O&M costs. DBS C2 shows the largest cost reduction. Its LCoH of 0.10 CHF/kWh is 33 % lower than the LCoH of the standard solar thermal system (0.15 CHF/kWh). Reasons for this are lower investment and maintenance costs compared to the standard solar thermal system and higher energy savings due to the solar and fossil integration into one large tank. System C1 shows nearly the same LCoH as C2 but the amount of energy saved is significantly lower because the small drainback storage of C1 is not complying with DHW requirements, see 3.3.1.

For all systems, the LCoH is found to be between 0.14 to 0.15 CHF/kWh except for DBS C cases where lower values of 0.10 - 0.11 CHF/kWh are obtained. Differences for the cost of the useful heat are less pronounced between concepts with values ranging from 0.20 CHF/kWh for DBS C cases to 0.21 - 0.22 CHF/kWh for the other systems.

If subsidies and incentives are taken into account, the same trends with lower values are found, see Table 15.

Table 15: Summary of the cost calculations with subsidies and incentives.

	Standard solar thermal system	DBS A	DBS B	DBS C1 (case: 805 L storage)	DBS C2 (case: 1610 L storage)
LCoH with subsidies	0.10 CHF/kWh	0.09 CHF/kWh	0.10 CHF/kWh	0.07 CHF/kWh	0.06 CHF/kWh
Cost of useful heat of the overall system with subsidies	0.19 CHF/kWh	0.19 CHF/kWh	0.19 CHF/kWh	0.18 CHF/kWh	0.17 CHF/kWh

Overall, DBS A is an interesting concept, requiring less investment despite slightly lower energy savings for nearly the same thermal energy price. As initially proposed, the add-on integration design is still to be improved to overcome the problem of existing storages with no spare/free connections for an additional energy source integration. In contrast, DBS B is not really interesting with costs remaining high and with no energy saving advantages. Most interesting concept turns out to be DBS C2 where a 33 % LCoH reduction is foreseen using an all-in-one large storage. Given the volume unsuitability (too small) of the storage in DBS C1 and the cost advantages of DBS C2 despite its higher investment, the following results will only consider DBS C2.

3.6 Parametric studies

In the previous results, the solar collector field was sized to fit the case study conditions and was set to 17 m^2. In order investigate the influence of this parameter on the indicators f_{sav} and cost of useful heat for DBS A and C2, seven larger solar fields were considered. Since the size of the drainback storage is directly related to the size of the solar collector field, the influence of the storage volume was also investigated for DBS A. To improve the integration design of this latter, its use in a preheating configuration was further analysed.

3.6.1 Optimisation of the solar collector field size

In this analysis, the storage capacity was kept constant and the investment costs for the collector were assumed to increase linearly with the surface of collector. The presented cost results take into account subsidies and incentives.

Figure 13 shows that for both DBS concepts A and C2 the influence of the collector size is weak on the energy cost but with more impact on the fractional energy savings that increase with increasing solar collector area. For both concepts the curves on energy cost also suggest an optimum collector field size where the energy cost declines with increasing solar field size up to 40 m^2 (minimum) after which it slowly rises. These values correspond to a cost of useful heat of 0.177 CHF/kWh for DBS A and 0.164 CHF/kWh for DBS C2.
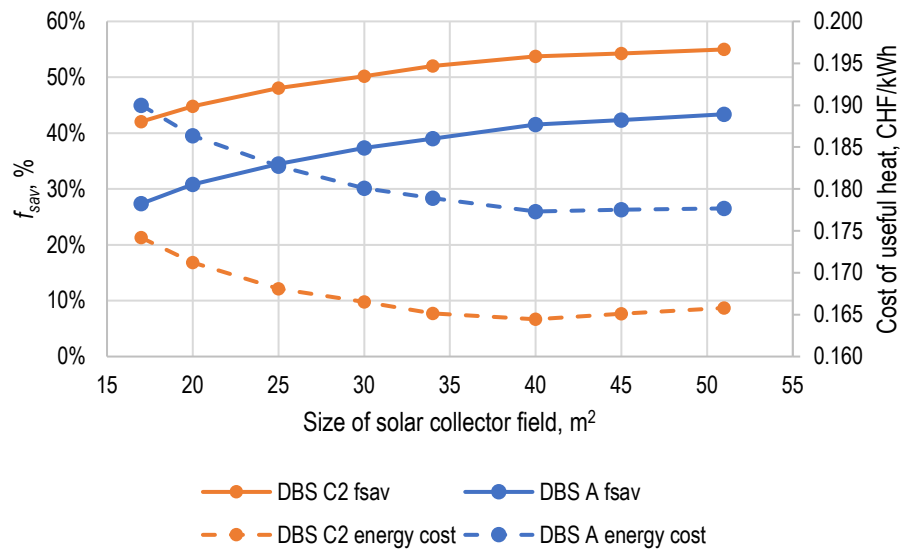
Figure 13: Influence of the collector field size on the fractional energy savings and energy cost (with subsidies) for DBS A and C2.

3.6.2 Optimisation of the drainback storage size

A larger storage volume of 1610 l was considered for DBS A, denoted as DBS A2, and its influence on the energy and cost indicators investigated. The influence of the drainback storage size in DBS A2 shows the advantages of a larger volume with increased solar collector field, see Figure 14. An optimum solar collector size is no longer possible to define here as the energy cost continuously decreases for the range of collector field sizes considered.
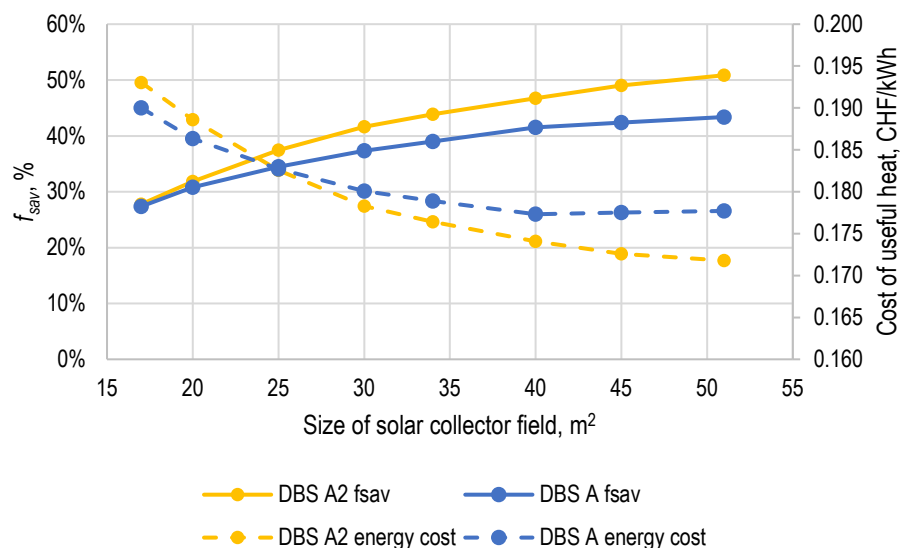

Figure 14: Influence of the drainback storage volume with the collector field size for DBS A (DB storage of 805 l) and A2 (DB storage of 1610 l).

3.6.3 Alternative integration design: DBS A in preheating mode

To overcome the integration difficulties of DBS A mentioned in chapter 2.7, the use of this concept as a solar hot water preheating system was evaluated. The configuration is presented in Figure 15 and shows the outlet of the drainback storage preheating the fresh water inlet to the existing DHW storage via a plate heat exchanger.
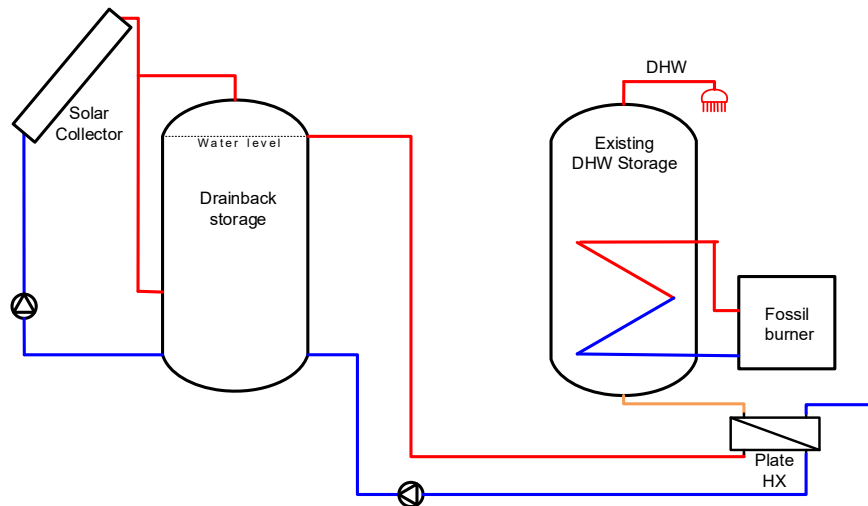

Figure 15: Configuration of DBS A in preheating mode (fresh water is preheated by the plate hx).

Three solar collector field sizes were simulated. Results show that the preheating configuration achieves higher energy savings and lower LCoH when compared to the initially proposed DBS A, and this for all simulated collector field sizes, see Table 16. However, no significant cost benefits are obtained by enlarging the solar collector field from the reference size of 17 m^2.

Table 16: Summary of results of DBS A in preheating mode.

	DBS A Preheating configuration		
	17 m^2	**20 m^2**	**25 m^2**
Investment cost	21'965 CHF	23'151 CHF	25'130 CHF
O&M cost (including the gas cost)	1'913 CHF/a	1'879 CHF/a	1'942 CHF/a
Energy saved (gas)	7'615 kWh/a	7'945 kWh/a	8'378 kWh/a
Fractional energy savings	32 %	33%	35%
LCoH	0.12 CHF/kWh	0.12 CHF/kWh	0.12 CHF/kWh
with subsidies	*0.07 CHF/kWh*	*0.07 CHF/kWh*	*0.08 CHF/kWh*
Cost of useful heat of the overall system	0.21 CHF/kWh	0.21 CHF/kWh	0.21 CHF/kWh
with subsidies	*0.19 CHF/kWh*	0.19 CHF/kWh	*0.19 CHF/kWh*

3.7 Conclusion

A reference case for the simulation studies was defined, corresponding to a DHW requirement of 270 m³ per year. The conventional fossil fuel system for this case study is a 15 kW gas boiler with a 750 litre tank. The cost of the useful heat delivered by this system to cover the entire heat demand was found to be 0.19 CHF/kWh. The standard solar thermal system for this case study is composed of a 17 m² solar field with 1500 litre tank, complying with MoPEC recommendations [26]. Despite the higher investment, the cost of the useful heat of the overall system, including solar and conventional part with MoPEC subsidies, is the same as for the conventional fossil fuel boiler and the LCoH of the solar thermal system is found to be 0.10 CHF/kWh. This system is only appropriate in the case of a complete renovation of the DHW production system as it requires the replacement of the existing tank for a larger one with two heat exchangers.

The analyses show that coupling a new solar thermal system into an existing tank is not trivial but is possible and can result in a relevant reduction of heat from the auxiliary heater. For the add-on concepts DBS A and B, the integration of solar thermal energy in the fresh water before it enters the existing DHW tank seems to be a feasible and also an energy-efficient solution. With 17 m² of solar collectors, DBS A provides almost the same solar fraction as for a standard solar system.

Cost results show that the use of plastic components, piping and tank, would reduce significantly investment costs of solar thermal systems. Combined with the reduced operational cost for DBS and the resulting economies on the glycol changes, the overall reduction of investment cost is significant, reaching 18% when comparing DBS A with the standard solar thermal system.

DBS B presents no advantages from the energy and cost point of view. The cost savings made by not installing a solar tank are balanced by the components that are still necessary to operate properly the DBS. This fact, associated with the performance reduction due to the absence of a solar tank, makes the economic results of the DBS B the least interesting. However, DBS B may still be the preferred choice when space is limited and the original DHW tank shall – for whatever reasons – not be replaced.

Economic analysis on the heat cost reveals DBS C as the economically most interesting solution. To comply with the heat demand, the volume for this system should be twice the volume of DBS A because there is no pre-existing tank in this configuration as the old tank is disposed. DBS C2 is the most promising system regarding energy savings and costs, reaching an LCoH of 0.10 CHF/kWh without subsidies. However, this system means the DHW is produced via a fresh water module which according to the advisory board, is not a common Swiss market practice and thus, not widely accepted yet.

Based on these results, the lab pilot system was chosen and designed according to DBS A, a system with no fresh water module, fitting better the expectations of the Swiss market in terms of renovation scenarios.

4 Thermohydraulic simulations

A challenge when designing the drainback systems is the proper sizing of all components that are influencing the drainback function. For the sizing of components and systems, today, there is a lack of information and design rules. To be able to size the lab system in a method-based way, thermohydraulic simulations were performed in the project, as they are the only available method to get insights into the relevant properties which need to be assessed for dimensioning the system.

Based on the results of the previous chapters, a prototype of a drainback system was designed, consisting of four flat-plate collectors and a storage tank.

This section basically follows the design procedure for the experimental setup. It can also serve as a practical guide for the design of DBS.

4.1 Methods

The collector loop of the chosen system variant was designed using HYDRA [27] which calculates the flow, temperature, and pressure distribution in single-phase operation. These data are used to assess the suitability of the chosen collector type and the collector field arrangement.

The newest version of THD [28] is used for the dimensioning of the pump, to assess the venting capability and to design the flow resistance needed to achieve overpressure in the collector field. The latter, in order to prevent evaporation at elevated temperatures.

The transients during filling, draining and stagnation are analysed using TRACE [29], a thermohydraulic system code developed for the safety assessment of nuclear power plants. Two-phase flows are simulated based on a 6-equation two-fluid model where each phase is represented by one-dimensional conservation equations for mass, momentum, and energy. The gas phase is modelled as a mixture of water vapour and a non-condensable ideal gas. The absorption and desorption of gases across the phase boundary is not considered.

4.2 Collector design and modelling

4.2.1 Design of a prototype collector

The collectors are prototypes based on the commercially available type COBRA AK2.8V of company Soltop AG. The draining capabilities were improved by two measures:

- The straight sections of the meander are not in parallel but have an angle of 4° in between, as shown in Figure 16.
- The collector array is tilted by 0.5° to allow draining of the headers.

To keep the effort to produce the prototype as small as possible, the header dimensions of 20 mm inner diameter were not reduced. Therefore, the flow velocity will be much too small for complete deaeration. This will be discussed in the sections 4.3.1. and 4.3.2.

Because the average distance of the meander tubes is increased due to the spreading by 4°, the efficiency of the collectors will be slightly lower compared to a collector with parallel meander pipes.

The four collectors are connected in C-configuration, i.e., inlet and outlet are on the same end of the collector array (see Figure 51). The collector with largest distance to the connections of the array was oriented in such a way that the meander enters the upper header pipe at the very end of the header. By

this, the whole header pipe is flowed through and partial stagnation due to dead header pipe segments in this collector is avoided.
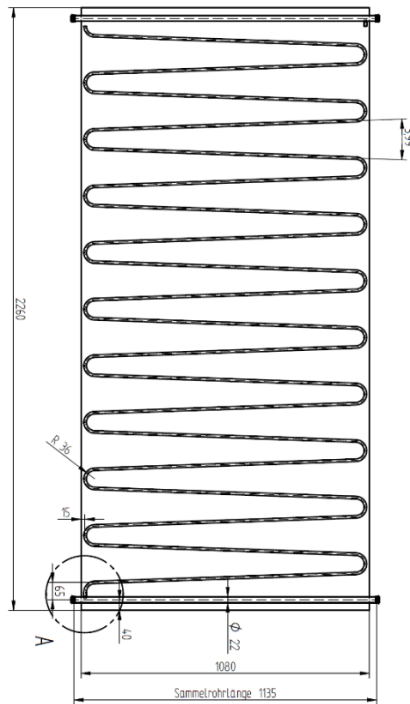

Figure 16: Drawing of the collector absorber with inclined meander pipe.

4.2.2 Empirical collector model

The efficiency factors of the original collector need to be altered according to the changes made for the prototype. This is done with SimCol (FHNW), a simulation tool based on the analytical collector model by [30] and [31], enhanced by correlations for the absorber edge-effect [32], and for the heat transfer across inclined gaps with non-isothermal boundaries [33]. Table 17 shows the efficiency coefficients of the original collector and the prototype collector, as well as the dry stagnation temperature and the temperature from solving Equation (1) for $\dot{q}_u = 0$.

$$\dot{q}_u = G\eta_0 - a_1\left(T_{fav} - T_a\right) - a_2\left(T_{fav} - T_a\right)^2 \tag{1}$$

Table 17: Collector efficiency coefficients and stagnation temperatures.

Coefficients			Collector type	
		Unit	Original	Prototype
Average tube distance		mm	90.2	102.5
Zero-loss coefficient	η_0	-	0.857	0.849
Heat loss coefficient	a_1	W/Km^2	4.160	4.160
Heat loss coefficient	a_2	W/K^{2}m^2	0.0089	0.0089
Dry stagnation temperature at 1000 W/m^2 and T_a = 30°C			195	195
Zero gain temperature at 1000 W/m^2 and T_a = 30°C				179.3

4.2.3 Transformation of the empirical collector model into a cylindrical model

To derive a one-dimensional cylindrical model suitable for TRACE, it is necessary to linearize the empirical model according to [34], based on a weighted average of the dry stagnation and zero gain temperatures.

$$T_S = 0.35 \cdot T_{\dot{Q}_u=0} + 0.65 \cdot T_{S,dry} \tag{2}$$

Solving Equation (1) for zero gain and using the parameters representing stagnation conditions, i.e. G_S = 1000 W/m^2 and $T_{a,S}$ = 30 °C, results in the average absorber temperature for zero gain, $T_{Qu=0}$. The stagnation temperature of a dry, stagnating absorber under the same conditions, $T_{S,dry}$, is taken from the test report. The useful gain related to the absorber area is formulated as a linear function,

$$\dot{q}_u = G\eta_0 - U_L \left(T_{fav} - T_a \right) \;, \tag{3}$$

where the heat loss coefficient is defined by evaluating the linear model for zero gain.

$$U_L = \frac{G_S \eta_0}{T_S - T_a} \tag{4}$$

Figure 17 shows the efficiency curve of the empirical model, dashed line, and the efficiency according to the linearized model.
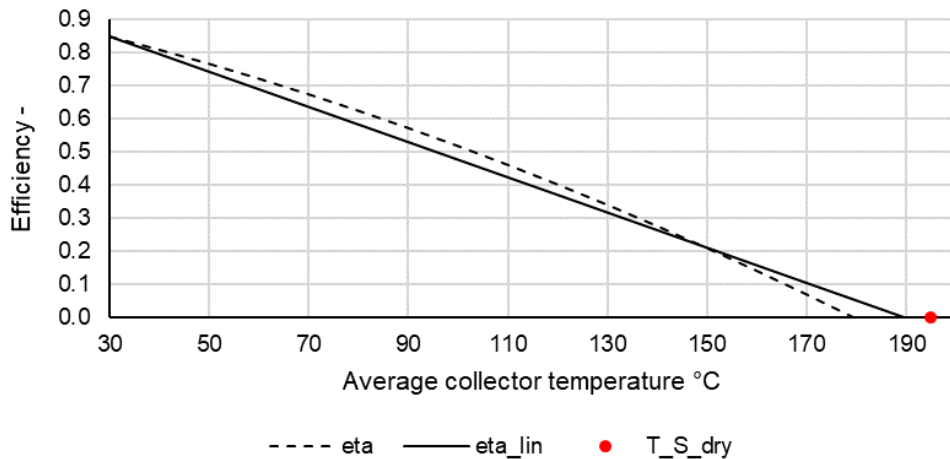

Figure 17: Comparison of the empirical and the linearized model of the prototype collector.

Both the header regions and the meander region of the absorber are represented by a cylindrical model, as shown in Figure 18, consisting of a pipe and an insulation layer.
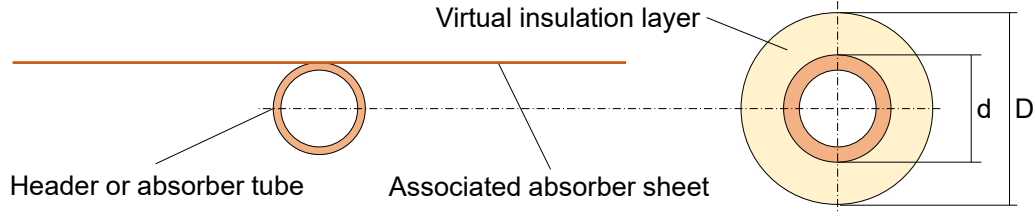

Figure 18: Representation of a tube-and-sheet absorber by a cylindrical model.

The mass of the absorber sheet and the associated tube are combined into a single virtual tube. The outer diameter of the insulating layer is determined so that the sum of all outer surfaces is equal to the absorber area. To simplify, the pipe temperature is set equal to the fluid temperature. This allows to define the heat conductivity of the virtual layer associated with the absorber region, X, as a constant. The radiation boundary condition is not defined directly but indirectly via the temperature of the outer surface at stagnation conditions,

$$\dot{Q}_u = 0 = GA\eta_0 - U_L A\left(T_{p,S} - T_{a,S}\right) \quad \Rightarrow \quad T_{p,S} = T_{a,S} + \frac{G\eta_0}{U_L} \tag{5}$$

The useful gain expressed by heat conduction in the virtual layer is,

$$\dot{Q}_{u,X} = \frac{\lambda 2\pi l_X}{\ln\left(D_X/d_X\right)}\left(T_{p,S} - T_a\right) . \tag{6}$$

Combination with Equation (5) yields the heat conductivity,

$$\lambda_X = \frac{G_S A_X \eta_0}{2\pi l_X \left(T_{p,S} - T_a\right)} \ln\left(D_X/d_X\right) \tag{7}$$

The results of this analysis are listed in Table 18.

Table 18: Physical data of the prototype absorber and the TRACE model.

Parameter		Unit	Total	Headers	Absorber tube
Absorber area		m^2	2.435	0.17	2.265
Sheet thickness		mm	0.5		
Length	Prototype	m		1.135	25.178
	Model	m		1.135	23.220
Inner diameter		mm		20	9
Outer diameter	Prototype	mm		22	10
	Model	mm		22.86	11.95
Specific heat conductivity	Model	W/Km^2		0.0156	0.0773

4.2.4 Flow and temperature distribution

The collector is modelled using HYDRA, based on the efficiency parameter from section 4.2.3 and the geometry data of the absorber. All stationary calculations were done for an irradiance of 1000 W/m^2 an inlet temperature of 50 °C and an area specific flow rate of about 31 l/hm^2.

Figure 19 shows the flow rate distribution. Due to the large header diameter the pressure loss is very small. Consequently, its influence on the flow distribution is practically negligible, and the exit temperature distribution will be almost uniform.
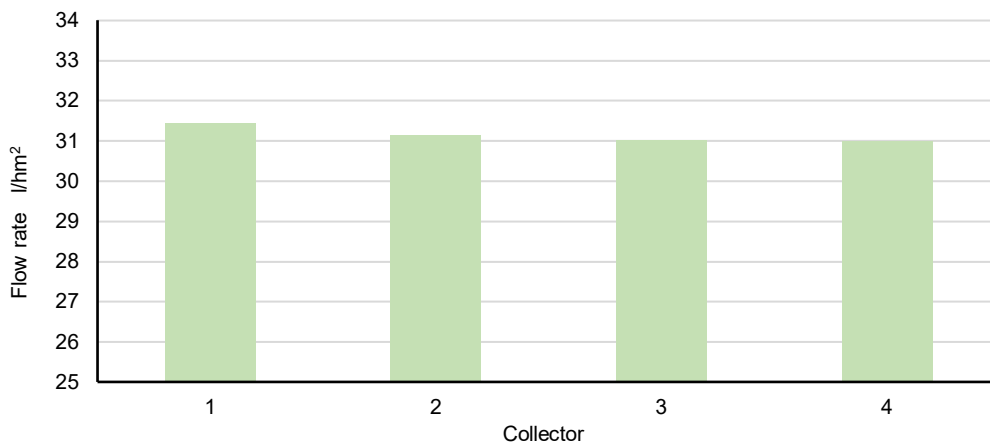

Figure 19: Flow rate distribution for an average flow rate of 31 l/hm^2. Header pipe inner diameter 20 mm.

With systems that are operated with water, it must be guaranteed that the pipes are installed with a downward slope. For this reason, the collector arrays will be rather short, and consist of a few collectors only. This would allow to decrease the header pipe diameter considerably. Figure 20 shows the flow distribution for a header inner pipe diameter of 13 mm. The effect on efficiency is far below 1% and therefore negligible.
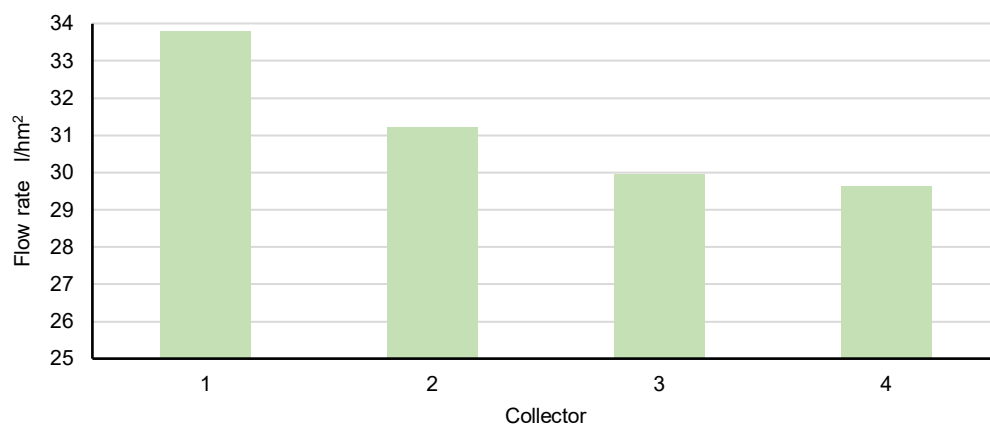

Figure 20: Flow rate distribution for an average flow rate of 31 l/hm^2. Header pipe inner diameter 13 mm.

However, the inhomogeneity of the flow distribution will cause a corresponding temperature distribution. It must be confirmed that the maximum collector outlet temperature is well below the saturation

temperature so that partial stagnation will not occur. In the present case, as shown in Figure 21, the maximum deviation from the average temperature at the collector field is negligible.
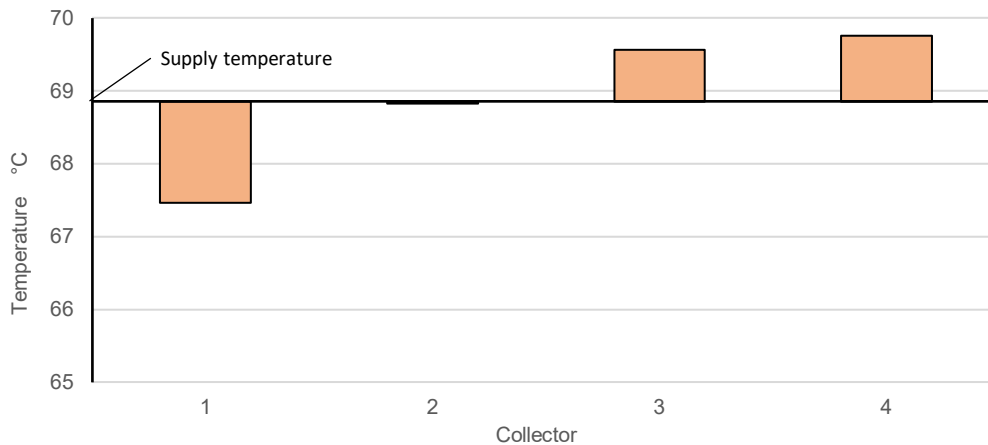

Figure 21: Corresponding temperature distribution for irradiation of 1000 W/m^2 and inlet temperature of 50 °C. Header diameter 13 mm.

4.3 Stationary, single-phase operation

4.3.1 Dimensioning of pump and flow resistance

Choice of pipe diameter and pump type are based on the following requirements:

- The flow velocity in the downward leading supply line must exceed the self-venting velocity. The pump should be applicable for multi-family houses of up to 3 levels height, i.e., about 12 m circuit height.

- To avoid under-pressure and/or vaporization at the summit of the circuit, the flow resistance in the supply line must compensate the static head of the liquid column above the drainback vessel. To be at the safe side, the pressure at the summit should be around 0.2 bar above atmospheric pressure.

Both requirements can be lessened by placing the drainback vessel at a higher position, as is illustrated in Figure 22 b). However, this might not be possible in an existing building. Therefore, it was decided to investigate solutions where the storage tank also constitutes the drainback vessel as shown in Figure 22 a).
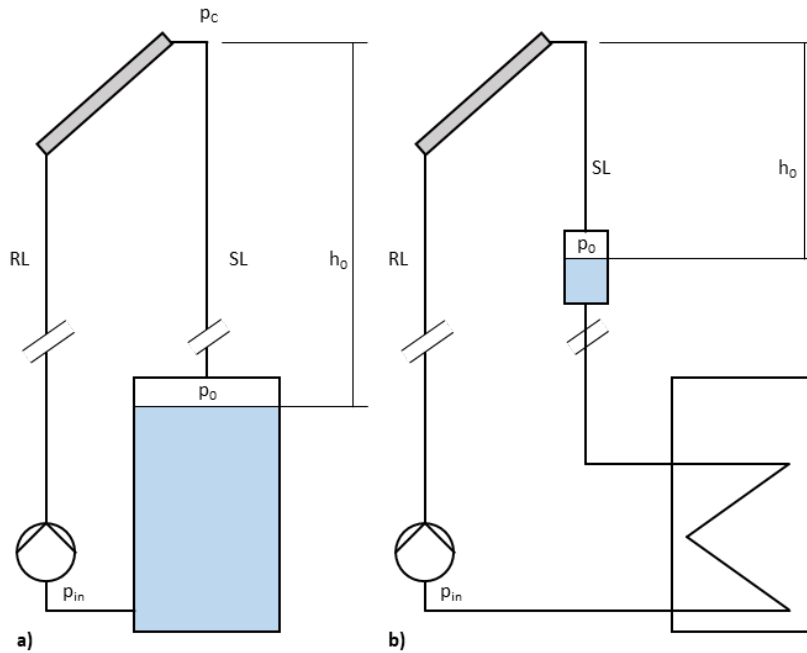
Figure 22: Drainback systems with a) combined DB and storage tank b) detached DB vessel.

Based on practical considerations, a plastic pipe with an inner diameter of 12 mm and a wall thickness of 2 mm was chosen for the solar loop, except for 1 m stainless steel pipe at the connectors of the collector field. In the lab demonstrator, the circuit height is 15.2 m.

Based on a detailed scheme of pipe routing (see Annex: Figure 72 and Figure 73), the system was modelled using the latest version of THD. For details of the circuit modelling and the operation parameters see Annex B, Figure 64. Some manufacturers of DB-systems achieve the required pump head by serial connection of two standard impeller pumps. This solution was discarded because of too high costs. Instead, a single stage regenerative turbine pump of the type SPECK Y-2340-SR was chosen (dimensions of circuit and pump characteristic see Annex, Figure 65 and Figure 66). The actual characteristic was determined from a later experiment in the lab, where the pump speed was set by a control signal of 3 V, resulting in the operational diagram shown in Figure 23.
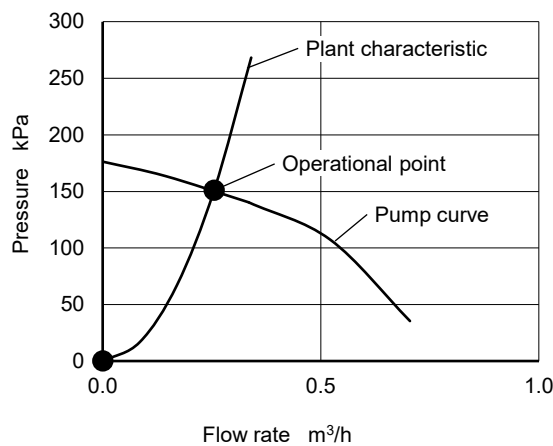

Figure 23: Pump and plant characteristics.

To avoid cavitation and to ensure efficient operation the following pressure conditions must be met:

- In all operational states, the pressure at the pump inlet must be higher than the minimum pressure needed to avoid cavitation.

- In all operational states, the pressure at the collector outlet must be well above the saturation pressure so that partial stagnation is avoided.

These are the same requirements valid for pressurized systems. In drainback systems, however, they are more difficult to meet. Because of the phase boundary, the air is always saturated with vapour. Furthermore, absorption and desorption of atmospheric gases across the phase boundary takes place which also depends on pressure and temperature. Both phenomena affect the system pressure.

On the other hand, the filling and commissioning of a drainback system should be as easy as possible, i.e., without special requirements for the initial pressure. Therefore, atmospheric pressure was taken as the initial pressure upon commissioning. Consequently, the required pressure at the collector outlet must be generated by a flow resistance in the supply line, which compensates the gravitational pressure of the corresponding water column.

Figure 24 shows the pressure profile along the circuit. The dashed line corresponds to the virtual state of a pressurized circuit where the liquid content is at rest. For a temperature of 20 °C, the flow rate is 26 l/(hm^2). The markers indicate the junctions between components, pump, and pipe sections. The first junction is the connection to the storage tank. The pump increases the pressure by 1.5 bar. Downstream of the pump, the pressure decreases due to friction and the increasing height. In THD the collector array is represented as a single component with the length of the array. The pressure at the exit of the collector array is about 0.35 bar. Further downstream the pressure increases again because the increase of gravity pressure dominates the friction. At the end node of the last pipe section a flow resistance with a drag coefficient of $\zeta = 600$ is modelled. In the experimental setup this resistance is realized by a control valve. By passing the valve, the pressure drops to the level of the pressure of the storage tank 1.6 m below the gas phase above the water level. Without the flow resistance, the pressure at the summit of the circuit (upper collector header) would drop to the vapor pressure, which would cause partial stagnation.
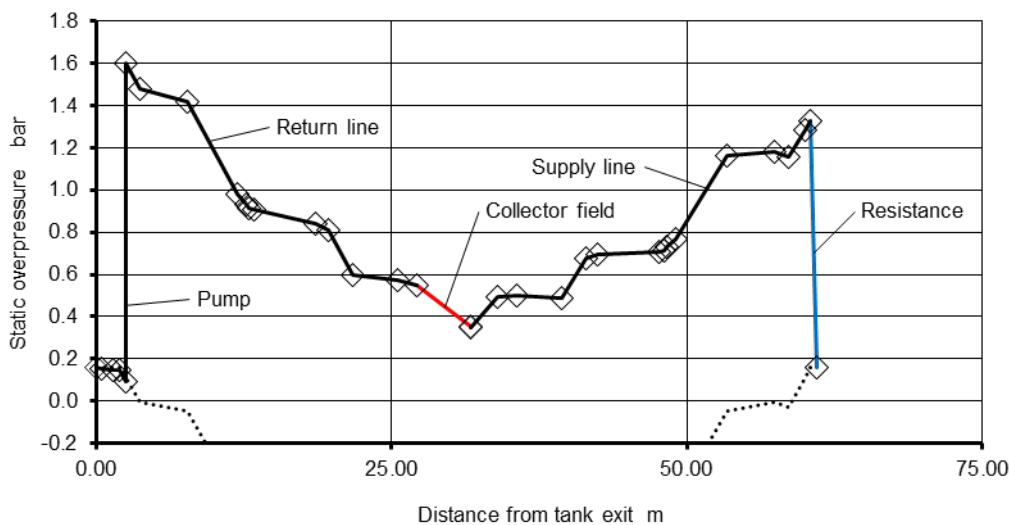

Figure 24: Pressure profile along the circuit.

4.3.2 Venting by flow forces

After the pump starts, the circuit is filled with water while the air is displaced via the supply line into the drainback vessel. In all pipe sections the flow velocity must be sufficiently high so that air pockets are swept away by flow forces. The velocity where this criterion is met is called self-venting velocity. It depends not only on the geometry of the pipe but also on the fluid properties. It should be mentioned at this point that the knowledge on self-venting is still sparse compared to other two-phase flow phenomenon, especially for pipe diameters below 50 mm and inclination angles larger than 20°. As part of his master thesis, Dällenbach [35], as cited in [36], derived a correlation between the Froude number, the Morton number, and the inclination angle, Φ.

$$\mathrm{Fr} = \frac{w_{sv}}{\sqrt{gd}} = \left[0.8\,\mathrm{Mo}^{0.0392} \sin\left(1.96\phi\right) + \mathrm{Mo}^{0.0213} - 0.075 \right] \tag{8}$$

The Froude number in equation 8 contains the self-venting velocity w_{sv}. To vary the fluid properties at room temperature, two sets of experiments using water and a water-glycol mixture were conducted. This allowed to express the effect of fluid properties on the self-venting velocity by the Morton number which is a function of the fluid properties (see Equation 9). Figure 25 shows the self-venting velocity of water at different temperatures in a 16 mm and a 20 mm pipe. The self-venting velocity is highest at inclination angles around 45 °, because around this angle, buoyancy drives the gas pockets to the pipe crest where the flow velocity is smaller than in the centre region. Thus, the gas pockets are less easily displaced by the water flow. In a vertical downward flow, gas bubbles located near the wall are driven towards the pipe axis by the so-called lift-force [37]. Therefore, the gas bubbles tend to stay near the axis where the local velocity is highest. As a result, the self-venting velocity in a vertical pipe is smaller than in an inclined pipe. It can also be seen that the velocity decreases with increasing temperature. This can be explained by the Morton number, Equation (9), because the fourth power of viscosity decreases more rapidly than the third power of surface tension, while the density is practically constant.

$$\mathrm{Mo} = \frac{\mathrm{We}^3}{\mathrm{Fr}^2\,\mathrm{Re}^4} = \frac{g \cdot v^4 \rho^3}{\sigma^3} \tag{9}$$
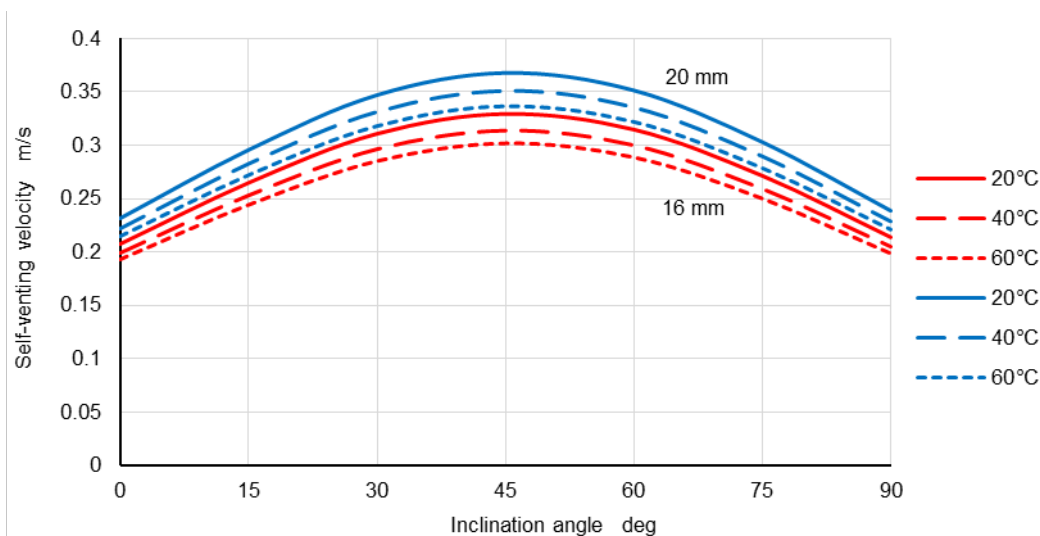

Figure 25: Self-venting velocity of water at different temperatures in pipes with inner diameters of 16 mm (red) and 20 mm (blue).

Figure 26 shows the flow velocity (black line) in the collector loop for a pipe with 12 mm inner diameter. The flow velocity is higher than the self-venting velocity (red line) in all sections of the circuit and in the

upper header of the first collector. Hence, self-venting of the collector loop is assured. Zero values indicate rising pipe sections where free gases are moved by buoyancy alone. The collector array is represented as a single component. Therefore, the velocities in the header of the second, third and fourth collector are not known. From the ratio of the flow velocity and self-venting velocity in the first upper header it can be concluded that the other upper headers will probably contain some air.
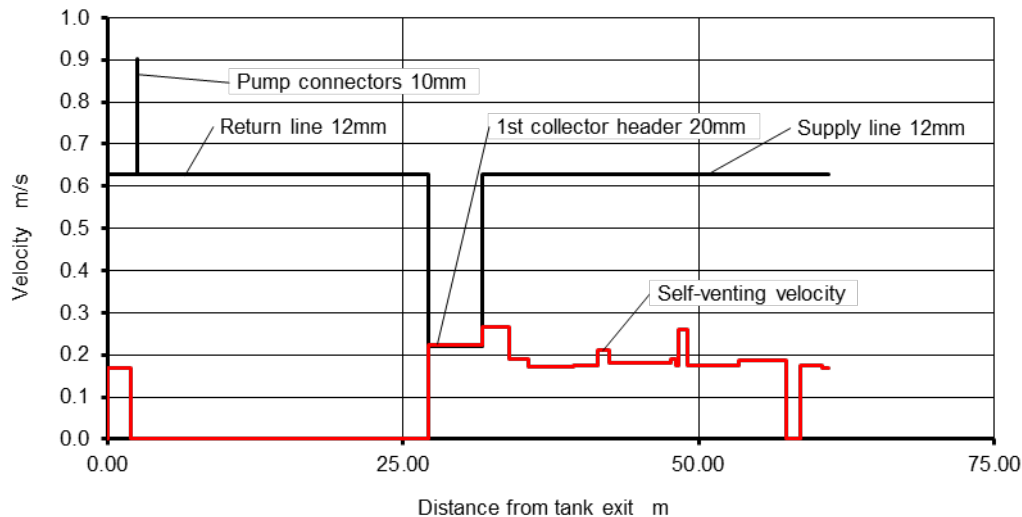

Figure 26: Flow velocity and self-venting velocity

4.4 Transients during filling, draining and stagnation

4.4.1 Modelling with TRACE

With the now known data for circuit and pump the DB-system was modelled for transient simulations using TRACE. Both the liquid phase and the gas phase are represented by three one-dimensional conservation equations for mass, momentum, and energy. The gas phase is modelled as a mixture of an ideal non-condensable inert gas, e.g., nitrogen, and water vapour. Absorption and desorption across the phase boundary are not modelled. Figure 27 shows the representation of the circuit using the graphical model editor SNAP (Symbolic Nuclear Analysis Package) [38]. The pump is modelled as a time dependent single junction, where the flow rate is defined in a table as a function of pump head. The valve, constituting a bypass, is opened to allow flow in both directions when the pump is off. The top of the storage tank and the supply line are connected by a venting pipe and a check valve with zero opening pressure. During pump operation, the pressure build-up in the supply line causes the check valve to close. As soon as the pump stops, the check valve opens due to the reversed pressure difference, and air enters the supply line.

The meander tube was modelled by a pipe with 200 cells and a corresponding heat structure according to Table 18. The inclinations of the header tubes and pipe sections were set in accordance with the design of the experimental setup.

In the present context the void fraction, ε, is defined as the volume ratio of the gas phase and the total volume of a pipe section defined by the cell in the TRACE model. A void fraction of 1 represents a section completely filled with gas.
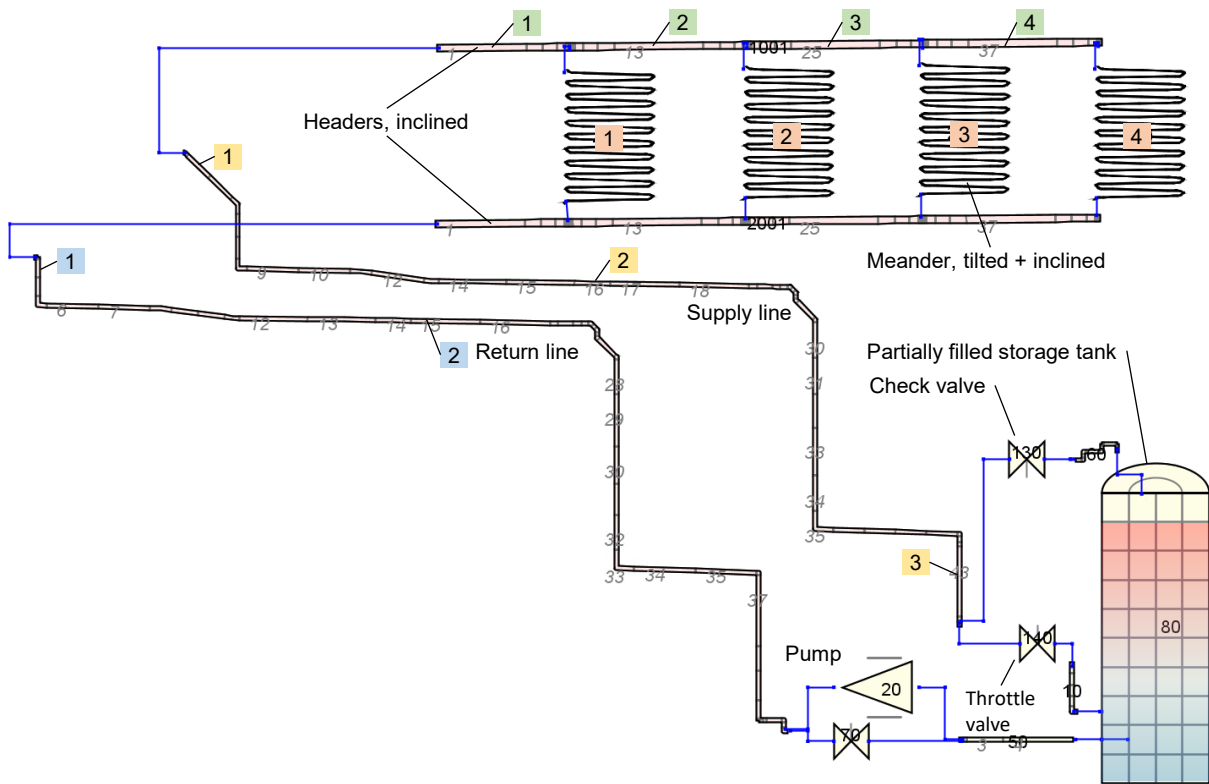
Figure 27: TRACE-model of the circuit.

To facilitate interpretation of the simulation results, the pipes were modelled with a monotonic slope, according to the design of the lab facility. However, the pre-insulated pipes used to set up the experimental system cannot be laid perfectly straight. In fact, from observations during the experiments, it can be concluded that sections with a slight counter-slope must exist, although the exact form could not be determined. Consequently, it must be assumed that these sections contain water from the previous operation.

4.4.2 Comparison between experiment and simulation

Simulations of venting and draining were performed under the same initial and boundary conditions as in an experiment. The experiment was conducted with the lab DBS on June 4, 2021. The pump was running at a comparatively low speed, which allows to discuss imperfect venting certain pipe sections. The initial pressure and temperatures were set according to the experimental data. The gas phase was assumed to be saturated with vapour. The non-condensable partial pressure was set accordingly. The storage tank was modelled as a 3-d volume of 1 m^3 with 10 axial layers, which are divided into two radial and four azimuthal sections. The initial volume of the gas phase of 100 l was set by defining a void fraction ε=1 within the uppermost layer. The global solar irradiation is 1000 W/m^2. The ambient temperature and the irradiance were defined by a table generated from experimental data.
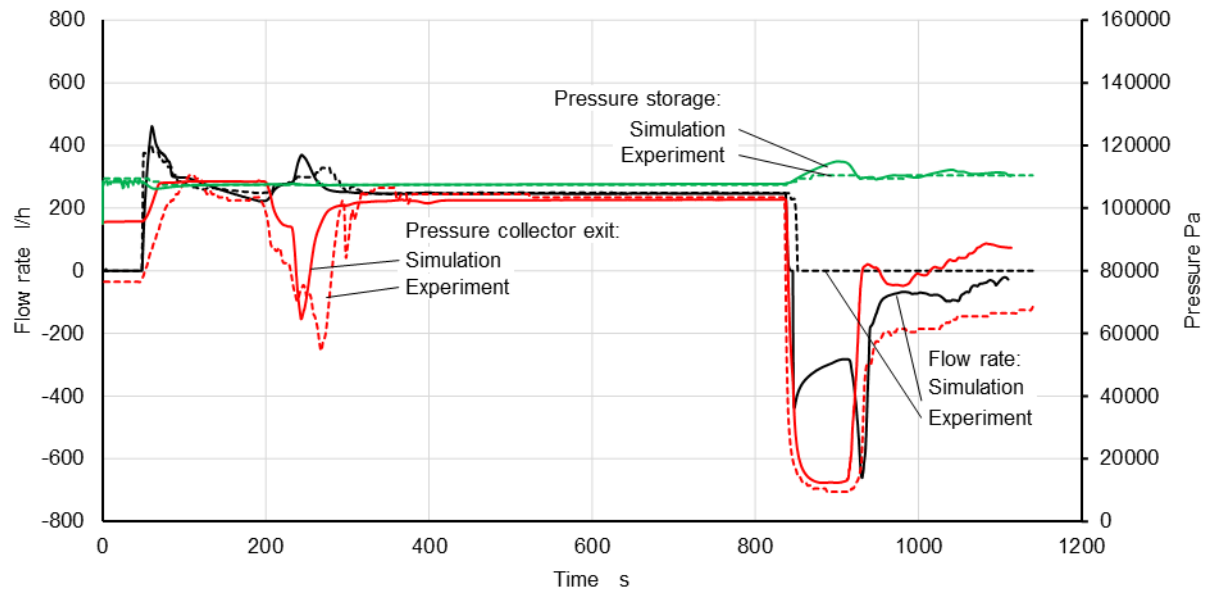
Figure 28: Measured and simulated flow rate and pressure at the collector exit and in the storage tank.

In the experiment, the pressure at the collector exits exhibits larger fluctuations than in the simulation. This is most probably due to imperfect pipe routing as explained in the section above. In general, the measured and simulated data for the flow rate and the pressure agree quite well. The draining is initiated by the pump stop at 840 s. As soon as the flow comes to a standstill, the pressure loss also disappears. As a result, the pressure at the collector outlet drops to a value which is defined by the current pressure of the gas phase in the storage tank, the height of the water column and the vapour pressure of the water within the collector: $p_{col} = \max\left(p_{DB} - \rho g h, p_v \right)$.

Due to hydrostatic imbalance caused by the air inside the storage tank, the water is accelerated in backward direction. The downflow of water in the return line, as shown Figure 28, is caused by a corresponding influx of air from the storage tank into the supply line. The experiment doesn't show this because the sensor measures only in positive direction. The main part of the draining process takes about 60 s. However, the downflow of water from the collector field through the supply and return line continues much longer. This downflow causes friction between the liquid and the gas phase. Therefore, the pressure within the collector rises only slowly towards the pressure of the gas phase in the storage tank.

As can be seen in Figure 27, the connecting point of the air venting pipe is lower than its local highpoint. Therefore, air can be temporarily trapped within the storage tank when, due to the pressure loss caused by the throttle valve, the height of the water level within the supply line rises above the connecting point. This is probably the main reason for the long draining time.

In the simulation, the initial pressure within the collector equals the pressure of the gas phase in the storage tank. In the experiment, however, the initial as well as the final pressure is about 20 kPa lower. This deviation can be explained by the imperfect draining, both in the preceding and the current experiment. Due to the counter-slope in the near horizontal parts of the supply- and return line, pressure can build up in the lower sections of the pipe, which prevents the water from flowing down. The pressure above the trapped water is lower by the pressure generated by the trapped water column. This situation is shown schematically in Figure 29.
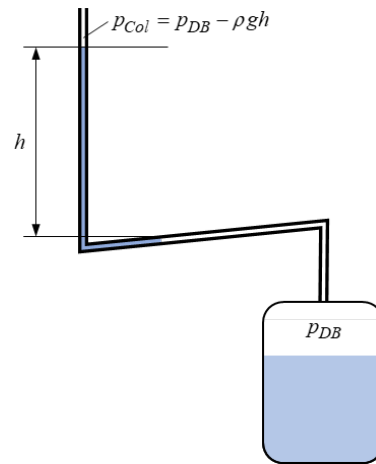
$$p_{Col} = p_{DB} - \rho g h$$

Figure 29: Pressure difference caused by trapped water

Figure 30 shows the liquid temperatures of the supply and return line near the collector inlet and exit, and the irradiance. The good match between the temperatures measured and simulated during operation of the collectors shows that the new linearized collector model (see section 4.2.3) is valid. Deviations might be caused by the heat capacity of the temperature sensor.
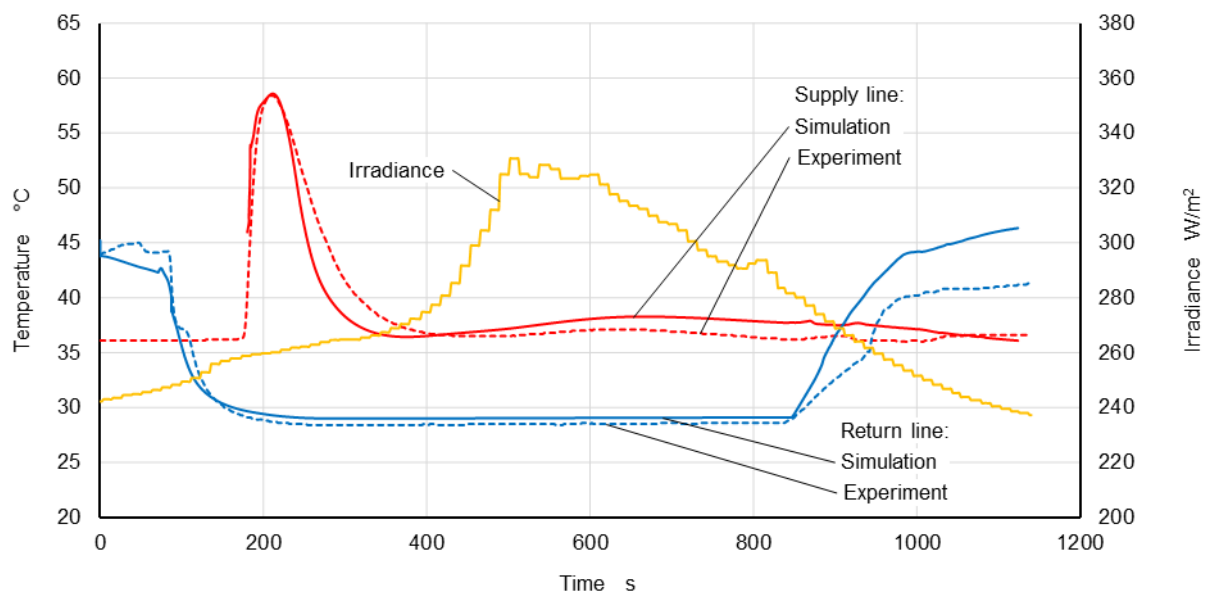

Figure 30: Measured and simulated temperatures and irradiance.

4.4.3   Filling and draining

To illustrate the filling and draining, a simulation over a time span of 600 s was carried out. The irradiance was set to zero and both the initial and ambient temperature was set to 30°C. The pump was started at 20 s and switched off again at 400 s. The mass flow and the pressure at different locations of the circuit are shown in Figure 31 and Figure 32, respectively. After the pump start, the mass flow first increases within a few seconds to its maximum. The return line is filled from below and the counter pressure of the growing water column increases, which causes the flow rate to decrease again. At about 150 s the water has reached the collector exit and starts to flow into the upper end of the supply line. Consequently, the

sum of the hydrostatic pressure in the liquid-filled part of the circuit decreases, which causes the flow rate to increase again. At 200 s the water has reached the vertical section of the supply line above the storage tank. Five seconds later the pressure in the upper header reaches its minimum of about 68 kPa. At the same time the water reaches the flow resistance. The pressure increases to a value of around 100 kPa while the flow rate drops to 0.07 kg/s. At 400 s the pump is switched off. Due to the hydrostatic imbalance created by the height of the gas volume inside the storage tank (in other words: the missing water column) the check valve opens and gas from the tank enters the supply line and rises towards the collector field against the downflowing water. Due to the forces between the rising gas bubbles and the water, the liquid mass flow in the supply line decreases sharply. Due to high interfacial friction, water is even driven in upward direction. Within about one second after the pump stop the flow direction in the return line is reversed. Almost the whole liquid content of the collector field is drained via the return line. Only a fraction of the liquid content of the upper header is drained via the supply line. This is in accordance with the experiments, where the draining via the return pipe can be derived by the temperatures at the flow and return connections of the collector field (see Figure 30).
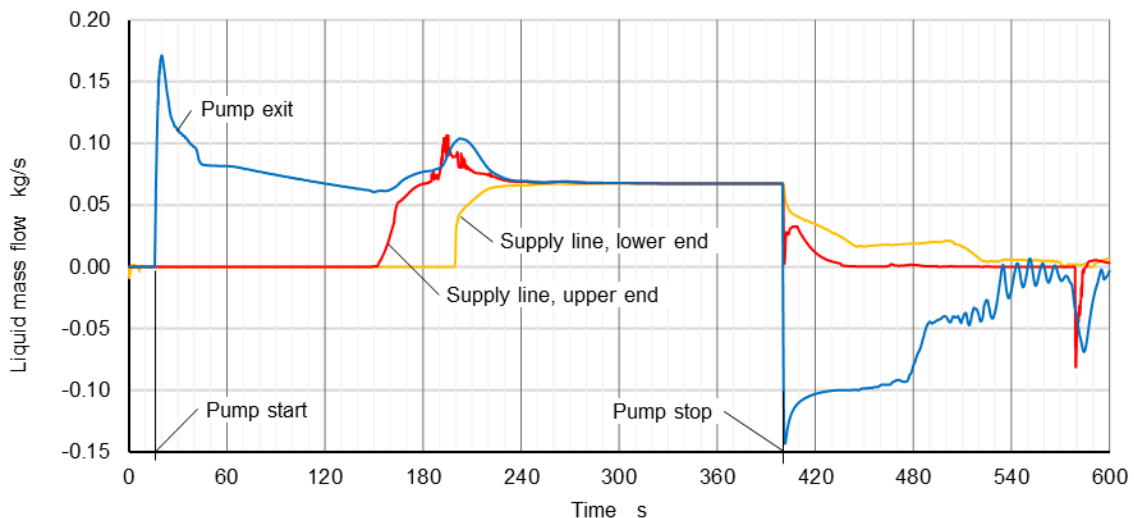
Figure 31: Mass flow at different locations of the circuit.

After the pump start, water displaces the gas content from the circuit into the storage tank. Due to the flow resistance at the exit of the supply line the gas content within the circuit is compressed while the gas volume within the storage tank is expanded by the same amount. Secondly, the warer level uin the tank decreases as the circuit is filled. Both effects cause a slight decrease of pressure inside the tank. After the pump stops, the pressure at the highpoint drops sharply and reaches a minimum corresponding to the vapor pressure, as can be seen in Figure 32.
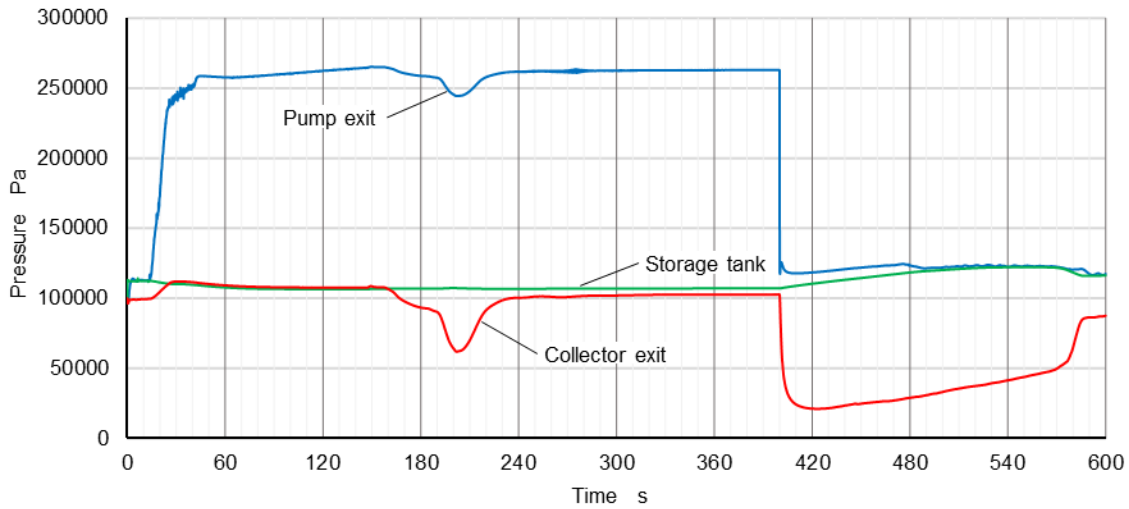
Figure 32: Pressure at different locations of the circuit.

After pump start at t=20s it takes about 130s for the water to reach the upper headers, and a further 150s to reach a stationary state. Figure 33 shows the void fraction within the header sections corresponding to the numbers shown in Figure 27. Self-venting is achieved in the first three headers and in the supply line. In the fourth header where the flow velocity is lowest, self-venting is not achieved, which is indicated by a void fraction larger than zero. Apparently, the interfacial friction is too low to mobilize the gas volume. However, the venting of the meanders is not affected, as can be concluded from the uniform increase of the meander content and the equality of their maximum value.
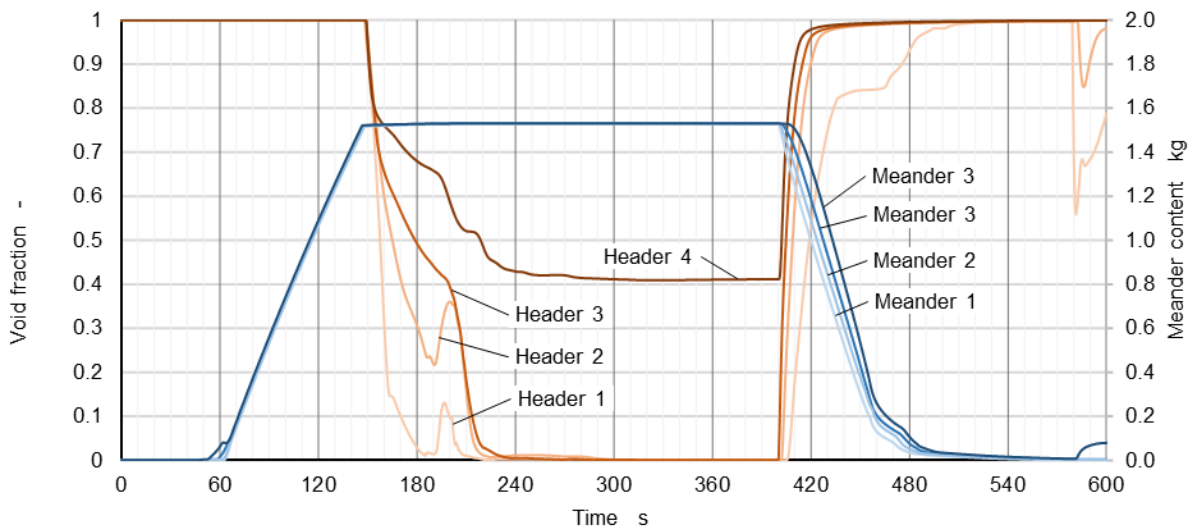
Figure 33: Void fraction within sections of the headers and the content of the meanders.

Figure 34 shows the void fraction at the inlet and in the vertical section of the supply line above the throttle valve. At t = 240 s the vertical section is nearly filled. A two-phase flow with a low gas content is present up to t=320 s, after which the void fraction drops to zero and a single-phase flow is established. Shortly after pump stop at t = 400 s air enters and nearly fills the upper header (see Figure 33). A fraction of the water inside the supply line is carried upwards by the air flow and starts to enter the upper header at t = 440 s, which can be seen from the sharp decrease of the void fraction.

Figure 34: Void fraction within the supply line.

4.4.4 Stagnation

In solar drainback systems, similar phenomena occur during stagnation as in non-drainback systems. After draining, some water remains within the headers and the meander 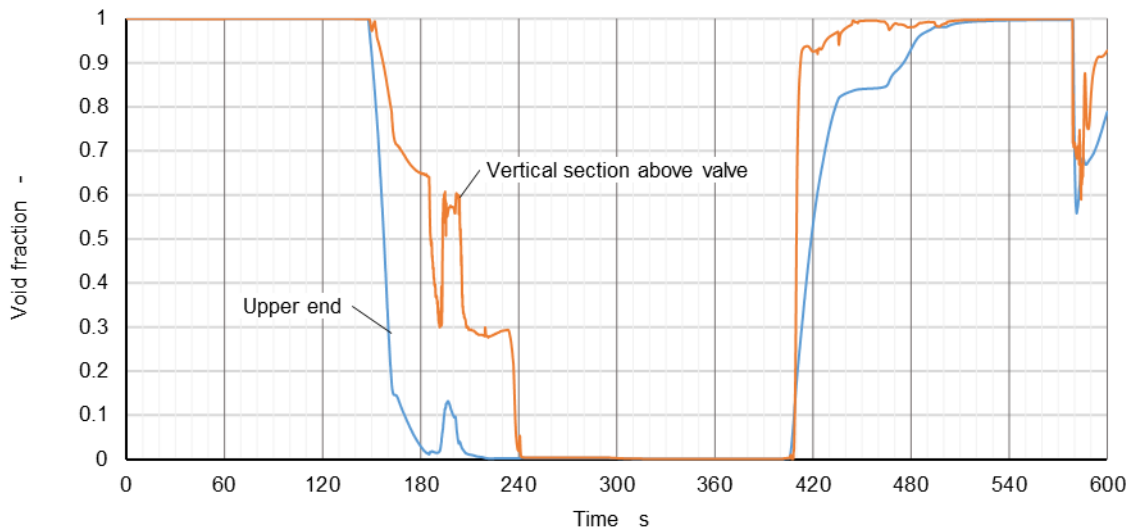tubes. Upon reaching the boiling point, the residual water begins to evaporate. The enthalpy flow of the steam is a function of the saturation temperature and the wetted fraction of the absorber. The steam enters the circuit and compresses the gas content in the supply and return lines, and in the storage tank. The pipe walls are heated up by the condensing steam.

To illustrate the stagnation processes the simulation time was increased to 1800 s and the initial temperature of the water content of the storage tank was set to 80 °C. The ambient temperature and the initial temperature of the collectors and the pipes was set to 30°C. The irradiance is 900 W/m^2. The pump is switched on as soon as the collector temperature exceeds the storage tank temperature by 6 K. After 600 s the pump is switched off and stagnation begins. The main simulation results shown in Figure 35 are interpreted as follows.
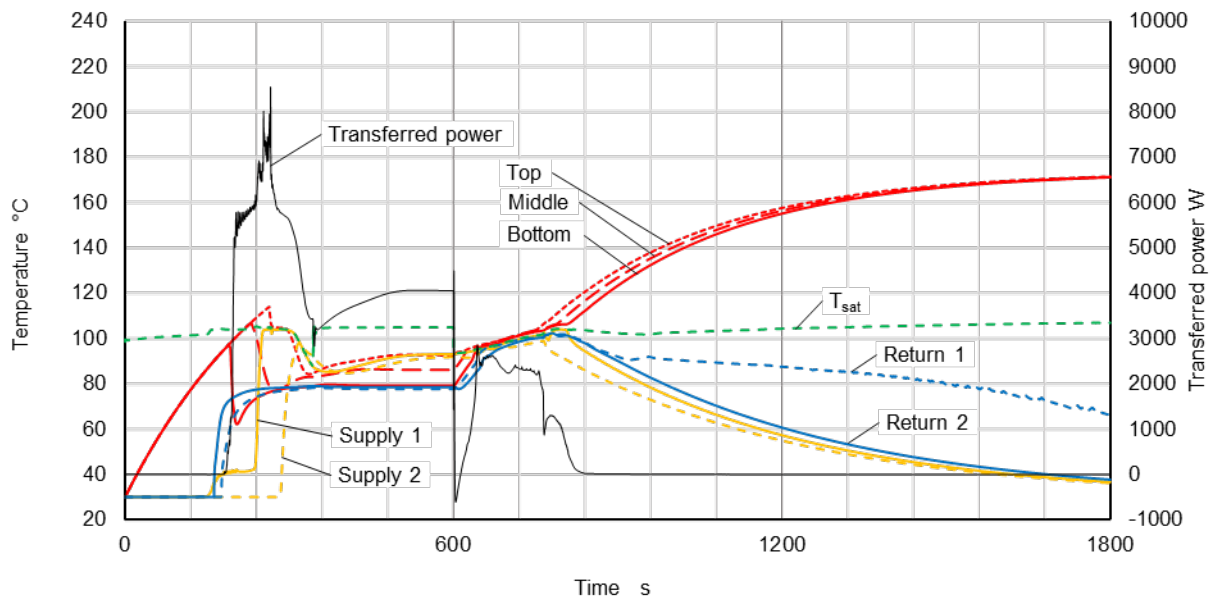
Figure 35: Temperature of the meander tube and in the supply and return lines. Total transferred power across the inner pipe wall of the meander tube.

The red lines show the temperatures of the nodes 5, 100 and 195 corresponding to the top, middle, and bottom section of the meander tube. The absorber temperature rises until water reaches the respective section. The temperature drops sharply while the accumulated heat is released into the water. The top section of the absorber reaches a temperature above the saturation temperature. Flow boiling occurs as the water enters the overheated regions, which causes the peaks in the transferred power. At t=240s the water enters the supply line in saturated state until the initial overheating of the absorber is carried away.

At 600s the pump is switched off. The pressure drops and the water within the collectors immediately starts to evaporate. This is indicated by the small peak of the transferred power, which is followed by a sharp decrease to a value below zero. The sharp decrease can be explained by the backflow of hot water from the upper regions of the absorber into regions with lower temperature. Therefore, for a short while, thermal power is transferred from the water into the meander tubes. Due to this process and the continuing irradiation, the absorber temperature increases and eventually reaches saturation conditions. In the meantime, the transferred power reaches a second local maximum, and subsequently decreases until it reaches zero at about t = 840 s. During this time, the residual water evaporates. The temperature of the top, middle and bottom node rises slowly until dry out is reached. After that, the supply and return line are no longer heated by condensing steam, and the temperature decreases while the absorber temperature rises to the stagnation temperature.

Due to the large gas volume in the system of more than 100 l, the pressure increase is very moderate, which is shown in Figure 36. Consequently, the saturation temperature stays low. Such a large air volume seems to be uneconomical. However, reducing it will result in a higher pressure and therefore higher saturation temperature.
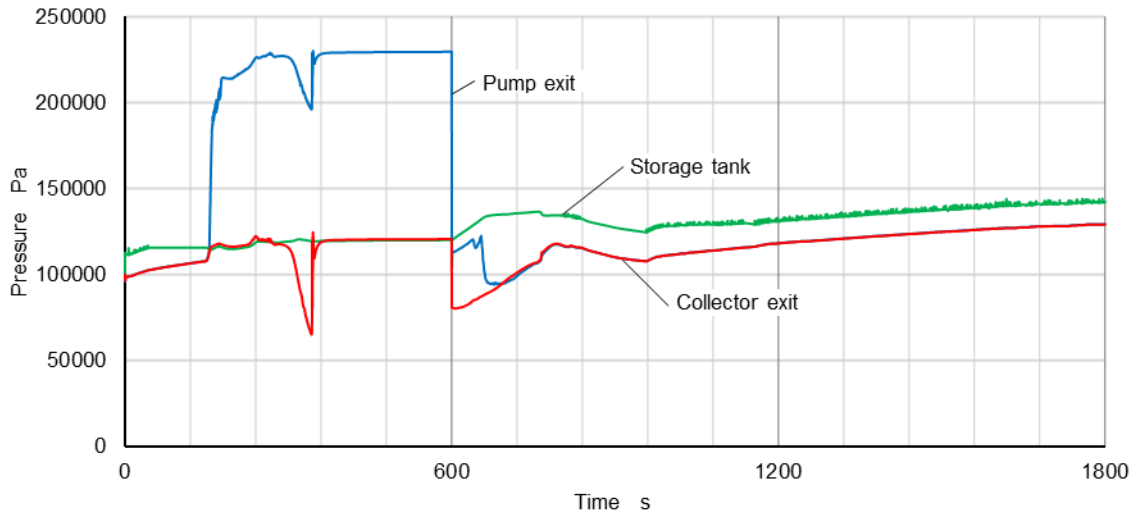
Figure 36: Absolute pressure transients for an initial gas volume of 100 l in the storage tank.

4.5 Effect of dissolved gases on the pressure

Another influence on the differences of experiment and simulation shown in Figure 28 might be attributed to gas solubility. The aim of this section is to determine whether the effect of nitrogen solubility on the system pressure must be accounted for. The solubility of gases in liquids is expressed by the volumetric solubility parameter, λ_i [39].

$$\lambda_i = \frac{V_{i,N}}{m_l\, p_{i,N}} \text{ in the units } \frac{\text{m}^3}{\text{kg} \times \text{bar}} \tag{10}$$

$V_{i,N}$ is the volume of the dissolved gas whose partial pressure at the liquid surface is equal to the norm pressure, $p_{i,N} = 1.013\,\text{bar}$, at the norm temperature, $T_N = 0\,°\text{C}$. Figure 37 shows the volumetric solubility of nitrogen in water, based on the data of [40].

Figure 37: Volumetric solubility of N_2 in water.

A two-phase circuit with increasing temperature in a constant volume was modelled using VBA under Excel and simulated using parameters shown in Figure 67 in Annex B. Figure 38 shows the 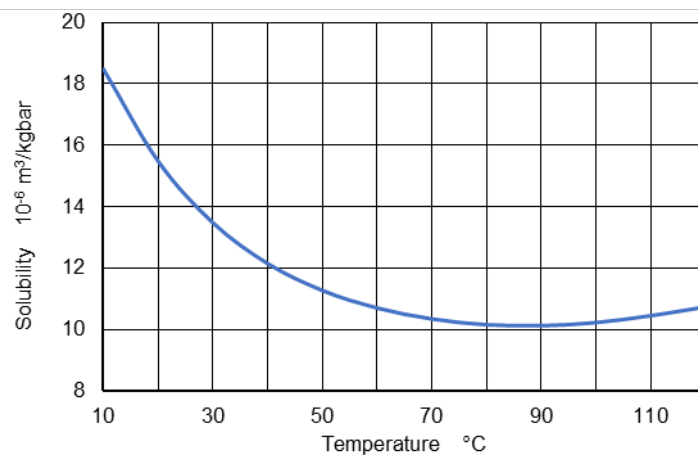simulation results for water, which was assumed to be saturated with nitrogen at time 0 s. Without desorption, the pressure depends only on the vapour pressure of water, the increase of pressure of the gas itself due to the temperature increase, and the free amount of nitrogen being compressed by the thermal expansion of liquid. With gas desorption, the pressure increase is much higher. This phenomenon reduces the danger of underpressure at the summit of the solar circuit considerably. On the other hand, the saturation temperature (evaporation temperature) of the water rises also, which might be a problem when using plastic pipes for the circuit.
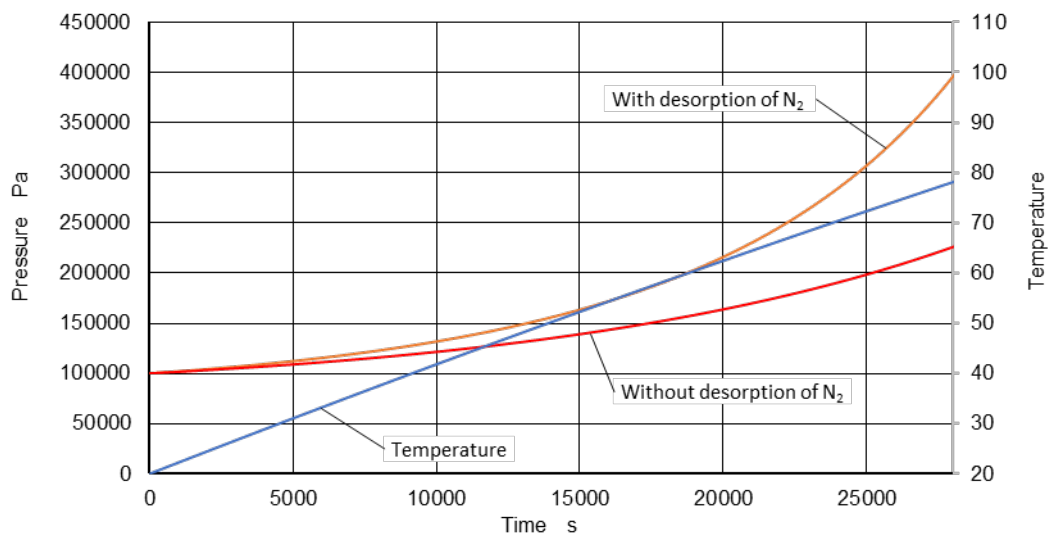
Figure 38: Effect of nitrogen on the system pressure as a function of temperature
(water saturated with N_2 at t = 0 s).

4.6 Design procedure for collectors and circuits of drainback systems

The design of a drainback system is the engineering task of the manufacturer, who must determine the specifications and operating conditions through calculations and simulations. The results must be presented in a way that allows the installer to build and commission a system without errors.

The first part of system design is always the thermodynamic sizing and cost assessment using appropriate software tools like Polysun.

The second part encompasses the dimensioning of the absorber tubing, the pipe network, and the pump. Furthermore, self-venting of the collectors and of solar circuit sections exposed to ambient if water is used as HTF must be proven. To ensure an absolute system pressure > 1 bar at the collector outlet, the necessary flow resistance in the supply line must be designed. Because energy and momentum equation have to be solved at the same time, a thermohydraulic approach is needed.

The thermohydraulic design requires the following steps:

1. Specify the mass flow related to the collector area, corresponding to the intended operation of the system (high- or low-flow).

2. Design the collector absorber tubes and the header tubes continuously inclined so that they can be drained by gravity.[7]

3. Determine the pipe diameters inside the collector with an absorber model using e.g. HYDRA [27] or Absorber-Master [41]. The pipes should be small enough to enable self-venting at low flow rates.

4. Model the collector array with the maximum desired number of absorbers connected in parallel via manifolds. Set the specified flow rate and calculate the flow- and temperature distribution at 1000 W/m^2 irradiance. Prove the following and adjust the pipe dimensions if necessary:

   - Self-venting is achieved at least in the upper header pipe at the connection of the flow pipe.

   - The maximum collector array outlet temperature should exceed the average temperature by less than 5 K to avoid local stagnation conditions in the collector field when running at high temperatures.

5. Model the whole circuit using THD. Choose a pipe diameter for the circuit that guarantees self-venting. Identify the largest height difference between drainback tank and the highpoint of the collector field. Choose a pump whose stagnation head is about 2 m higher than the height difference. Set the minimum return temperature, e.g. 20 °C and run simulations using 0 W/m^2 irradiance and atmospheric pressure in the drainback tank as boundary conditions. Vary the pump model and the flow resistance at the lower end of the supply line until:

   - the desired flowrate is reached and,

   - the pressure at the highpoint of the collector is around 0.2 bar above atmospheric pressure.

With these settings, the dimensioning is on the safe side regarding normal operation. However, there are additional steps to prove safe operation.

6. Proving operational safety requires the following steps. These steps are interdependent and therefore cannot be processed sequentially.

   - Choose a safety valve with a response pressure corresponding to the maximum allowed system pressure which defines the saturation temperature.

   - Choose a drainback vessel with an initial gas volume so that the maximum pressure during stagnation stays well below the response pressure of the safety valve.

   - Choose a pipe insulation with a sufficiently high heat loss coefficient so that the pressure stays below the response pressure of the safety valve.

   - Choose a piping system that can withstand the maximum pressure and the associated saturation temperature.

   - Choose a pipe insulation material for the pipes near the collector connections that can withstand the maximum temperature of the pipe wall which can be set to the maximum saturation temperature.

---

[7] If water is used as HTF: remaining water in the headers e.g. near the pipe connection is not problematic in winter (freezing) as far as the pipe's cross section is nowhere filled completely with water.

4.7 Conclusions and outlook

4.7.1 Model validation

The system code TRACE has proven very useful to realistically model genuine features of drainback systems. The dataset of the simulation results contains the time evolution of the state variables of each node, which provide deep insights into the transient processes.

In general, the simulation agrees quite well with the experiment. The deviations are due to model imperfections but also due to circuit geometries (imperfect pipe laying) that could not be reflected properly in the model design. One of the more fundamental uncertainties arise from solubility of atmospheric gases in water, which is not modelled in TRACE. It was shown in section 4.5 that the effect of gas solubility should be taken into consideration. This is also pointed out by Rühling and Schabbach [7] who did the so far only experimental investigation in this field

4.7.2 Stagnation behaviour

In section 4.4.4 it has been shown that the effects of stagnation on temperature and pressure must also be considered in drainback systems. At least in the upper part of the circuit, temperatures far above 100°C may occur. This means that commercially available, cheap plastic pipes and fittings cannot be used in this part of the system. Furthermore, it is obvious that the pressure and the resulting saturation temperature are strongly influenced by the initial volume of the gas phase and the dissipation rate of the pipes.

4.7.3 Further work

The empirical collector model and thermohydraulic tools Absorber Master, HYDRA and THD are well suited for a preliminary dimensioning of components and the drainback system. However, for the dimensioning aspects that depend on the two-phase flow phenomena, additional tools are needed.

Derivation of a practical method to assess stagnation safety was beyond the scope of this project. This method would include the following models, which are to be calibrated by TRACE simulations and, where necessary, by experiments:

- Validation of the calculation of the residual amount of liquid within the absorber after draining.

- Time evolution of the enthalpy flow of the steam leaving the collector field.

- Condensation of steam in the supply- and return line in the presence of non-condensable gases.

- Absorption and desorption of non-condensable gases across the phase boundary, and its effect on the system pressure.

The residual amount of liquid and the time evolution of the steam enthalpy flow are the determining parameters for the maximum pressure and temperature [34]. These quantities do not only depend on the collector hydraulics and the dimensions and routing of the pipes but also on the volume of the gas phase, on the water content and on the dissipation capacity of the pipes.

Connections between pipes and fittings are usually not tight against underpressure, except metallic and brazed or soldered joints. It can be expected that, over time, the circuit builds up pressure due to repeated situations where underpressure occurs (e.g. each time the circuit is drained). On the other hand, circuits are also affected by diffusion of water through gaskets and other non-metallic parts of the circuit. This countereffect will lead to a corresponding decrease of pressure. Also, the possible disappearance of oxygen from the gas phase due to reaction with wall materials must be considered. These questions should be answered based on long-term monitoring of a well-documented operational drainback system.

5 Drainback system: design and experiments

5.1 Storage tank with integrated drainback volume

A solar storage tank was developed and tested in the lab. The design of the tank is based on the project ReSoTech 2 [11]. The aim is to keep the manufacturing costs low, to reduce the system components, and to enhance the thermal efficiency of the storage and of the solar collectors. The main characteristics of the storage are:

- The storage tank envelope is mainly made out of glass fibre reinforced polymers. This allows for a reduced weight, which is a relevant factor for the market [2], and for corrosion safety in the presence of gases (a possible issue for drainback-concepts).

- The design of the built-in components like diffusors or stratification devices has to be simple and low in price without leading to an operation that is disturbing stratification and thus, reducing the efficiency of the storage.

- Because water is used as heat transfer fluid in the solar loop, the solar loop can be connected to the storage directly with double ports (no heat exchanger needed).

- Due to the direct connection of the solar loop, the drainback volume can be integrated into the storage.

A consequence of the direct connection of the solar loop to the storage (without heat exchanger) is the possibility that air is coming down at start or during operation of the solar loop, causing disturbance of the stratified water layers inside the storage. Larger volumes of air that enter into the storage via the solar flow pipe are expected to disturb the stratification of the storage water ("whirlpool effect") and should be avoided. Hence, the behaviour of the two-phase flow during filling and operation was analysed with a simplified test rig in the lab at ambient temperatures.

5.1.1 Lab tests of storage inlet geometries for the solar drainback loop

The goal of the lab tests was to evaluate the effect of different devices in the storage on the stratification during and after refilling the solar loop with water and to find low-cost stratification devices that are also able to manage air that enters the storage via the solar flow port.

A rectangular storage made of sheets of glass and having one side non-insulated for visual observation was used for the experiments. The storage has a cross section of 0.64 m^2 and a water level of 1.59 m, which results in a total volume of approx. 1 m^3. The test arrangement was built in the lab without a collector and long pipes (Figure 39 a). However, as the volumes of the collector field and of the pipes of the solar loop are needed for the test, a mock-up volume of 23 litres was put in place. An electric heater within the solar loop emulation was used to mimic the heating of the collector. For draining, when the pump is switched off, a small pipe was mounted between the air volume at the top of the storage and the flow pipe. It was possible to close this small pipe with a hand valve.

Because the walls of the storage are made of glass that cannot be penetrated with pipes, all connections of external hydraulic loops had to be inserted via the storage top. Hence, all tested inlet geometries were attached to a vertical copper pipe with a 90° elbow at the end, which was installed inside the storage (Figure 39 b). The horizontal opening of this elbow was at a relative storage height of 56 % (storage bottom: 0 %).

Six temperature sensors (T3 to T9) were mounted inside the storage, equally distributed over the storage height. There were also sensors to measure the temperature of the incoming and outgoing water flow. The storage had no cover and thus a high heat loss at the top, which was measured in a test

without loading/unloading (Figure 40). The flow through the hydraulic loop and thus, the storage, was measured with a Coriolis mass flow sensor. It was possible to set this flow via a PID controller in order to ensure a constant load.

(a)   (b)
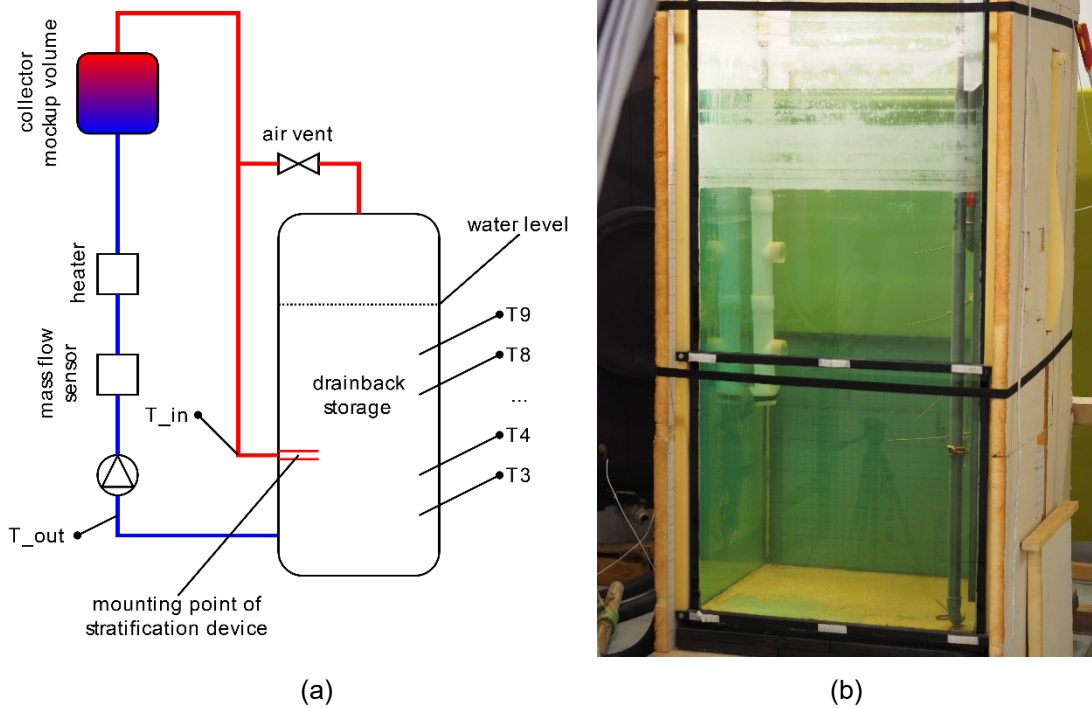
Figure 39: Drainback test arrangement. (a) Scheme of the storage and the collector loop emulation with a small tank (mock-up volume) representing the hydraulic volume of the collector field. (b) Side view into the storage with stratification device Type D (white pipe) inside the storage on the left.

Figure 40: Temperature decrease of the storage water due to heat loss to ambient. The lab storage was uninsulated at one side and had an open top (z: relative height of the temperature sensors from storage bottom, e.g. 27 % for T3).

Inlet geometries

Four different inlet geometries (Figure 41) for the connection of the solar flow pipe to the storage were analysed with experiments:
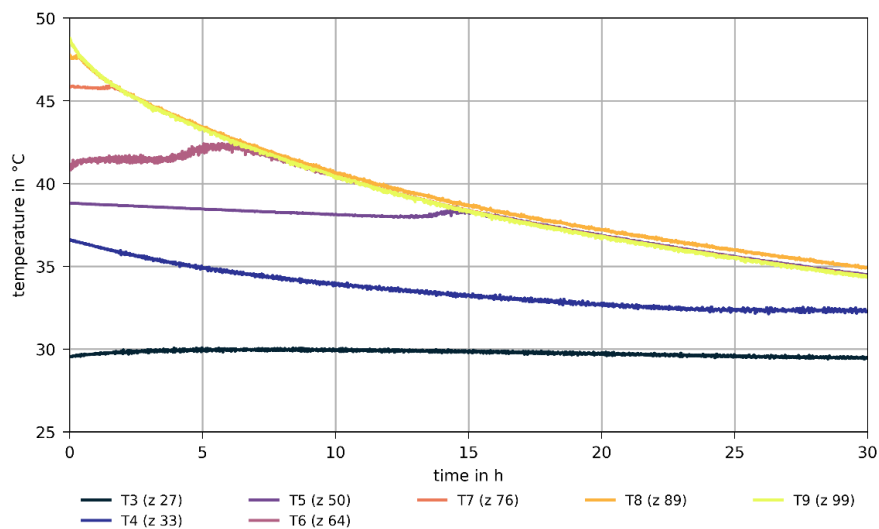
- Type A is the most basic version: a horizontal opening into the storage with an inner diameter of 1 inch (2.54 cm)

- Type B is identical with the basic inlet but has a funnel glued to a vertical pipe right above the inlet, which can lead air to the water surface without influencing the temperature stratification (funnel mounted: see Figure 39 b)

- Type C is an adapted version of Type A with an extension of the outlet diameter up to 60 mm (approx. 2.4 ") and a length of this extension of 100 mm.

- Type D is a market available stratification device from Solvis GmbH with four inlets. Each inlet has a passive shutter pad made of silicone that closes the inlet if the density of the water inside the device is lower (i.e. the water is warmer) than the one of the surrounding water.

The inlet for Types A to C is positioned at 56% of the filling height. The heights of the four inlets of the Type D device range from 66% up to 100% with distances between the openings of 26 cm.

For sizing storage inlets on medium heights of the storage, the design rules shown in Table 19 can be found in literature.

Table 19: Design rules for storage inlet geometries ([42] [43]).

Flow velocity	The cross section of the opening has to be large enough to reach a flow velocity below 0.1 m/s
Length of cross section expansion	3 to 6 times the length of the hydraulic cross section
Elbow upstream	Upstream to the opening into the storage, an elbow (90° bow with normal/small bending radius) has to disturb the flow

The mass flows in the lab tests are either 150 kg/h or 500 kg/h. For the inner diameter or Type A this gives a flow velocity of 0.08 resp. 0.27 m/s and for Type C a flow velocity of 0.01 resp. 0.05 m/s. Hence, at a mass flow of 500 kg/h, Type A (and Type B) has an inner diameter that is slightly too small with respect to the cited literature.
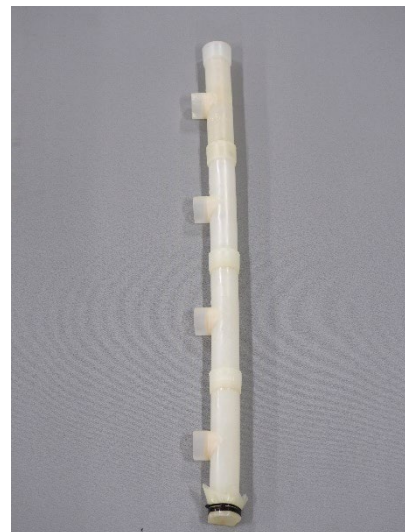
Type A: 1"-port (2.54 cm)

Type B: 1"-port with air funnel

Type C: 2.4"-port (6 cm)

Type D: Solvis stratification device

Figure 41: The four inlet geometries that were analysed with stratification experiments.

Test procedure

The water temperature of the storage tank was conditioned as follows:

- 50 °C for the upper 36 % of the water volume
- 30 °C for the lower volume (64 %)

The part of the solar circuit above the storage water level was drained during pre-conditioning. The pump was then turned on with the controller set to either 150 kg/h or 500 kg/h mass flow. By this, water leaves the storage at the bottom, is pumped through the heater and the collector mock-up and enters the storage through the mounted inlet device. By starting the pump, the air is displaced and enters the DB-storage either through the solar inlet or through the venting pipe at the storage top. The path is determined by the specific experiment chosen. There are two possible options for the air vent valve: a) always open and b) open until deaerated and then closed manually.

During the experiment with a duration of three hours, the water which is taken from the storage was heated up in the solar loop:

- In the first 90 minutes, the water was heated up from approx. 30 °C to 40 °C

- For another 90 minutes it was heated up to 55 °C

At a high mass flow of 500 kg/h the storage volume was fully replaced before the test was completed. For a flow of 500 kg/h, the volume would theoretically be completely replaced in 1.3 h (78 min), but the test duration was 3 h (180 min).

Results

<u>Air separation via the venting pipe on top of the DB storage</u>

With a small venting pipe that is installed on top of the DB storage and that is connected via a manual valve and a T-piece to the solar flow pipe (Figure 39a), air is supposed to be separated from the flow after starting the solar pump. By this, the insertion of a large air volume into the tank via the solar connection should be avoided, and the stratification of the storage water remains largely undisturbed. This dynamics of the separation and insertion of air was analysed by experiments.

The tests showed that keeping the valve on top of the storage permanently open leads to an unstable state which results, dependent on the flow rate, in either overpressure or negative pressure at the T-piece of the flow pipe. As a result, either air is sucked in via the venting pipe on top of the storage and is entrained into the storage via the solar inlet or cool water is lead to the hot top layer of the storage via the venting pipe. Both phenomena have negative effects for the stratification. Thus, only tests with closed valve after the starting phase[8] showed good results and are shown hereinafter. For the demonstrator DBS in the lab, this indicates the need of an automated valve to handle the air exchange via the pipe on top of the drainback storage.
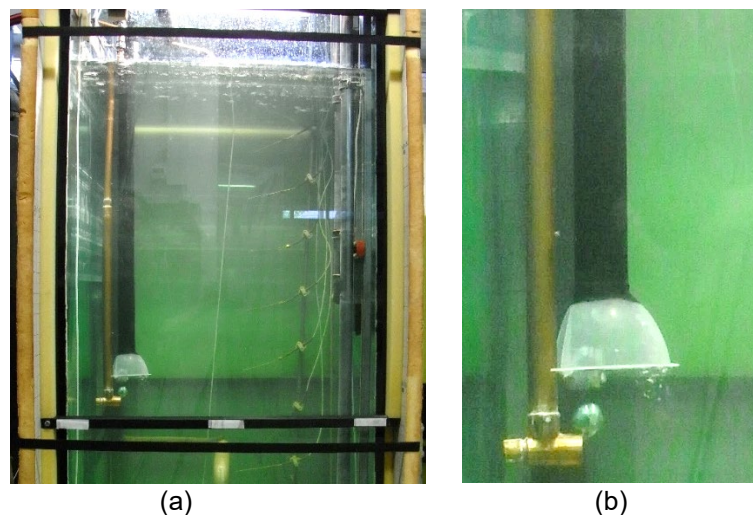

(a)   (b)

Figure 42: Type B device with 1" inlet and a funnel with pipe to collect and lead air above the storage water.
a): side view into the storage, b): zooming with air entering the funnel.

---

[8] During the starting phase itself, air has to be conducted from the mock-up volume to the top part of the storage.

However, the tests with the stratification devices Type B and D have shown that these devices are able to separate air entering the storage via the solar flow connection. Air can enter the storage either after starting the solar pump with high flow rates, which can lead to an insufficient separation of air in the T-piece of the solar flow, or also possibly during operation, after closing the valve of the venting pipe. During operation, gases might be present in the collector field that are flushed towards the storage or degassing happens due to the temperature increase in the collectors. The separation of air after entering the storage via the solar connection is shown for device Type B in Figure 42.

Effects on stratification

During the test with device Type A (1" inlet at a relative height of 56 %) the layer T7, which is 30 cm above the device, is mixed to lower temperatures when the inlet temperature is at 42 °C (Figure 43, around 1 h). When starting the charging with higher temperature (> 1.4 h), the whole volume, including T5 which is 10 cm below the inlet, is fully mixed until the end of the experiment. However, the lower temperature sensors (T3 and T4) and the outlet temperature stay at lower levels for longer time. Device Type B with the same inlet but including a funnel shows similar behaviour like Type A.
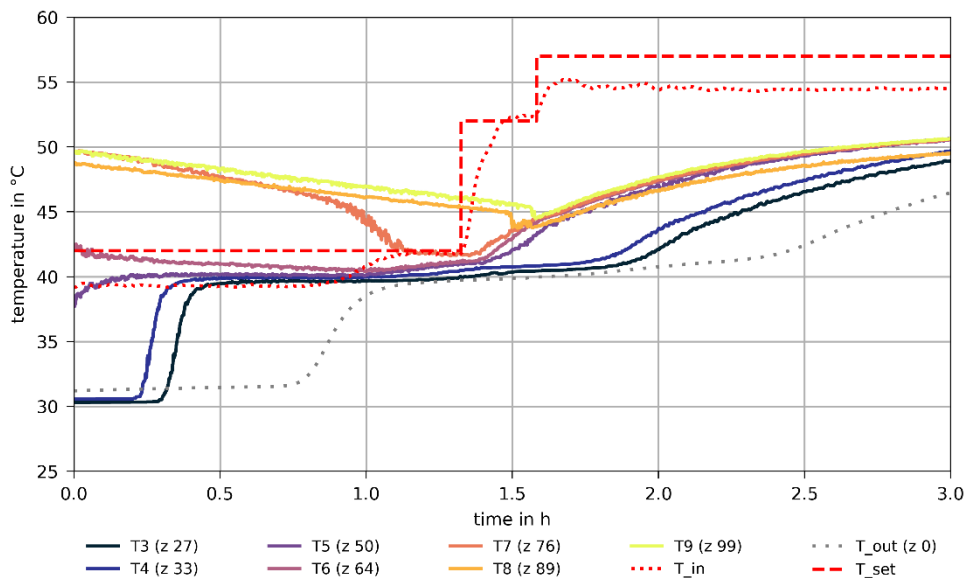
Figure 43: Storage and port temperatures with solar inlet Type A at 500 kg/h flow. Inlet height at 56 %.

A slightly better behaviour can be seen for Type C (Figure 44). Here, the pre-conditioning slightly differs as also T6 is at a high temperature level. A downmixing of T6 or T7 before increasing the inlet temperature (at 1.5 h) cannot be seen. However, the mixing of the upper layers, after the temperature increase of the inlet flow, shows a similar intensity like for device Type A.

Figure 44: Storage and port temperatures with solar inlet Type C with closed valve and 500 kg/h flow.

Device Type D (Figure 45) shows a stronger mixing in the first part of the experiment (< 1.5 h) as T6 and T7 are slightly mixed down. The loading at high temperature (> 1.5 h) is done with a good stratification as the different storage heights (T3 to T9) heat up one after the other.
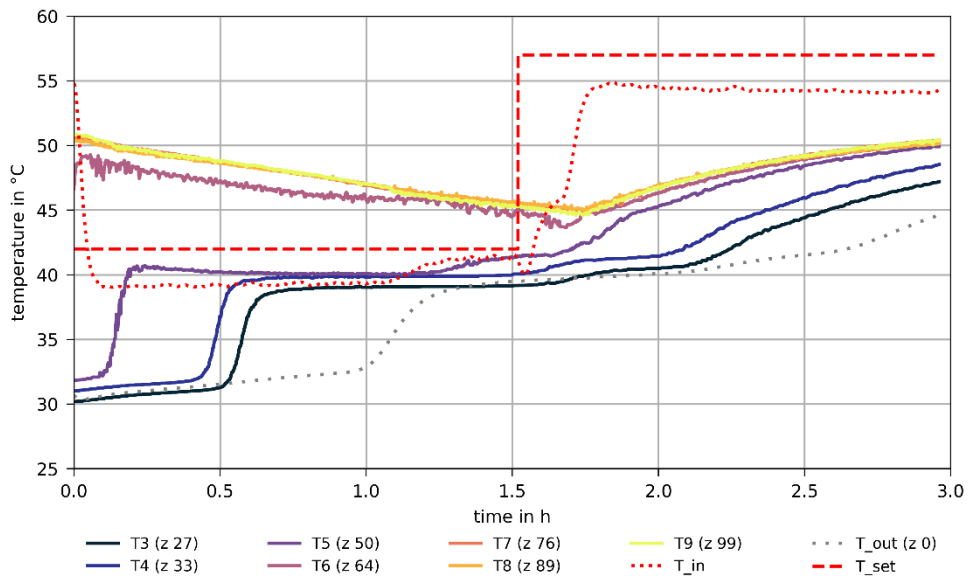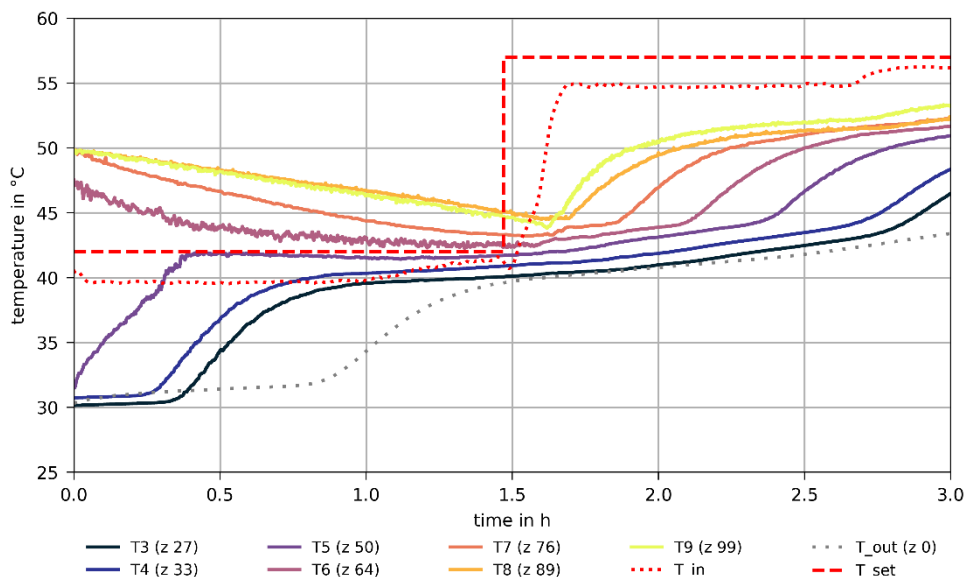

Figure 45: Storage and port temperatures with solar inlet Type D with closed valve and 500 kg/h flow.

The better stratifying of device Type D can be seen when compared directly as in Figure 46. After 1.7 h, where T9 and the inlet and outlet temperatures are shown for Types A, C, and D. However, the results show that the differences between the devices regarding stratification might not be relevant, as:

- The temperature differences between T9 and the inlet temperature differ not strongly between the devices and reaches approx. 3 K for Type D versus approx. 5 K for the other types.

- The temperatures of the solar return (line "T_{out}" in the graph), which are relevant for the efficiency of the collector field, do not differ over a long period of the lab test. Only at the end of the test (> 2.7) a slightly lower return temperature (43 °C versus 45 °C) can be seen for Type D.

A limitation of these conclusion might be the duration of the test of 3 h, as 20 minutes before test end the outlet temperatures Tout start to differ, with Type D showing a lower temperature.

Another finding from Figure 46 for simple cylindrical inlets is that the increase of the inlet diameter (Type A versus C) does not enhance the performance. For both devices, the temperatures T9 and T_{out} are very similar.

Figure 46: Temperature of uppermost storage water layer (T9) and outlet temperature for the three Types A, C, and D during 3 hours at 500 kg/h inlet flow rate.

The test with the same stratification devices but only 150 kg/h flow rate shows similar results (see Figure 47 where only two devices are shown: Type B and D). The final temperature differences (T9 - T_{out}) are 12.4 °C for Type B and 15.9 °C for the Solvis device (Type D). However, the length of the tests may be too short for the flow rate of only 150 kg/h and therefore the significance might not be as high as with the 500 kg/h tests.
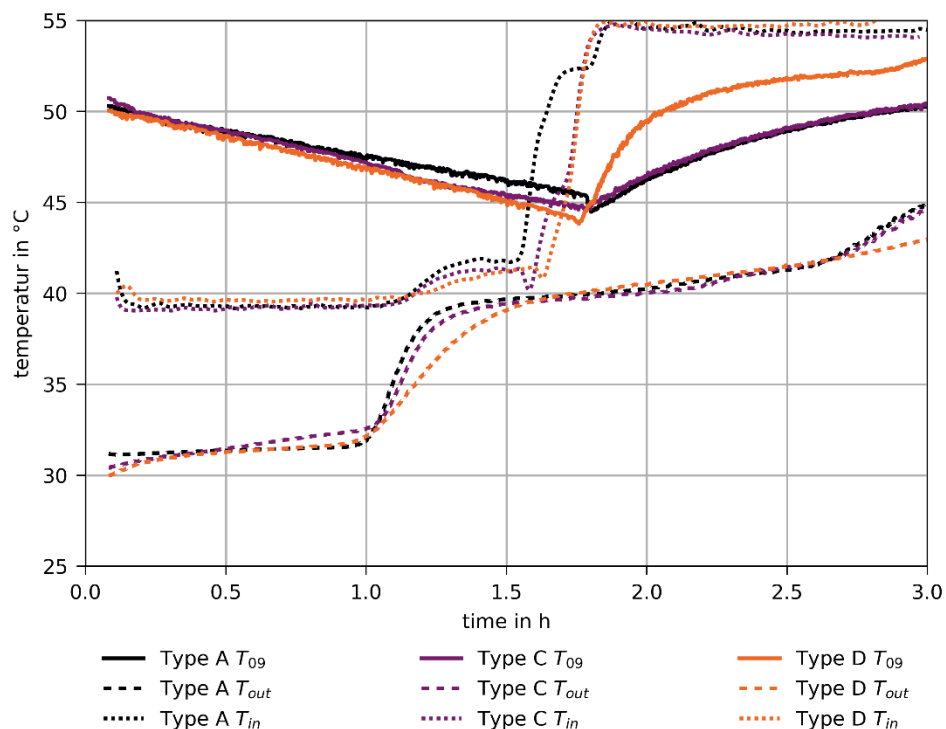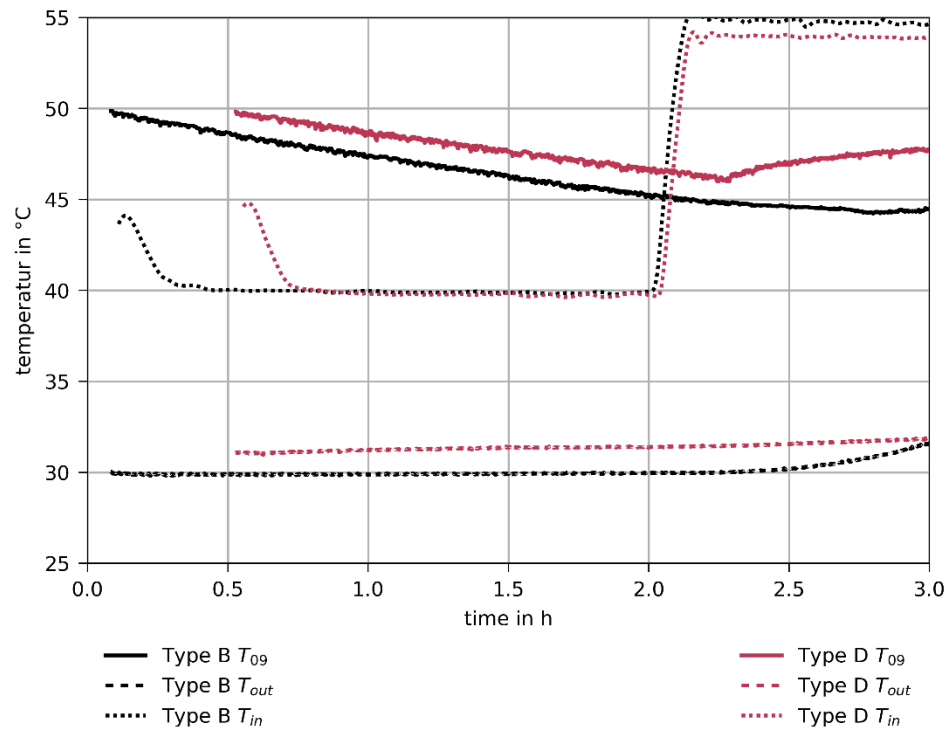
Figure 47: Temperatures of uppermost layer (T9) and outlet temperature for the two Types B and D during 3 hours at 150 kg/h inlet flow rate.

Conclusion

The best separation of air coming from the solar loop towards the storage after starting the solar circuit pump was reached when the venting pipe on top of the storage was open to let the air enter the storage on top. Then, after closing the valve of the venting pipe, only a few air bubbles were pumped into the storage through the solar inlet pipe which had no negative effect on the stratification of the storage water. If a strong air entrainment occurs during operation, both, a funnel above a simple inlet port (Type B) or a stratification device (Type D, "Schichtladelanze") is able to separate and lead the air into the drainback air volume at the top of the storage without disturbing stratification.

The stratification tests have shown slight advantages when using Type D which is a market available stratification device, as Type D allows for stratified charging over the full storage height in case the storage is loaded with temperatures higher than the storage temperatures. However, the differences of the return temperature of the solar loop between the devices are low (< 5 K) and thus, the effects on the efficiency of the collectors and of the solar gains are expected to be minor. Further, when loading the storage with Type D at temperatures colder than the upper layers, a down mixing of these layers was measured, which is a negative finding.

The inlet geometries of Type A to C are very simple and low in price. With respect to the effects on stratification observed with the lab tests and with respect to the manufacturing costs, the simple inlet geometries of Types A to C seem to be favourable for the use in the DB storage.

5.1.2   Storage tank design

The design of the solar buffer storage with integrated drainback volume is based on the simulation analysis (see chapter 3.7) and the previous lab tests.

The solar DB-storage that was investigated within the drainback system in the lab, was produced by a manufacturer based on the following specifications:

- Storage wall material: glass fibre reinforced plastic (GRP)

- Integrated drainback volume (top part of the storage volume)

- Dimensions: inner diameter 0.8 m, height 2.1 m

- Inner volume 1'000 L, water volume 805 L (adjustable)

- Insulation: 150 mm soft polyurethane foam

- Weight: 130 kg (thicker, heavy walls chosen for more safety margin in the lab tests)

- Maximum permanent loads: water at 90 °C, 3.7 bar (excess pressure)

- Manhole for installation of stratification devices (no internal heat exchangers)

As the manufacturer of the storage had problems to tighten the planned threaded metal fittings of the ports into the glass fibre reinforced plastic of the tank wall, for the lab storage (Figure 48) it was decided to realise the ports with flanges.

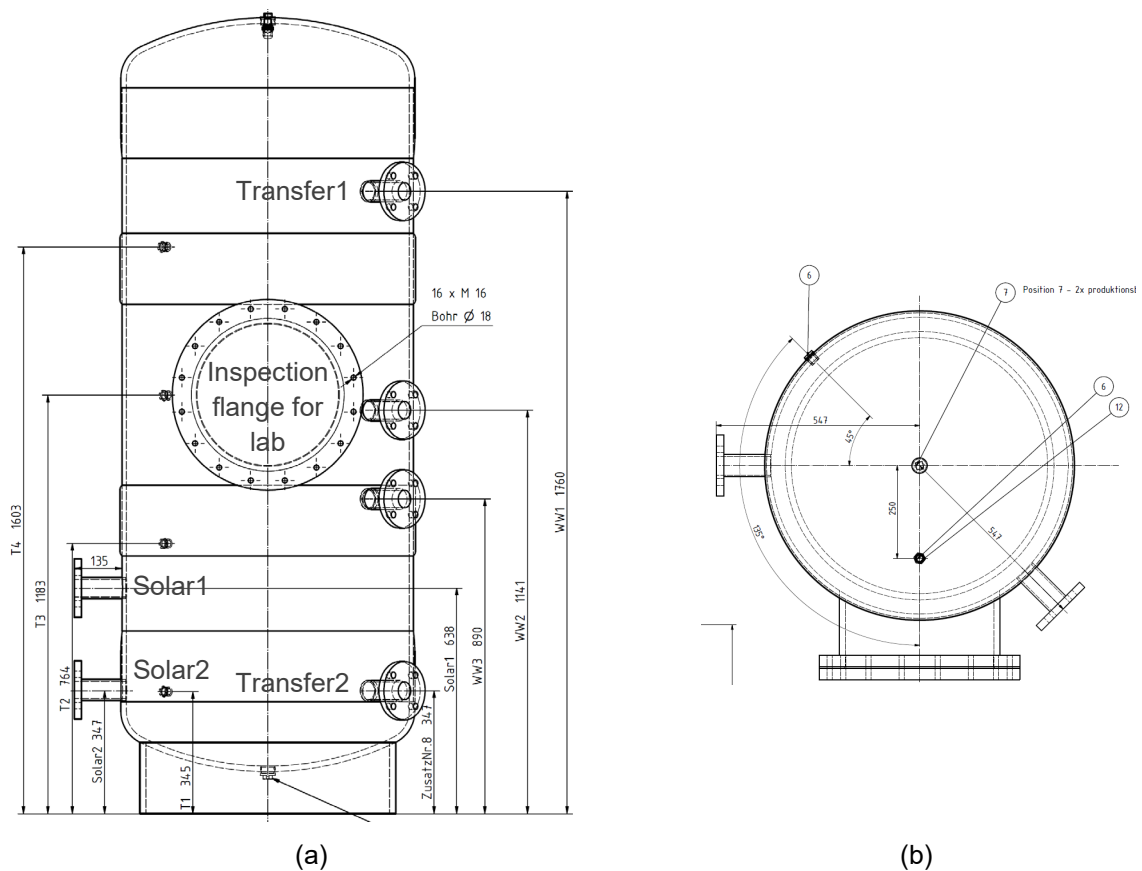(a)   (b)

Figure 48: Drawing of the drainback storage with inspection flange to mount built-ins for the lab tests, a) side view with labelled connections for solar and transfer loop, b) cross section.

The solar inlet was designed following the rules given in Table 19: the inlet specifications are 45 mm inner diameter with a length of this cross section of 150 mm. A flow rate of 500 L/h corresponds to a velocity of 0.09 m/s, which is 10 % below the recommended speed according to the design rules.

Given the system design that was chosen for the lab test (DBS A, Figure 7), next to the solar loop, a heat transfer loop is connected to the DB storage that transfers the solar heat to the DHW storage tank via a plate heat exchanger. This way for transferring heat was chosen, as only little changes in the existing DHW installation are needed when retrofitting with this solar thermal system. However, in this variant the heat transfer can only be done when warm water is tapped. Typically, a plate hx is operated with same mass flows on both of its sides. For the system size selected, the flow rate of the DHW tapping can reach maximum values of up to 1'600 kg/h (see Annex, page 91 for details). The mass flow rate of the heat transfer loop of the DB storage can reach the same maximum value. To avoid turbulences at the storage inlet of this loop, a flow pacifier (Figure 49 a - c) was designed according to the criteria listed in Table 19.

(a)   (b)

(c)   (d)
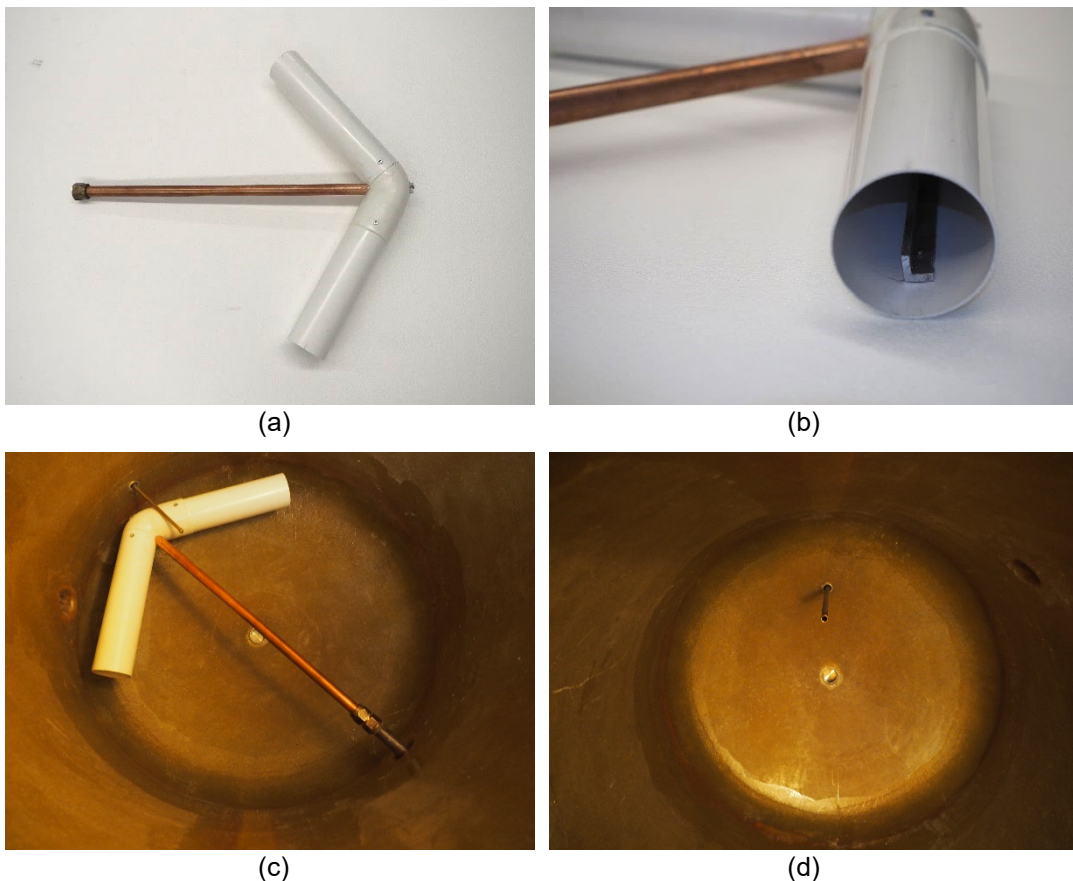
Figure 49: Flow pacifier at the DB storage inlet of the heat transfer loop (a - c) and (d) venting pipe at the top of the storage.

The water temperature of the storage is measured with four immersion temperature sensors (Pt1000) that are evenly distributed over the storage height. At the same heights, additional four Pt1000-temperature sensors are fixed with tape and heat transfer compound onto the outer surface of the storage tank (below the storage insulation). In case the response of the surface sensors is fast enough, this simple way of measuring the storage water temperatures could be chosen instead of the immersed sensors.

The later tests (Figure 50) have shown that the measurement difference between the surface sensors and the immersed sensors are below approx. 1.5 K if the heat exchange via the loops is below approx. 10 kW. At 20 kW transfer power with 1'050 L/h flow through the transfer loop, the surface sensors temporarily show a difference and thus an error of max. 10 Kelvin within the time delay of about 15 minutes.

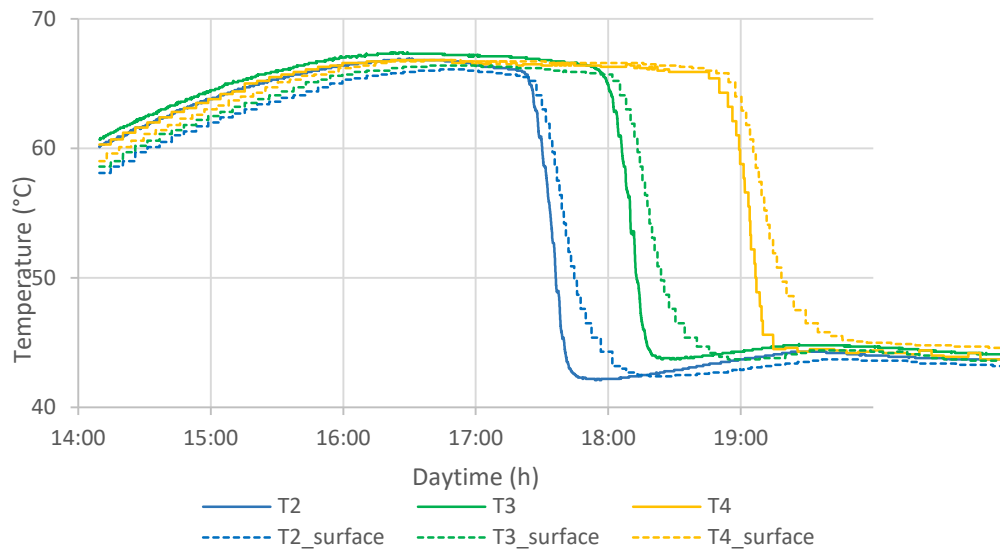Figure 50: Storage temperatures measured with immersed sensors (solid lines) and surface sensors (dashed lines) mounted between the storage GRP's wall and the storage insulation during solar loading (t < 16:00) and during heat transfer to the DHW storage with a power of approx. 20 kW (t > 17:00).

The results show that for the control of both loops cost effective surface sensors could be used. With the storage used in the lab, the lower dead band of the solar controller should be increased by approx. 1.5 K to assure a stop of the solar loading early enough. In the transfer loop, the short-term mismatch of the measured temperature is expected to be unproblematic. It would possibly lead to an unnecessary run of the transfer pump only for a short time of about 15 minutes if DHW is tapped and the solar storage temperature is close to the fresh water temperature. An optimized wall thickness of the DBS storage, which has an increased thickness of 10 mm for the lab test, would reduce the time delay of the surface sensors.

5.2   System design

The aim of operating the DBS in the lab is, on the one hand to prove and demonstrate the feasibility of the system concept and its efficiency, and on the other hand to test stable and as well unstable parameter sets of mass flow and pressure. By also analysing unstable operating conditions, knowledge is gained about the sensitivity of the specific DBS to run into malfunctions. The parameter sets of interest will be derived from the thermohydraulic simulations and applied in the demonstrator. Measurement data from the experiments will be used to validate the simulations.

<u>Hydraulic scheme</u>:

The lab installation (scheme see Figure 51) consists of a solar thermal drainback system which is connected to a DHW storage via a plate heat exchanger. In the lab system, no auxiliary (e.g. gas burner) was used, which would also heat the domestic hot water in a field installation. For control and monitoring purposes, several temperatures, flow rate, and pressure sensors were installed (detailed scheme see Annex D, Figure 71). The system control was implemented in an UVR16x2 controller of Technische Alternative GmbH.
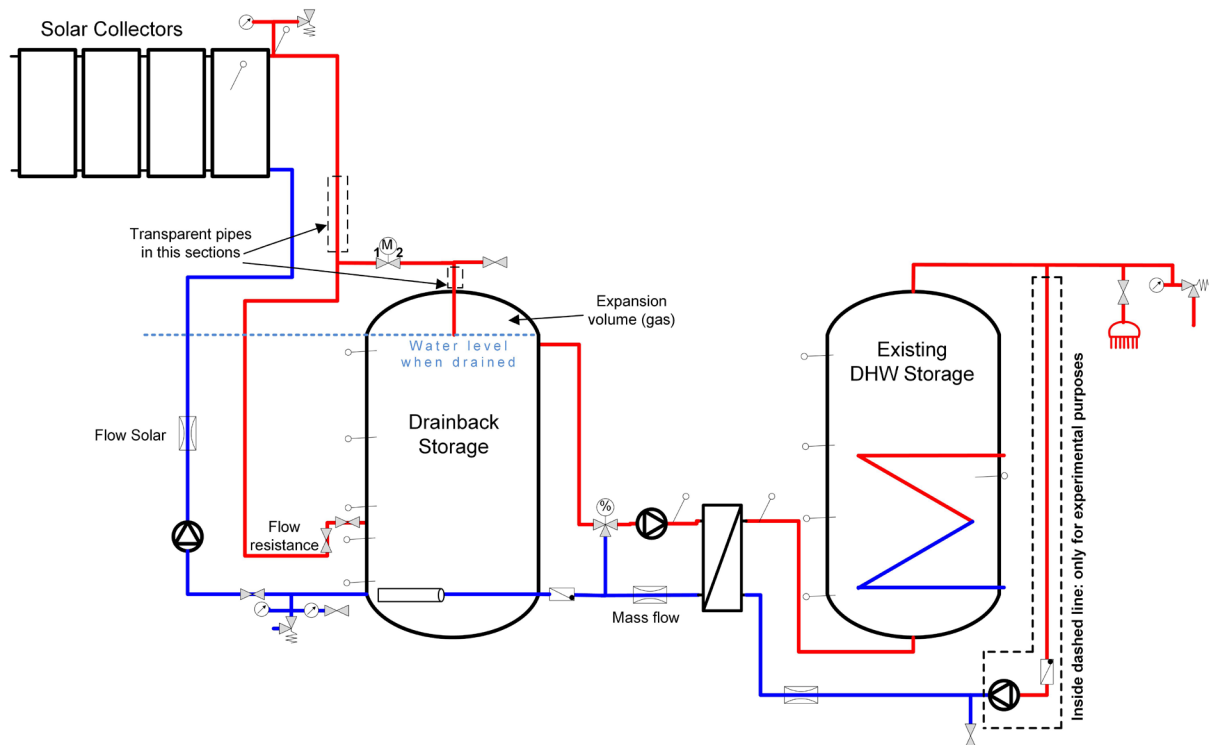
Figure 51: Hydraulic scheme of the solar drainback system with connected DHW storage as installed in the lab.

<u>Collectors</u>:

Four collectors with 2.43 m^2 absorber area each, based on the standard collector Cobralino AK 2.8V of Soltop AG, were installed on the institute's roof with orientation to south and 45° inclination. The collectors were produced by Soltop with inclined meanders (Section 4.2.1). The collectors are mounted in parallel with flow and return connection on the same side of the collector field and with an inclination of the header pipes to the horizontal of 1°, allowing them to drain (Figure 52).

Figure 52: The four collectors of the demonstrator DBS mounted on the roof in parallel.

Solar loop:

The solar loop was built with pipes and with fittings that contain plastic (Figure 53), as the drainback function of the system guarantees an overheating protection for the solar loop. Both, the return and the flow pipe have a length of 30.5 m. The height between storage and collector is 15.2 m. For the section of the loop outside the building (18 m length) a pipe made of polybutene was used, which guaranties frost safety in case the water does not fully drain (e.g. in pipe valleys). The loop section inside the building (12.5 m) was built with a composite pipe made of PEX and aluminium as this pipe keeps its shape and thus, can be installed more rapidly. Both types of pipe are commonly used for sanitary installations and their resistance against steam and frost impact was proved ReSoTech [11] within boundaries that can be kept in a drainback installation. Both types of pipes have an inner diameter of 12 mm. Push-fit fittings that can be mounted by hand (without electric tools) were mainly used for the installation of the solar loop.

In-between the collector's flow and return connections and the plastic fittings of the solar loop, corrugated stainless steel pipes of 600 mm length were placed. The metal pipes reduce the impact of hot steam onto the plastic after draining and prevent excessive conduction of heat from the header pipes of the collector (~200 °C possible) to the plastic fittings of the solar loop.

Figure 53: Components of the solar loop, push-fit fitting (black), corrugated pipe (grey) with 6 mm PE insulation and protective foil (blue).

A relatively thin insulation was used for the solar loop pipes that is provided by the pipe manufacturer together with the pipe itself (pipe pre-insulated): an insulation of 6 mm Polyethylene foam with a heat conductivity of 0.04 W/(mK). As this thickness is clearly below the recommendations of MoPEC [10][9] and the insulation typically offered by manufacturers[10], the influence of the increased heat losses through the 6 mm pipe insulation were analysed by simulation of DBS A (system see chapter 3.1) in Polysun. The solar loop was modelled with two pipes (flow and return) of 15 m length in contact to the ambient air and 10 m length in contact to room temperature. The pipe insulation of the solar loop was varied between 40 mm and 6 mm. When using 6 instead of 40 mm insulation thickness, the yearly gas consumption of DBS A increases only by 1 ‰, which is not significant.

The velocity of air a surface is in contact with has a relevant influence on the heat loss of this surface.[11] To reduce the heat losses of the thin insulated pipes, especially caused by wind around the solar pipes outside the building, the solar pipes are installed inside a low-cost waterspout pipe made of PE with 70 mm diameter. To show an example of how a solar loop could be installed along a building's façade, the downpipe was realized with this waterspout also inside the institute's building (Figure 54).
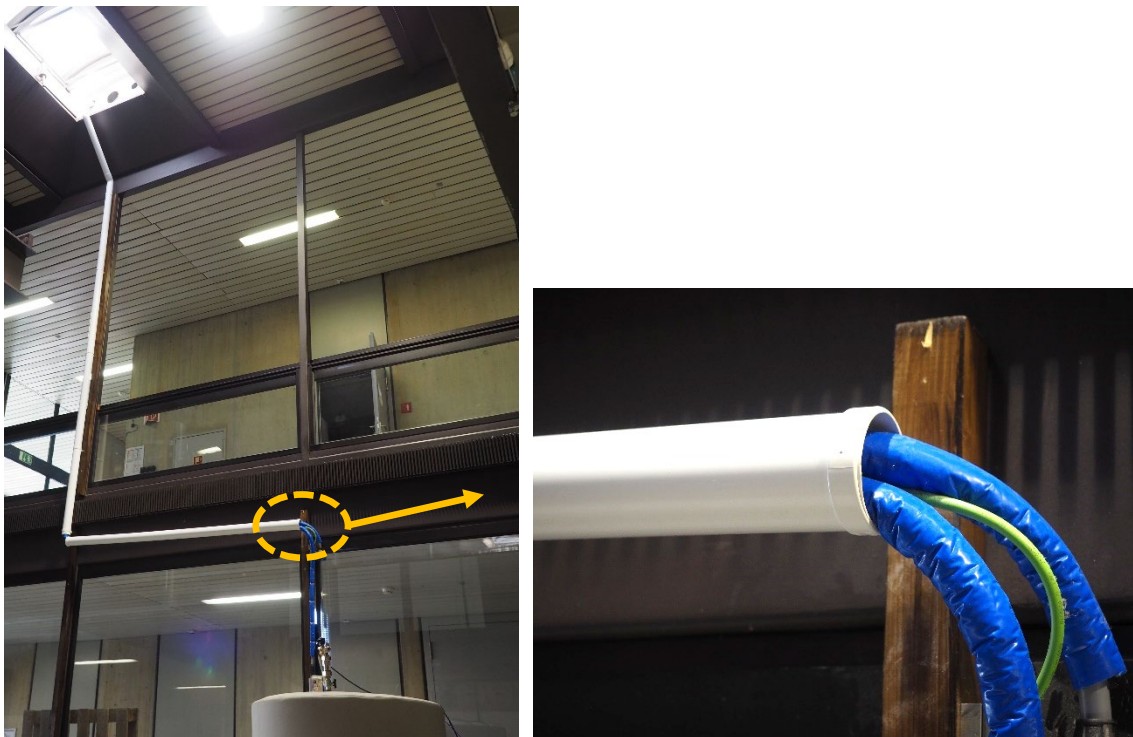
Figure 54: Solar loop, left: section inside the building, right: detail with opening of the waterspout pipe with the two pre-insulated solar pipes (in blue) and an electric cable of the monitoring sensors.

Two pipe sections made of glass were added near the DB storage for visual observation and detection of gas in the solar flow.

---

[9] Which recommends for pipes of DN10 to DN15: 40 mm insulation with λ 0.04 ± 0.01 W/mK

[10] E.g. https://www.torgen.ch/solar2.htm (21.9.2021): 13 mm insulation for pipes up to DN25 with λ 0.04 W/mK

[11] https://www.schweizer-fn.de/berechnung/waerme/rohrisol/rohrisol_start.php

Figure 55: Transparent pipe section (see arrows) of the solar loop for visual observation of gases within the flow.

<u>Solar pump</u>:

A single stage regenerative turbine pump (SPECK Y-2340-SR) is used as solar circuit pump (see chapter 4.3.1 for details).

<u>Storages and heat transfer</u>:

The solar drainback storage described in 5.1.2 was connected with an old DHW storage[12] (Figure 56 a). The heat is transferred from the solar storage to the DHW storage by a plate heat exchanger with 3'000 W/K specific heat transfer rate (Figure 56 b). With a flow detection sensor of Technische Alternative GmbH (sensor type STS01DC-3/4") a tapping on the DHW side can be detected. The water in the primary side of the transfer loop is pumped with a Grundfos UPM3 Solar 15-75 PWM GPS 70 pump. The temperature of the transfer is controlled by a passive thermostat to a maximum of 60 °C to avoid lime stone in the secondary side of the plate hx.

[12] DHW storage of CTC AG, 3/1000 L Combi-Boiler without electric rod.

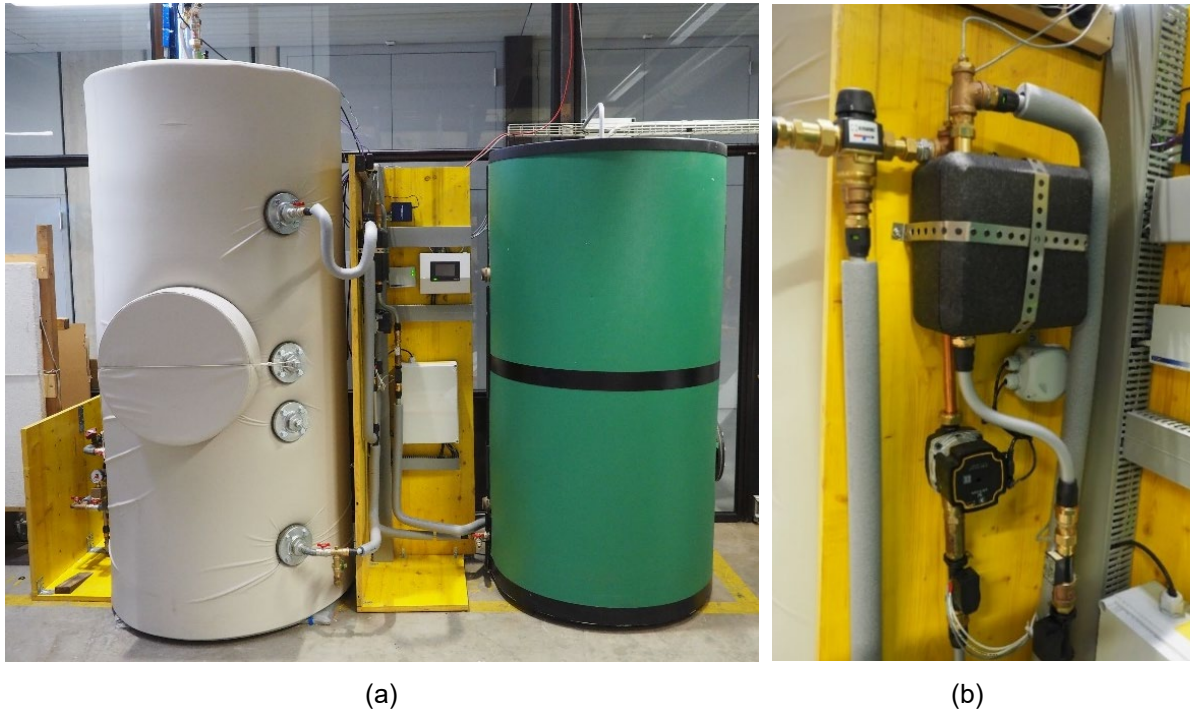(a)   (b)

Figure 56: Storages and heat transfer with a) solar drainback storage (grey) and DHW storage (green) and b) components for heat transfer and system control between the storages (passive thermostat, plate heat exchanger, pump, and flow detection sensor)..

5.3   Analyses

5.3.1   Storage: air handling and stratification

Inside the DB storage an air volume of approx. 150 litres provides the functions of a drainback volume of the solar loop and of pressure compensation. The venting and operation phase of the lab DBS was analysed to assess whether the air that is pushed into the storage when the solar loop is vented (i.e. filled up with water) is disturbing the thermal stratification of the storage water. Further, it was analysed whether the simple design of the solar inlet (see chapter 5.1.2) does initialize turbulences in the storage water.

A negative influence on the storage stratification when all air is vented via the solar inlet is shown in Figure 57. Here, the venting pipe on top of the storage was closed manually. Shortly after venting is started around 8:03 h, the upper water layers T4 and T3 are nearly fully mixed to the same temperature. Also T2, which is around 10 cm above the solar inlet is mixed to higher temperatures. These results show the need of a proper handling of air during venting of the solar loop.
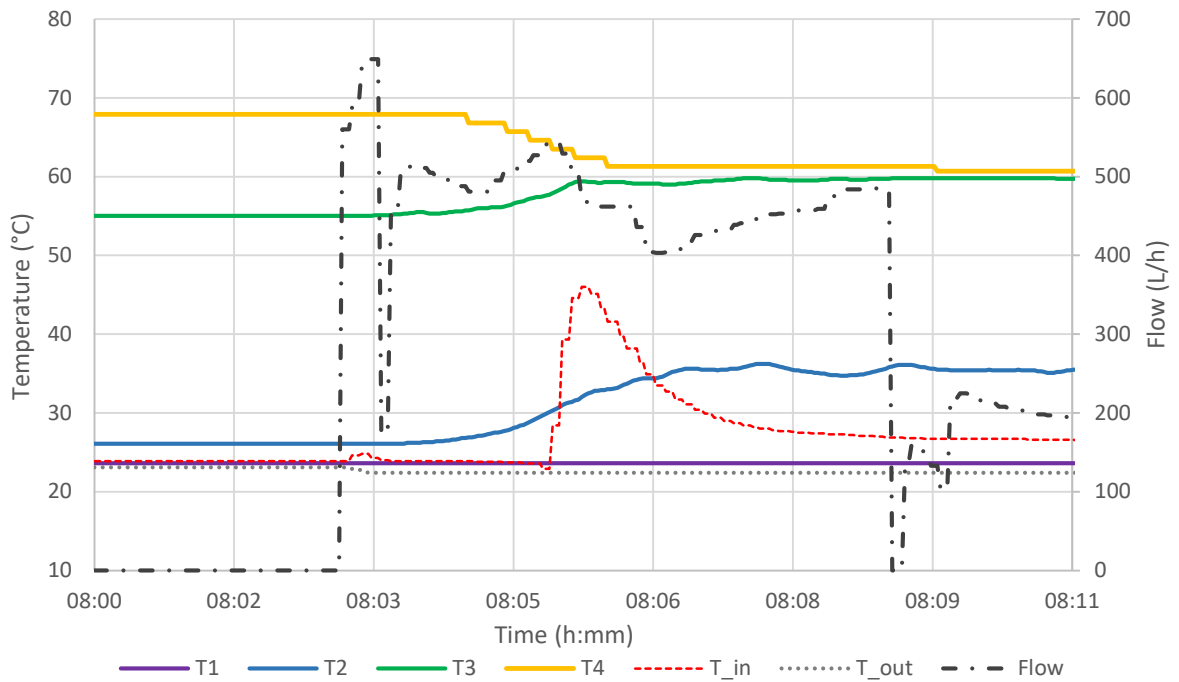
Figure 57: Disturbed stratification of storage water when venting the solar loop via the solar inlet. Venting starts around 8:03 h (flow starts).

When the air is lead through the venting valve and pipe on top of the storage, only little effects can be observed for T2 and T3 (Figure 58). Both water layers have only slightly higher temperatures of approx. 3 Kelvin.

The solar inlet is properly working also at high mass flows (Figure 59) like expected from the storage tests (chapter 5.1.1): the upper layers T3 and T4 are not mixed down during solar loading and the return temperature stay low.
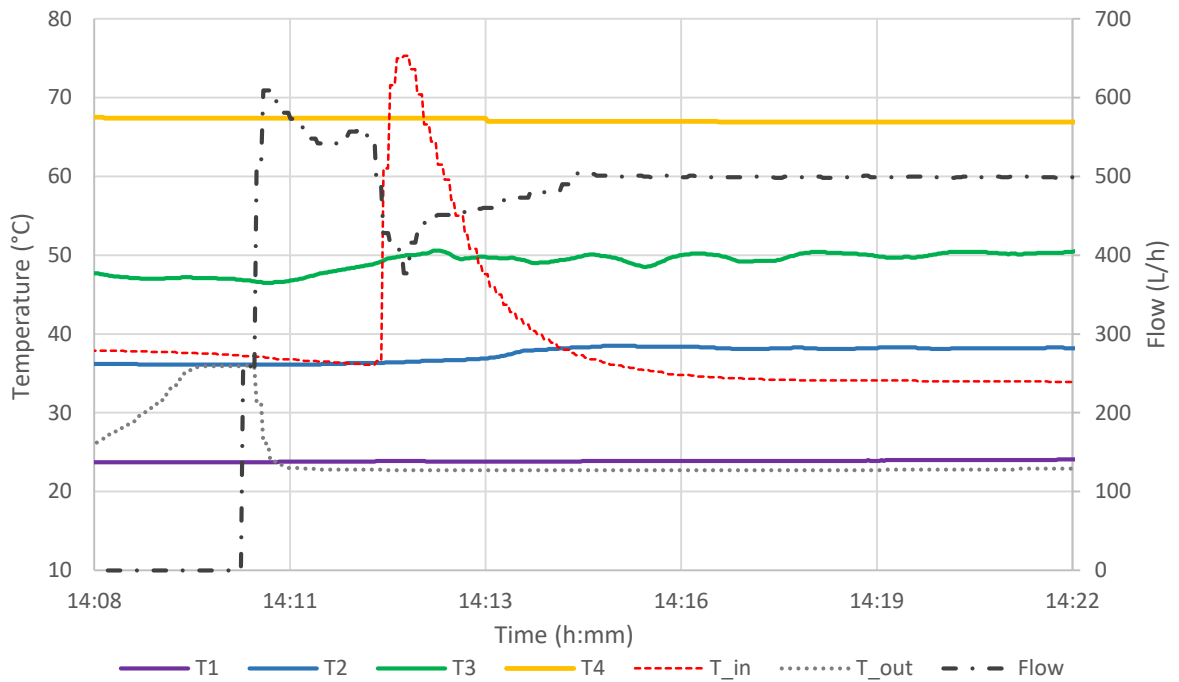
Figure 58: Preserved stratification of storage water when venting the solar loop via the venting pipe on top of the storage. Venting starts around 14:10 h.
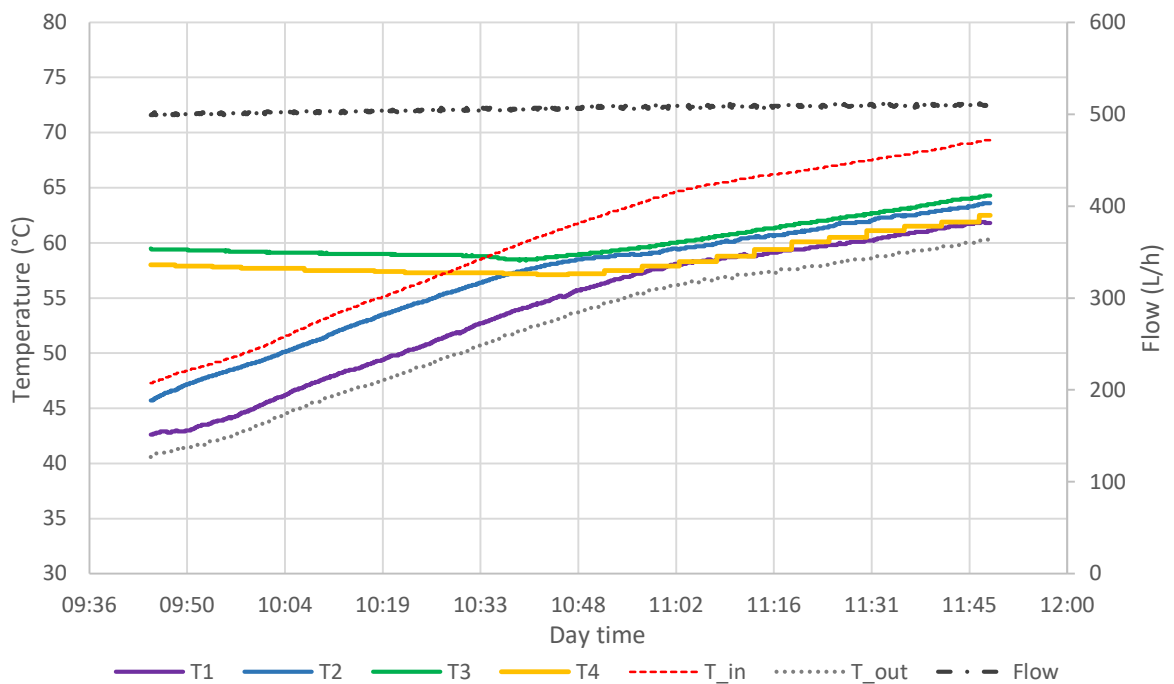

Figure 59: Solar loading of the storage with preservation of warm layers and fully mixing when loading with hot inlet temperatures.

5.3.2 Influence of the plate heat exchanger size on system performance

The sizing of the plate hx that transfers heat from the DB storage to the DHW boiler was done with the help of system simulations in Polysun. Measurement data of the plate heat exchanger in the lab was used to validate the simulated hx. In the simulations, the exchange power of the plate hx was varied to analyse the influence on the reduction of the yearly gas consumption which was used as main criterion for the sizing of the plate hx.

For the validation, different temperatures and mass flows for both the primary (i.e. solar) and the secondary (i.e. fresh water) side of the plate hx were used (see Annex, Figure 69 and Figure 70). The plate hx with Polysun catalogue No. 45 (capacity 3 kW/K) was matching well the lab data.

As in DBS A the heat transfer can only be done when DHW is tapped, the temporal and quantitative distribution of the DHW tapping during a day is relevant. Hence, a more realistic DHW tapping profile was used for the simulative sizing of the plate hx. The profile was generated with DHWcalc [44] with the following specifications:

- Multi-family house with 9 households
- Mean daily draw-off vol.: 700 l/day
- Min. flow rate: 6 L/h
- Max. flow rate: 1600 L/h
- No. of occupant categories: 4 (see Table 20)
- Time step duration: 1 min

Table 20: Flow rate setting for the DHW draw off profile generated with DHWcalc [44].

Category	1	2	3	4
Mean flow Rate (L/h)	60	360	840	480
Duration of draw-off (min)	1	1	10	5
Portion (%)	14	36	10	40
Sigma (L/h)	120	120	12	24

The result of the system simulation with different plate hx sizes, i.e. heat transfer capacities, shows that the size of the plate hx within the ranges analysed has a minor relevance for the non-renewable energy consumption (Figure 60). The installed hx with a capacity of 3 kW/K has a sufficient size and according to the simulations results, the increase of gas consumption compared to hx with four times higher capacity is only 3 %. Hence, the relatively small plate hx with 3 kW/K capacity used in the demonstrator fits well to this application and system size.
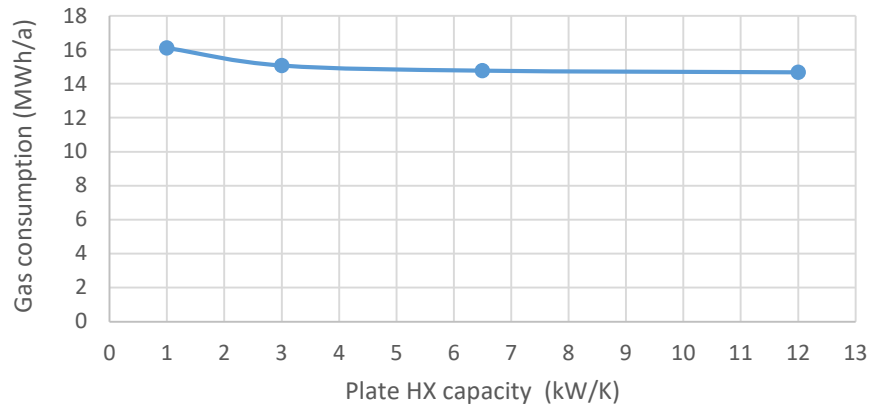
Figure 60: Simulated gas consumption of the DHW system for four different plate heat exchanger sizes used to transfer solar heat to the DHW boiler via the fresh water pipe.

5.3.3 Impact of freezing and high temperatures

As the solar circuit it partly built with plastic pipes and fittings and as water is used as heat transfer fluid, both, temperatures above the limits of use of the materials and below the freezing point of water might cause damages of the circuit. The effects of heat and freezing on plastic piping was analysed extensively in the lab in project ReSoTech [11] and it was shown that using these materials in DBS is possible.

Within the SimplyDrain project, the lab DBS was running during one winter which was relatively warm without longer frost periods. However, in February 2021 there was a period of around four days with ambient temperatures below 0 °C and even temporarily down to -10 °C (Figure 61). During these days the DBS was running several times. No defects on the components occurred.
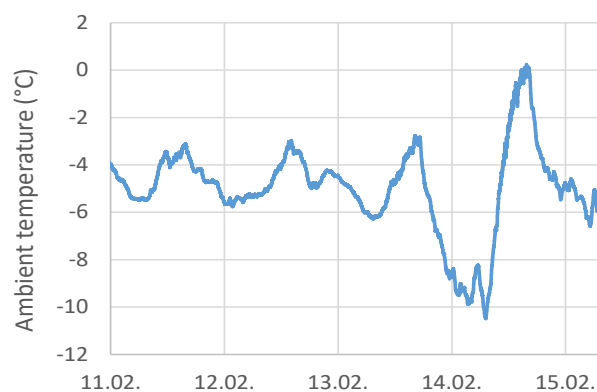
Figure 61: Ambient temperatures the collector and the piping of the water filled DBS were exposed to during the longest frost period in winter 2021.

Compensators are used to connect collectors of a collector field. Often short metal bellows are used as compensators. After draining a collector field, water can remain within the corrugations and freeze if the temperatures drop below 0 °C. As within the project ReSoTech [11] no icing tests were conducted with compensators, an icing test was performed for several types of this component within SimplyDrain. Nine compensators of different kind were slightly bended to increase the amount of remaining water, partly filled with water, and closed with silicone plugs. 120 cycles of freezing and melting were carried out (Figure 62).

The possible dilatation between the ends of the compensators was measured with a calliper rule recurrently after approx. 40 cycles during times with melted and with frozen water. No dilatation could be measured and no deformation or visual defects of the compensators were recognizable.

(a)　　　　　　　　　　　　　　　　　　　　(b)

Figure 62: Freezing test with compensators partly filled with water to mimic the case that water remains within the corrugations after draining the collector field. (a) part of the compensators, all closed with silicone plugs, (b) opened compensator with frozen water.

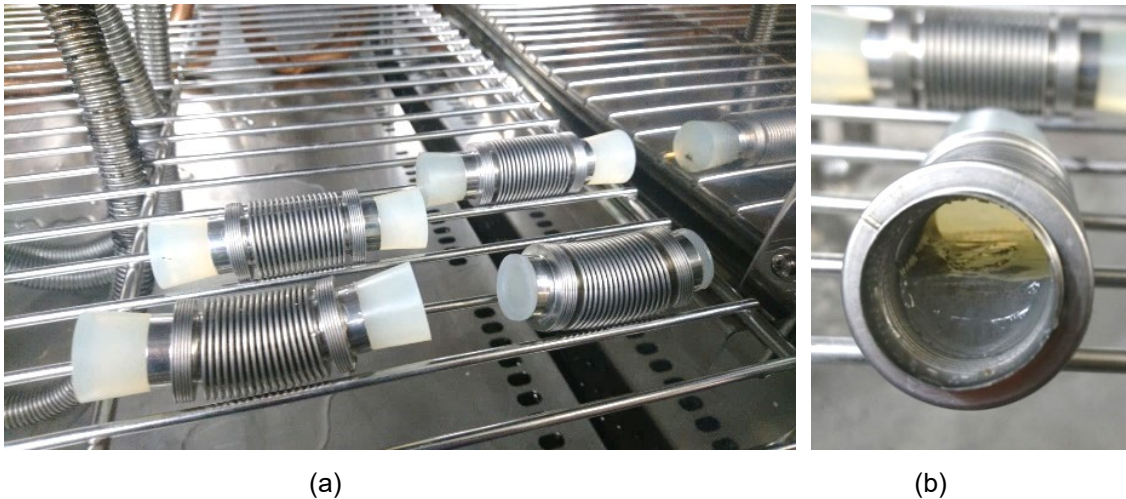The impact of high temperatures from the collector field to the solar circuit pipes is shown Figure 63. The figure shows frequencies of temperature classes in a period of approx. 6 months including summer months for times after draining, i.e. for temperatures near or above 100 °C (see colours). Like the thermohydraulic simulations predict, a longer impact of high temperatures is measured in the return pipes. The first 0.5 m of piping after the connections to the collector are made of metal pipes. The plastic pipes and fittings, stating after these 0.5 m only see moderate temperatures below 105 °C, and only for few hours.

Two effects influence the temperatures of the gas resp. steam that possibly enters the pipes after draining. First, the pressure inside the solar circuit affects the boiling point of the residual water that remains in the collectors after draining. The higher the system pressure, the higher the temperature of the steam that enters the pipes.

The absolute pressure of the lab DBS was mostly at approx. 1 bar and the maximum was at 1.5 bar, which corresponds to a boiling point of 100 °C or max. 110 °C, respectively. The absorber reached stagnation temperatures around 200 °C during times with high solar irradiation. However, for relatively short times high temperatures of only moderate levels were reaching only the first parts of the pipes (Figure 63).
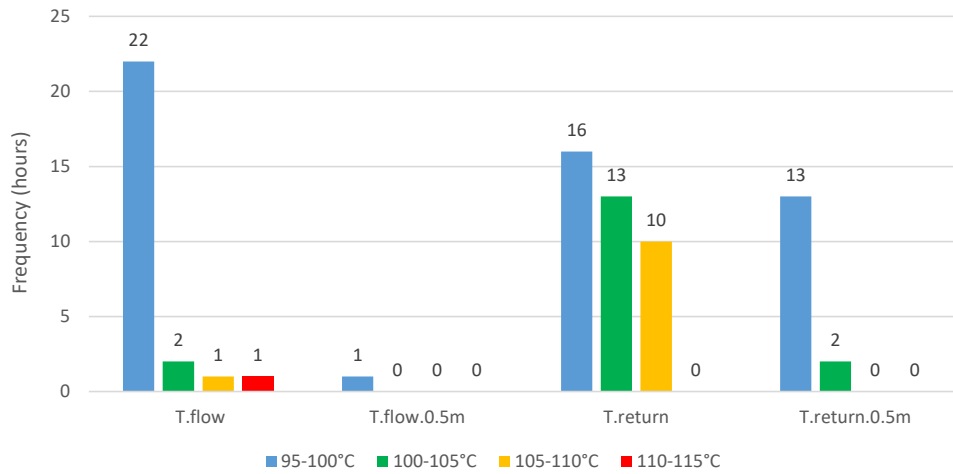
Figure 63: Exposure of the solar circuit to high temperatures from March to end of August 2021 (total: 3870 h). Measuring sites: T.flow and T.return at the collector connections (metal pipes), T.flow.0.5 m and T.return.0.5 m at start of the plastic pipes, insulated on a metal fitting surface in a distance of 0.5 m to the collectors.

6 Summary and conclusions

The market survey has identified 3-floor pre-1980 MFH as the main market for the DHW drainback systems analysed by this study. These buildings are widespread and present an urgent need of renovation, including their heating system that is reaching the end of the service life. Statistics show that these buildings account for 40% of the MFH buildings in Switzerland and fossils fuels represent the larger part of their energy consumption (62%). Representatives from companies that were interviewed indicate that renewable energies are not considered in their renovation strategy unless legal obligations exist. However, in the latter, a preference goes for solar thermal systems as quite often the space heat distribution in these old MFH still runs with traditional high temperature radiators, making solar thermal more suitable than heat pump systems. They also indicate that when it comes to replacing the fossil fuel heating system, both, boiler and storage are replaced with an equivalent, more modern system. No additional hydraulic connections are considered to add another energy source such as solar. Overall, the results show that ST systems are a viable option for renewable DHW production in old MFH buildings. However, to increase the adoption of ST systems in renovation actions, the two main issues pending are the integration point into the existing DHW system and the cost. These two issues have been tackled with the proposed DBS of SimplyDrain.

Of the three analysed drainback system concepts, DBS concepts A and C are the most interesting concepts in terms of cost of heat and LCoH. DBS C, the variant with replacement of the existing DHW storage with a solar (combi or DHW) storage and with a fresh water module, is slightly advantageous by being technically feasible and by fitting best to the typical retrofit situation in MFH, where the old DHW storage needs to be replaced. With a large storage volume, DBS C2 leads to the highest reduction of the LCoH (-33 %) when compared to the solar reference system and to fractional energy savings compared to the conventional gas-system of 42%. DBS A, the variant with a solar DB-storage connected to an existing DHW storage, is also shown to be interesting for cases where the existing DHW storage is kept, although these cases are not dominant according to our survey. However, with DBS A, an add-on can be offered that can be installed with very little effort and that nevertheless leads to a high solar coverage. In addition, DBS A is a cost-effective MuKEn standard solution. The concept presents the additional advantage of not using a fresh water module for DHW production (like DBS C), a technology still quite uncommon and often seen sceptical by professionals in Switzerland. Technically simple ways to couple DBS A to the existing storage have been described. In contrast, DBS B, a variant similar to DBS A but with only a DB vessel instead of a DB storage, is not of interest with costs remaining high and with no energy saving benefits.

A solar loop with drainback function consisting of one row of parallel connected solar collectors was designed with the help of thermohydraulic simulations. With the help of this analysis, first design rules for DBS with one solar loop and one collector row were formulated. Generally spoken, after thermodynamic sizing of a system with energy simulations and after a cost assessment, these design rules, respectively design steps, should be followed when designing a DBS. The rules consist of dimensioning of the absorber tubing, the pipe network, and the pump. Self-venting must be proven by calculations. Further, a slight overpressure of about 0.2 bar in the collector during operation should be ensured to prevent partial stagnation during operation. This can be reached by adding a flow resistance in the solar flow line. Also the overpressure within the circuit after draining should be low to avoid too high steam temperatures and by this, protect the plastic piping of the solar circuit.

A storage tank with direct integration of the solar loop without any heat exchanger, with integrated drainback volume and with water as solar heat transfer fluid was designed and tested in the lab. Different inlet geometries for the solar port were tested with respect to their ability to prevent mixing of the storage water and to separate air bubbles entering the storage via the solar port. Simple inlet geometries already showed a sufficient performance. If air is not separated well enough after starting the solar pump, a

funnel with a pipe that catches and conducts the air to the storage top or a vertical stratification device that reaches the storage top can be used.

DBS A, including a solar buffer storage with integrated drainback volume, was built in the lab and connected to an old DHW storage to prove the feasibility of the concept. Measurement data from the lab system was used for the validation of the thermohydraulic simulations. The heat transfer was realized with a plate heat exchanger by preheating the fresh water before it enters the DHW storage when DHW is tapped. As an advantage, this concept reduces the intervention at the existing DHW system greatly. However, the heat transfer is reduced to times when hot water is tapped, and the control of the transfer process has to be done properly. The lab DBS with water as heat transfer fluid and a solar circuit made of plastic piping could be operated successfully also during high strains in winter and summer months.

The present investigations were discussed with the companies from the advisory board as well as others, and the laboratory DBS was inspected. It was thus confirmed that the investigated ideas, such as the use of water as heat transfer fluid, the use of pre-insulated plastic pipes with push-fit fittings, and the integration of the drainback volume in a simple solar storage tank, are realistic and feasible. However, it has also been indicated that larger collector arrays with branched solar circuits are also relevant for the market, and thus, it is considered necessary to have knowledge and planning certainty also for these larger systems. Proposals for a heat transfer via the maintenance flange of the existing storage tank would be helpful and suitable stratification devices should be found. The companies see it as necessary that field tests are carried out with several DBS set up in order to validate the previously gained knowledge.

7 Outlook and next steps

With the present study, important physical phenomena influencing a stable and safe operation of drain back solar thermal systems (DBS) could be analysed for small system sizes with one collector row. However, important effects like the steam propagation into the circuit after draining, that is influenced by remaining water within the collector, and the solubility of non-condensable gases influencing the system pressure and the evaporation temperature, could not sufficiently be analysed. Further, a general investigation of principle system designs regarding the solar circuit being open or closed towards atmosphere and regarding height differences between DB volume and collector would be beneficial. The authors of this study see a need for a follow-up project where the investigations started in SimplyDrain can be extended to larger DBS and especially to DBS with branched circuits. The follow-up project should be subdivided into an explicit scientific part where the above-mentioned topics are addressed and a field implementation part, where, together with the interested companies, several DBS will be installed and analysed regarding reliable operation. Typical situations from the field with flat and pitched roofs are to be examined. The existing laboratory facility is to be adapted for this purpose and used again to validate the THS and to make a proof of concept in the lab. The planning recommendations, which could not be worked out in detail in SimplyDrain, are to be refined and expanded to include larger DBS. Publishing these recommendations should help in creating confidence for the proposed technology amongst the relevant stakeholders. Variants suggested by the companies for the heat transfer between storages should be analysed with laboratory tests. Variants of the overall system, if possible, with different size categories of the collector field (20, 40, 60, ... m^2) are to be designed by the institutes and installed by the companies. The functioning of these field systems should be evaluated with a scientific monitoring.

8 References

[1] T. Hostettler and A. Hekler, 'Statistik Sonnenenergie - Referenzjahr 2020', 2021. [Online]. Available: http://pubdb.bfe.admin.ch/de/publication/download/10539

[2] D. Philippen, M. Caflisch, S. Brunold, and M. Haller, 'ReSoTech 1 – Reduktion der Marktpreise solarthermischer Anlagen durch neue technologische Ansätze, Teil 1: Potenzialanalyse und Lösungsansätze', SPF Institut für Solartechnik, Rapperswil, Schlussbericht, 2016. [Online]. Available: https://www.aramis.admin.ch/Dokument.aspx?DocumentID=35218

[3] M. Müller, S. Perch-Nielsen, L. Bühler, and F. Ribi, 'Preise und Kosten thermischer Solaranlagen, Analyse der Preise in der Schweiz, Österreich und Baden-Württemberg', E. Basler+Partner, 2014.

[4] IEA, 'IEA SHC-Task 54, Price Reduction of Solar Thermal Systems'. 2019. Accessed: Sep. 20, 2019. [Online]. Available: http://task54.iea-shc.org

[5] J. Berner, 'Drain-Back-Systeme im Überblick', *Sonne Wind und Wärme*, pp. 60–61, 2012.

[6] T. P. Bokhoven, J. Van Dam, and P. Kratz, 'Recent experience with large solar thermal systems in The Netherlands', *Solar Energy*, vol. 71, no. 5, pp. 347–352, Nov. 2001, doi: 10.1016/S0038-092X(00)00124-9.

[7] K. Rühling and T. Schabbach, 'Eigendruckhaltung und Eigensicherheit kleiner Solaranlagen. Chemisch-physikalische Vorgänge in einem Zweiphasen-Kollektorkreis', presented at the 16. Symposium thermische Sonnenenergie, Bad Staffelstein, 2006.

[8] R. Botpaev, J. Orozaliev, and K. Vajen, 'Experimental Investigation of the Filling and Draining Processes of the Drainback System (Part 1)', *Energy Procedia*, vol. 57, no. 0, pp. 2467–2476, 2014, doi: http://dx.doi.org/10.1016/j.egypro.2014.10.256.

[9] M. Lehmann, M. Meyer, N. Kaiser, and W. Ott, 'Transformation der Energieversorgung - Umstieg von fossilen auf erneuerbare Energieträger beim Heizungsersatz (FP-2.8)', econcept AG, Zürich, 37, 2017. [Online]. Available: https://www.energieforschung-zuerich.ch/fileadmin/berichte/FP-2.8_Forschungsbericht.pdf

[10] 'Mustervorschriften der Kantone im Energiebereich (MuKEn 2014)'. Konferenz kantonaler Energiedirektoren, 2014. [Online]. Available: https://www.endk.ch/de/ablage/grundhaltung-der-endk/muken2014-d20150109-2.pdf

[11] D. Philippen *et al.*, 'ReSoTech 2 – Reduktion der Marktpreise solarthermischer Anlagen durch neue technologische Ansätze', SPF Institut für Solartechnik, Rapperswil, Schlussbericht, Apr. 2020.

[12] FSO, 'Enquête sur les agents énergétiques des bâtiments d'habitation', 2019.

[13] 'SIA 380/1 L'énergie thermique dans le bâtiment.', 2009.

[14] S. Schwab *et al.*, 'eREN Rénovation énergétique des bâtiments', 9782970100522, 2016.

[15] EnDK, 'Energieverbrauch von Gebäuden, Fact Sheet K', Schweizerische Energiedirektoren Konferenz EnDK, Bern, Bern, 2014.

[16] 'SIA 480 - Calcul de rentabilité pour les investissement dans le bâtiment', 2004.

[17] Prognos AG, 'Analyse des schweizerischen Energieverbrauchs 2000-2018 nach Verwendungszwecken', 2019.

[18] A. Cordin, V. Bernhard, and B. Stefan, 'HPT Annex 46 Domestic Hot Water Heat Pumps Task 1 Market Overview Country Report Switzerland', 2016.

[19] Swiss Confederation, 'Federal Constitution of the Swiss Confederation Article 89 (4)', 1999.

[20] EnDK, 'Stand Umsetzung MuKEn 2014', 2021.

[21] Swiss Confederation, 'RO 1018 Arrêté fédéral pour une utilisation économe et rationnelle de l'énergie', 1991.

[22] SIA, 'SIA 385/2 Installations d'eau chaude sanitaire dans les bâtiments – Besoins en eau chaude, exigences globales et dimensionnement.', 2015.

[23] Y. Louvet *et al.*, 'Economic comparison of reference solar thermal systems for households in five European countries', *Solar Energy*, vol. 193, pp. 85–94, Nov. 2019, doi: 10.1016/j.solener.2019.09.019.

[24] D. Siegrist and S. Kessler, 'Harmonisiertes Fördermodell der Kantone (HFM 2015) - Schlussbericht'. Konferenz Kantonaler Energiefachstellen EnFK

und   Bundesamt für Energie BFE, 2016. [Online]. Available: http://www.ow.ch/dl.php/de/586e3fdcf16be/HFM2015.pdf

[25] CEN/TC 312, 'EN 12977: Thermal solar systems and components — Custom built systems — Parts 1 – 5', 2018.

[26] L. Perret and J. Fahrni, 'Analyse der Auswirkungen der MuKEn 2014 auf die Märkte thermischer Solaranlagen und Photovoltaikanlagen', BFE, Ittigen, BFE Schlussbericht, Feb. 2015.

[27] R. Eismann and A. Genkinger, 'HYDRA – Rohrnetzdimensionierung für Solaranlagen. Bedienungsanleitung mit Beispielen', Institut Energie am Bau,Fachhochschule Nordwestschweiz FHNW, Muttenz, 2018.

[28] R. Eismann, S. Müller, and A. Genkinger, 'THD-opt: Validierung der Software THD zur thermohydraulischen Dimensionierung von Solaranlagen', Institut Energie am Bau,Fachhochschule Nordwestschweiz FHNW, Bern, 2018. [Online]. Available: https://www.aramis.admin.ch/Dokument.aspx?DocumentID=49944

[29] U.S. NRC, 'TRACE V5.0, Theory Manual. Field Equations, Solution Methods, and Physical Models', Washington, DC: Division of Risk Assessment and Special Projects, Office of Nuclear Regulatory Research, US Nuclear Regulatory Commission, 2007.

[30] Hoyt C. Hottel and Austin Whillier, 'Evaluation of Flat-Plate Collector Performance', presented at the Transactions of the Conference on the Use of Solar Energy, 1958.

[31] R. W. J. Bliss, 'The derivations of several "Plate-efficiency factors" useful in the design of flat-plate solar heat collectors', *Solar Energy*, vol. 3, no. 4, pp. 55–64, 1959.

[32] R. Eismann and H.-M. Prasser, 'Correction for the absorber edge effect in analytical models of flat plate solar collectors', *Solar Energy*, vol. 95, no. 0, pp. 181–191, 2013, doi: http://dx.doi.org/10.1016/j.solener.2013.06.009.

[33] R. Eismann, 'Accurate analytical modeling of flat plate solar collectors: Extended correlation for convective heat loss across the air gap between absorber and cover plate', *Solar Energy*, vol. 122, pp. 1214–1224, 2015, doi: https://doi.org/10.1016/j.solener.2015.10.037.

[34] R. Eismann, S. Hummel, and F. Giovannetti, 'A Thermal-Hydraulic Model for the Stagnation of Solar Thermal Systems with Flat-Plate Collector Arrays', *Energies*, vol. 14, no. 3, p. 733, 2021, doi: http://dx.doi.org/10.3390/en14030733.

[35] M. Dällenbach, 'Selbstentlüftungsgeschwindigkeit von Wasser und Wasser-Glykol-Gemisch in glatten und gewellten Rohren', Master Thesis, Eidg. Technische Hochschule ETH, Zürich, 2015.

[36] R. Eismann, *Thermohydraulische Dimensionierung von Solaranlagen : Theorie und Praxis der kostenoptimierenden Anlagenplanung*. Wiesbaden: Springer Vieweg, 2017.

[37] T. Hibiki, H. Goda, S. Kim, M. Ishii, and J. Uhle, 'Structure of vertical downward bubbly flow', *International Journal of Heat and Mass Transfer*, vol. 47, no. 8–9, pp. 1847–1862, 2004, doi: http://dx.doi.org/10.1016/j.ijheatmasstransfer.2003.10.027.

[38] K. Jones, J. Rothe, and W. Dunsford, *Symbolic Nuclear Analysis Package (SNAP): Common application framework for engineering analysis (cafean) preprocessor plug-in application programming interface*. US Nuclear Regulatory Commission, Office of Nuclear Regulatory Research, 2009.

[39] J. D'Ans, E. Lax, and R. Blachnik, *Taschenbuch für Chemiker und Physiker: Band 3: Elemente, anorganische Verbindungen und Materialien, Minerale: Bd. III*, vol. Bd. III. Springer, Berlin, Heidelberg, 1998.

[40] J. Alvarez, R. Crovetto, and R. Fernández-Prini, 'The Dissolution of N2 and of H2 in Water from Room Temperature to 640 K', *Berichte der Bunsengesellschaft für physikalische Chemie*, vol. 92, no. 8, pp. 935–940, 1988, doi: 10.1002/bbpc.198800223.

[41] S. Mathez, 'Absorber-Master: Optimierung der Absorber-Geometrie', *Wetzikon*, 2011, [Online]. Available: http://www.solarcampus.ch/index.php?id=de1032

[42] C. Gwerder *et al.*, 'Horizontal Inlets of Water Storage Tanks With Low Disturbance of Stratification', *J. Sol. Energy Eng*, vol. 138, no. 5, pp. 051011–051019, Aug. 2016, doi: 10.1115/1.4034228.

[43] M. Battaglia, L. Züllig, and M. Haller, 'BigStrat - Schichtung grosser Wärmespeicher', BFE Schlussbericht SI/500315-03, Aug. 2018.

[44] 'Dhwcalc: Program to Generate Domestic Hot Water Profiles with Statistical Means for User Defined Conditions', *ResearchGate*, Accessed: Jan. 25, 2017. [Online]. Available: https://www.researchgate.net/publication/237651871_DHWcalc_PROGRAM_TO_GENERATE_DOMESTIC_HOT_WATER_PROFILES_WITH_STATISTICAL_MEANS_FOR_USER_DEFINED_CONDITIONS

Acknowledgements

Annex A: Interview guideline

One of the expected results of the SimplyDrain project, financed by the Swiss Federal Office of Energy (SFOE), is a number of indicators to assess the possibilities of integrating drainback solar thermal systems (DBS) when refurbishing existing domestic hot water (DHW) systems in multi-family houses (MFH). In order to meet this objective, several interviews were conducted with experienced representatives from companies in the DHW and building sector to gather information of the actual market situation for typical DHW systems in MFH and the required technical aspects for integration of a DBS.

This document was a guideline for the interviews to be conducted. To better structure the interview, the questions are arranged by topics:

1. **Contact information:** interviewee basic information
2. **Building characteristics:** overview information on the current MFH market
3. **Technical room:** suitability of existing technical rooms for retrofitting of the DHW systems
4. **DHW system:** overview of existing DHW systems in MFH and technical information to assess the possibilities of integrating DBS
5. **DHW storage:** overview of the existing DHW storages in MFH and technical information to assess the possibilities of integrating DBS
6. **Miscellaneous:** other relevant information

The main outputs of the interview relate to issues such as storage tank sizes, preferable ways on how to combine new and old system components, and space typically available for additional components (e.g. additional storage tank, DB-vessel, plate HX).
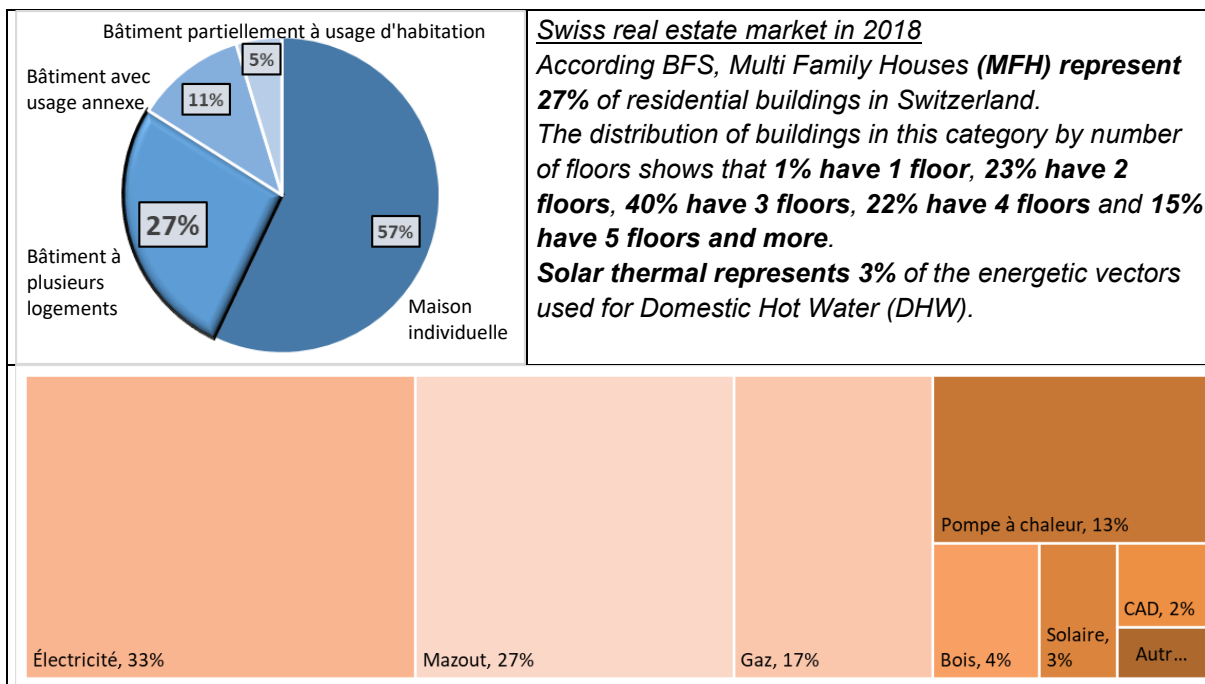
Interview guideline
Legend:
- Underlined numbering bullets – main questions

- Non-underlined numbering bullets – complementary questions
- Lettering bullets: information required within a question
- Arrows – predefined answer options

Date:

Contact information

Person		Domain of activity	
Company		Position	
Interest in receiving information and results from the current project?			
Comments			

Building characteristics

1- How many buildings the company manages/have information on?
2- Construction period?
3- What are the typical sizes of these buildings?
    a. Number of floors, including basement (if the technical room is there)?
    b. Height, from ground floor to the roof?
    c. Number of apartments? Or inhabitants?
4- Concerning the roof of these buildings, is there a standard? *Use google maps for external view if full address available!*
    a. Shape: Flat; Gable ; Shed(specify slope in degrees)
    b. *Orientation: South ; South-East ; South-West ; East ; West*
    c. Available surface? *Order of idea: absolute value or percentage*

Technical Room

1. Where is the technical room normally located? *where the DHW system is installed*
➜ Basement; Ground floor; Under the roof; Other (specify)
    ➜ DHW system next to the technical room ; On the same floor than the technical room ; Other
2. What is the general size of the technical room?
3. Floor area?
4. Height?
5. Entrance door size?
6. Direct access from outside?[13]
7. Is there typically any available space to install other equipment? *(approx. 1.5 a 2 m² max required for our concept A)*
8. Typical available space
    9. absolute value; floor percentage; enough for a small 300l storage?
10. Is it possible to fill this space with an additional renewable DHW system?

---

[13] This is an obligation depending on the capacity of the installed boiler DPI-24-15 page 6

➜ Is there other available additional room that could be used as technical room? If yes, where is it located?

11. Is there an opportunity for solar pipe routing in the building? *from the roof to the technical room*
➜ Existing duct passage? Riser zone within the building? Disused chimneystack? Outside of the building along the façade?

DHW system

1- What is the typical type of DHW system installed?
   ➜ Boiler with built-in DHW storage ; Separated DHW storage ; Tank in tank (DHW tank immersed in SH tank) ; Other (specify)
2- What is the typical final energy used for DHW system?
   ➜ Electricity ; Heat pump ; Gas ; Fuel ; Wood ; Other (specify)
   ➜ Is refurbishing work normally planned?
      o If yes, what is the share of the building stock concerned?
3- What are the main requirements/considerations for refurbishing the DHW system?
   ➜ Sizing rules? Systematically resizing of system or taken as it was? e.*g. recommendations by SIA384/1.*
   ➜ Is solar thermal considered?
4- During the design phase, is it considered to install a DHW system offering the possibility for later integration of a renewable energy system?
   ➜ DHW storage with double heating coil
5- When refurbishing takes place, is the DHW storage replaced?
6- Are fresh water stations common?
7- Is DHW re-circulation common?
   ➜ If not: will it be common? is it upcoming?
   ➜ How is the legionella problem taken into account?

DHW storage

1- What is the typical number of installed storage(s)?
   ➜ 1; 2; 3; 4; more (specify)
2- What is the typical size of the installed storage(s)?
   1. Volume?
   2. Height / diameter?
3- What is the hydraulic connections of the DHW storage?
   a. Locations / heights
   b. Dimensions (diameter)
4- Do the DHW storage offer the possibility to connect solar thermal system? *(extra not used connections)*
   3. Locations / heights
   4. Dimensions (diameter)
5- What is the type of DHW storage insulation?
   ➜ Demountable (mat or preformed pieces); Hardened foam around
6- Could the sensor position be changed with existing mounting positions?
7- Is electric heating rod common*? e.g. might be used as solar double port instead*
8- Do you have a preferable way to combine new and old system components for the DHW storage(s)? *e.g. 2 small storage or 1 larger storage*

Miscellaneous

1. What are the typical problems when retrofitting a DHW system?

2. What are the relevant legal boundary conditions when refurbishing DHW system?
3. What is your experience in integrating new DHW system, such as solar when refurbishing?
4. Are welding of new solar connections realistic?
5. If yes, where?
6. Size of the tubes?
7. If no extra ports available for solar and no welding possibility: is it realistic to use the heat exchanger of the fossil part? *(added t-pieces and unidirectional valves etc.)*

Annex B: Thermohydraulic model: specification of details

0	Kreislauf	Kreislauf+MAG	Blattfunktionen aktivieren	R. Eismann			© ETH Zürich		
		Die Summe aller Höhendifferenzen muss null sein:			0.00	Dicke			spezif.
			Wendel-	Parallele	Anzahl	Höhen -	Isolation	Fläche	Druck	Durchfluss
Kreislaufelemente	Rohrdim.	Länge m	Durchm. m	Rohre -	Winkel	diff. m	mm	m²	bar_ü	l/hm²
1 Druckhaltung		Höhe Referenzpunkt bezüglich MAG Anschluss :				1	am Referenzpunkt:		1.00	46
2 Rohr PE	16x4	0.5			1	0	19			
3 Rohr PE	16x4	1			1	-1	19			
4 Rohr PE	16x4	0.5			1	0	19			
5 Rohr PE	16x4	0.5			1	0.5	19			
6 Pumpe					Regelparameter zwischen 0 und 1:			1.00	Speck Y-2340-SR	
7 Rohr PE	16x4	1.2			1	1.2	19			
8 Rohr PE	16x4	4.02			1	0.4	19			
9 Rohr PE	16x4	4.29			1	4.29	19			
10 Rohr PE	16x4	0.747			1	0.48	19			
11 Rohr PE	16x4	0.2			1	0.2	19			
12 Rohr PE	16x4	0.43			1	0.05	19			
13 Rohr PE	16x4	5.215			1	0.4	19			
14 Rohr PE	16x4	1.04			1	0.25				
15 Rohr PE	16x4	2.05			1	2.02	19			
16 Rohr PE	16x4	3.79			1	0.05	19			
17 Rohr PE	16x4	1.63			1	0.2	19			
18 Kollektorfeld						1.63				
19 Rohr PE	16x4	2.3			1	-1.6	19			
20 Rohr PE	16x4	1.63			1	-0.2	19			
21 Rohr PE	16x4	3.79			1	-0.05				
22 Rohr PE	16x4	2.05			1	-2.05	19			
23 Rohr PE	16x4	1.04			1	-0.25	19			
24 Rohr PE	16x4	5.215			1	-0.4	19			
25 Rohr PE	16x4	0.43			1	-0.05	19			
26 Rohr PE	16x4	0.2			1	-0.2	19			
27 Rohr PE	16x4	0.747			1	-0.48	19			
28 Rohr PE	16x4	4.29			1	-4.29	19			
29 Rohr PE	16x4	4.02			1	-0.4	19			
30 Rohr PE	16x4	1.2			1	-1.2	19			
31 Rohr PE	16x4	0.5			1	0	19			
32 Rohr PE	16x4	0.5			1	0.5	19			
33 Rohr PE	16x4	0.5			200	0	19			

Figure 64: Circuit parameters of the solar drainback loop.
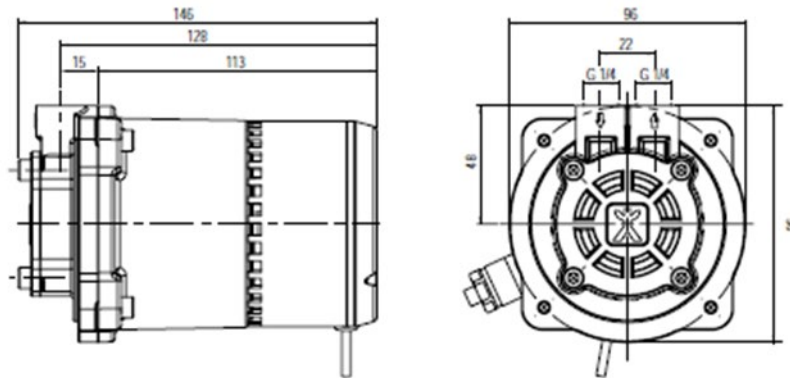
Daten / Data

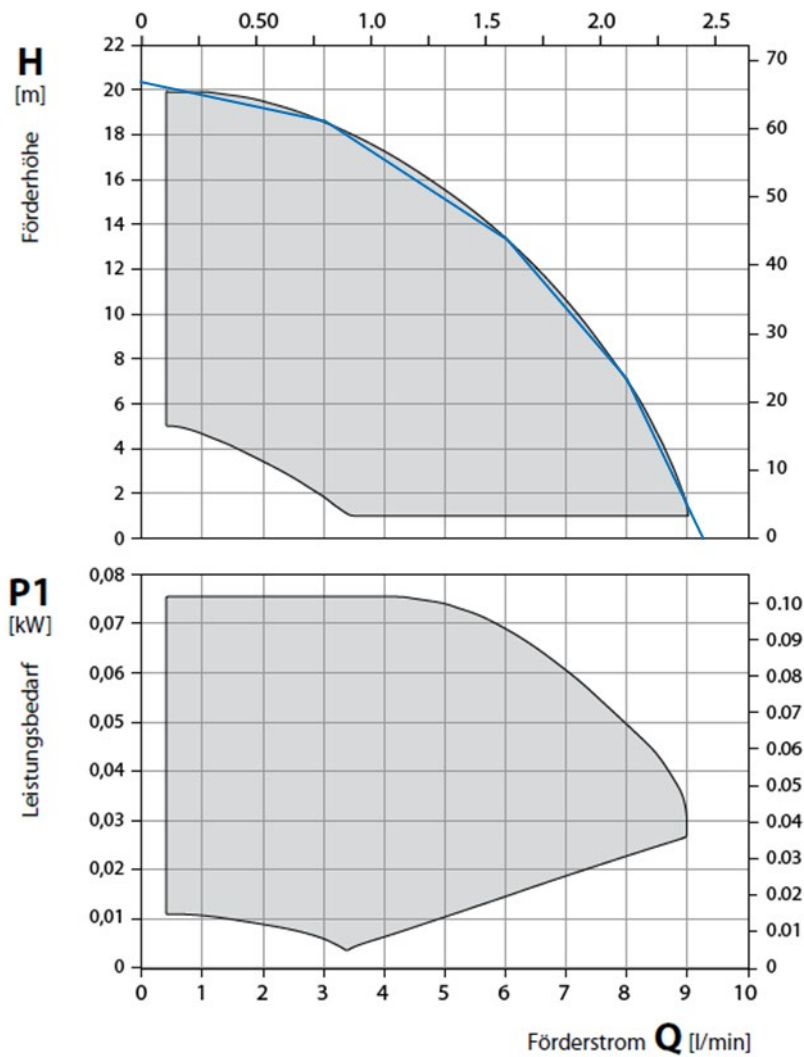| Type	EC-Motor Brushless motor				Anschlüsse Connections		Gewicht Weight		Wasser Water	Wasser-/Glykol-Gemisch Water/glycol mixture
	V	1/min	kW	HP	G_s	G_D	kg	lbs	t_{max}	t_{max}
Y-2340-SR	230	1500 - 3800	0,075	0.10	G 1/4	G 1/4	2,4	5.3	95 °C	95 °C

Figure 65: Specification of the solar pump.

Figure 66: Characteristics of the solar pump.

Two-Phase Solar Thermal Circuit	Simulation		Collector array characteristics		
Boundary and initial conditions			**Collector array characteristics**		
Constant or time series?	-	Constant	Conversion factor	-	0.8
Solar irradiation	W/m^2	1000	Heat loss coefficient	W/Km^2	3.4
Ambient temperature	°C	20	Heat loss coefficient	W/K^{2}m^2	0.01
Initial temperature	°C	20	Heat capacity per collector	J/K	4000
Initial gas pressure above atmospheric	bar	0	Collector area	m^2	2.2
Initial liquid holdup in collector	-	1	Number of collectors	-	4
Initial liquid holdup in drainback tank	-	0.95	Total collector area	m^2	8.8
Circuit characteristics					
Heat carrier liquid	-	Water			
Drainback tank volume	l	800			
Drainback tank height	m	2	Diameter	m	0.71
Circuit volume below liquid level at rest	l	5			
Supply line length	m	15			
Supply line diameter	m	0.012	Supply line volume	l	1.70
Return line length	m	15			
Return line diameter	m	0.012	Return line volume	l	1.70
Collector array volume	l	8	Total initial gas volume	l	46
height differrence liquid level - collector exit	m	10	Total initial liquid volume	l	765
Zeta value at the end of supply line	-				
Operational conditions					
Pre-set flow rate	l/hm^2	40			
Pump type					
pre-set operational pressure at collector exit	bar	0.1	relative to atmospheric pressure		
Operational pressure at collector exit		Pre-set			
Model options					
Drainback tank state	-	Mixed	Desorption of gas allowed?	-	no
Simulation time	h	8	Absorption of gas allowed?	-	no
Time step size	s	10			

Figure 67: Model parameters of the two-phase solar circuit.

Annex C: Details of lab tests and DHW calculations

C.1 Component heights of the lab storage for stratifications tests

Table 21: Heights of temperature sensors and solar loop connections of the DB storage used in the lab test.

Sensor / Connection	Height from bottom (cm)	Rel. height
T9	155	99%
T8	139	89%
T7	120	77%
T6	100	64%
T5	79	51%
T4	52	33%
T3	43	28%
Inlet	87.5	56%
Inlet with stratification device	49 to 100	
Outlet for conditioning	104	67%
Outlet during test	2	1%

C.2 Domestic hot water: maximum flow rates of tapping

The maximum flow within the cold water pipe due to tapping of hot water by inhabitants is estimated as follows:

- According to norm EN 806-3 (simplified procedure for calculation of inner pipe diameters), six apartments correspond to 48 loading unites (LU) (EN 806-3, page 8)
- In SimplyDrain, we size the DHW system for nine apartments. Linear scaling of the norm data which might be allowed as the scaling factor is near 1, gives 46/6*9 = 72 LU
- 72 LU correspond to a flow rate of 0.9 L/s (see Figure 68)
- To estimate the cold water flow into the DHW storage, we assume that for tapping, fresh water of 10 °C and hot water from the DHW storage of 60 °C is mixed to a tapping temperature of 35 °C. This halves the 0.9 L/s of warm water tapping to 0.45 L/s fresh water that enters the DHW storage.
- Thus, the maximum flow rate of fresh water that passes the plate hx (hx used for transferring solar heat to the fresh water before entering the DHW storage) is 0.45 L/s or 27 L/min or 1'600 L/h.
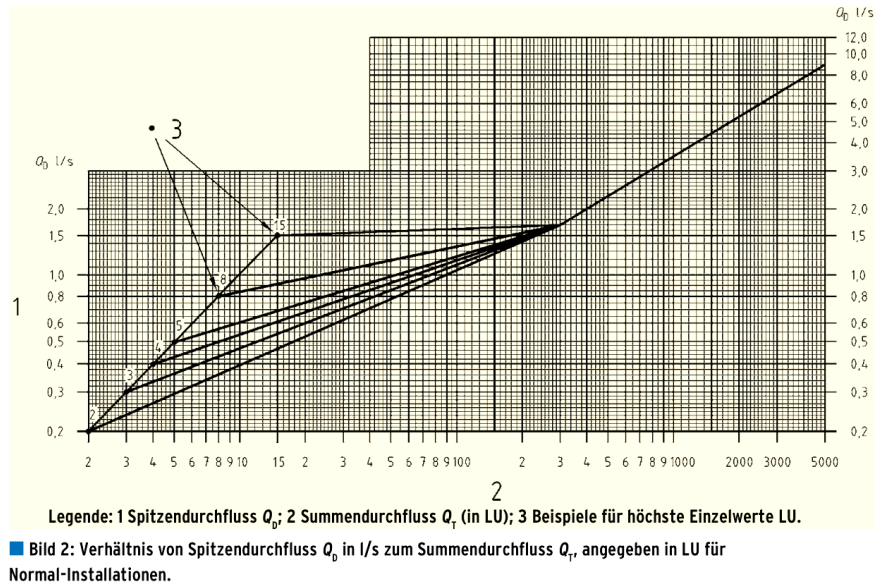
Legende: 1 Spitzendurchfluss Q_D; 2 Summendurchfluss Q_T (in LU); 3 Beispiele für höchste Einzelwerte LU.

■ **Bild 2:** Verhältnis von Spitzendurchfluss Q_D in l/s zum Summendurchfluss Q_T, angegeben in LU für Normal-Installationen.

Figure 68: Ration of maximum flow (Q_d in L/s) and cumulated flow (Q_T in LU) for DHW installations (source: EN 806-3 cited in IKZ-Haustechnik, Heft 22/2006).
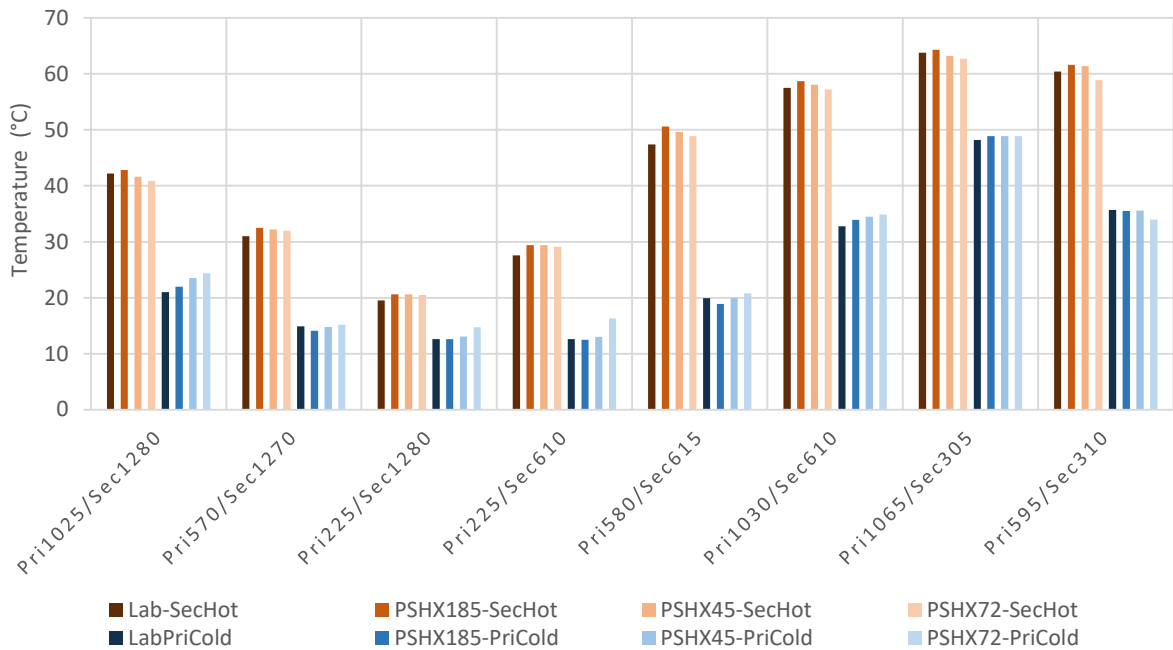
C.3 Validation of plate heat exchanger

Figure 69: Water outlet temperatures of the primary and secondary circuit of the plate hx for the measurements in the lab and for three plate hx in Polysun (Polysun catalogue no. 185, 45, and 72) and different sets of mass flows in the primary and secondary circuit in kg/h.
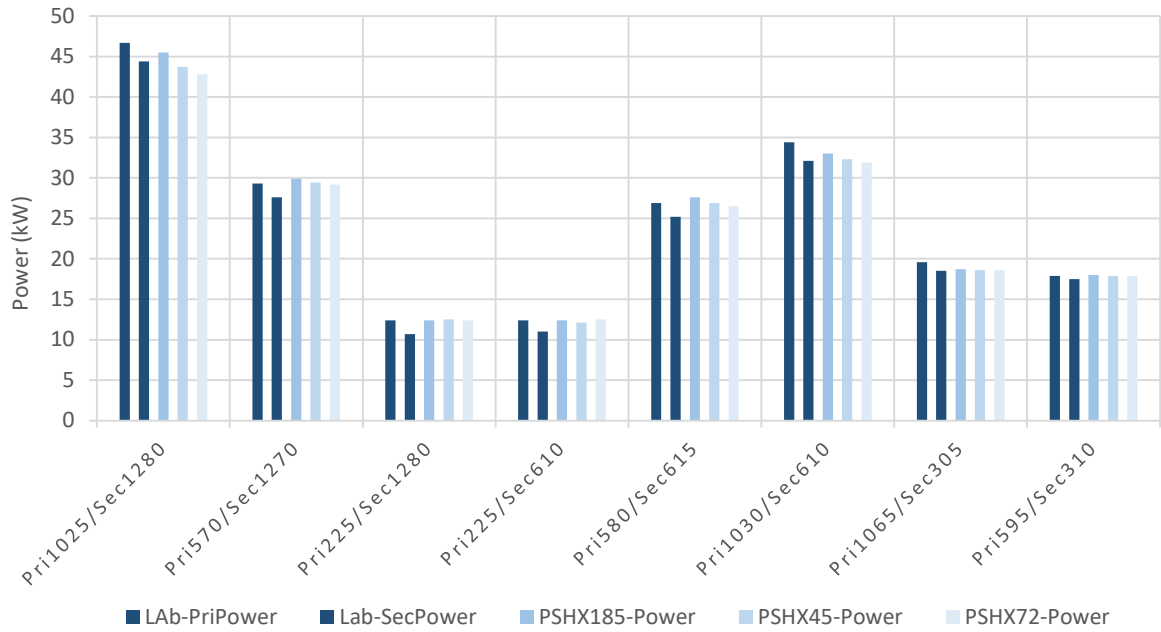
Figure 70: Exchange power of the primary and secondary circuit of the plate hx for the measurements in the lab (measured per circuit) and for three plate hx in Polysun (Polysun catalogue no. 185, 45, and 72) and different sets of mass flows in the primary and secondary circuit in kg/h.

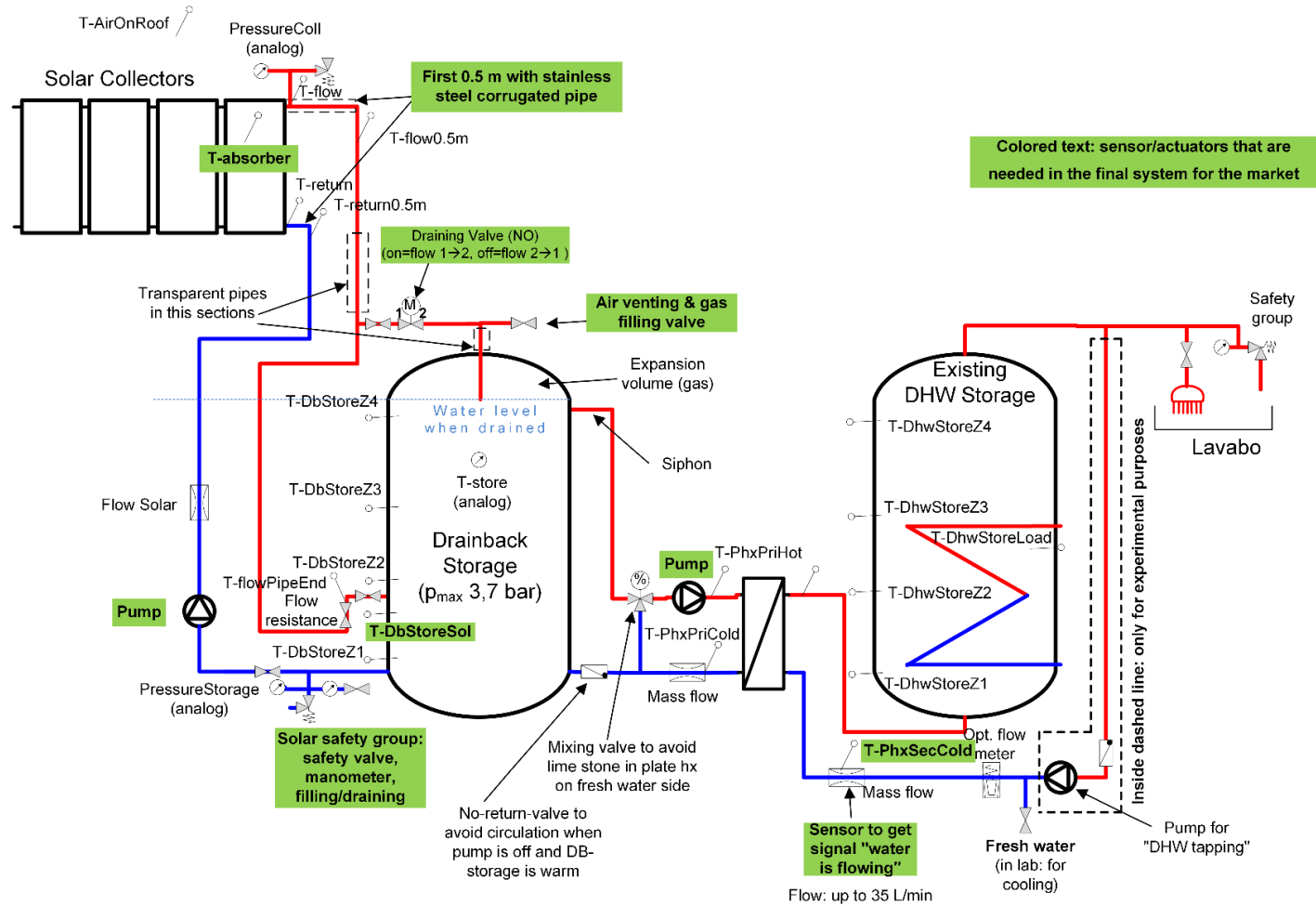# Annex D: Lab system

D.1   Hydraulic scheme

Figure 71: Detailed hydraulic scheme of the DBS installed in the lab.
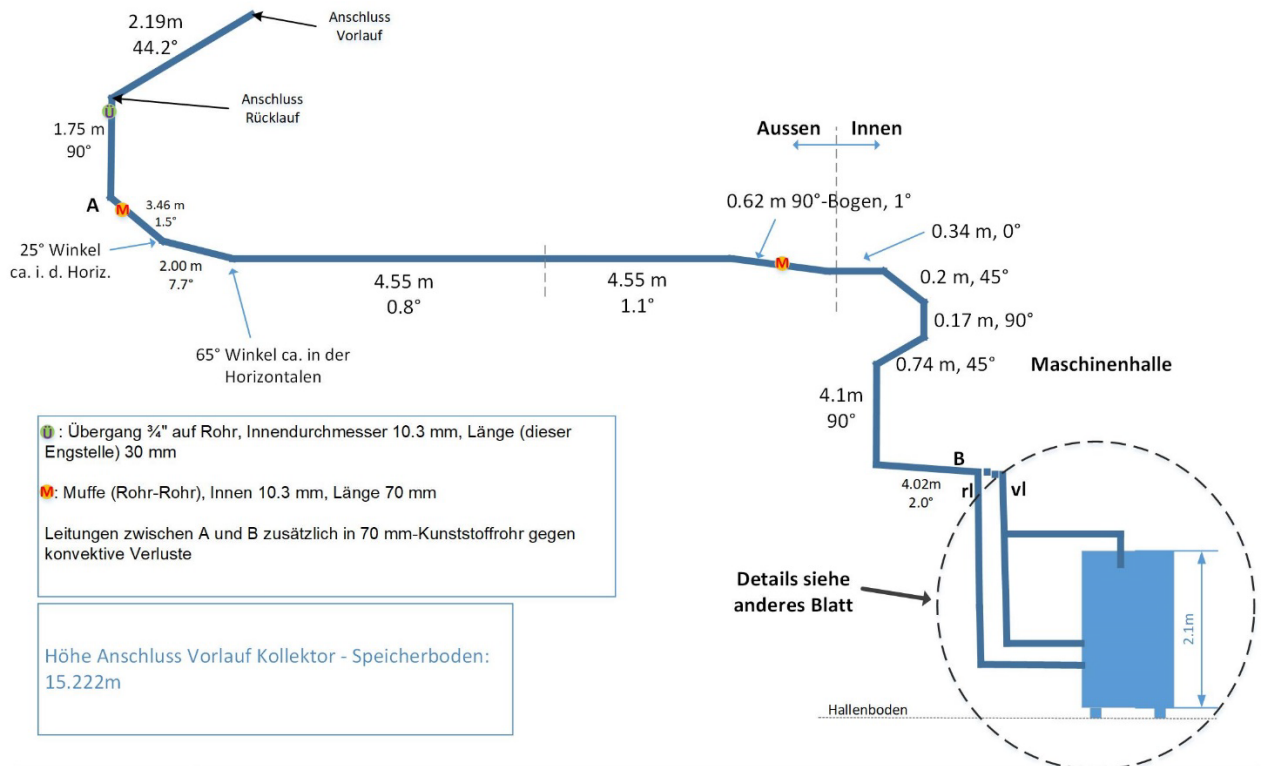
D.2 Lab system: Geometry of piping

Figure 72: Pathway of the flow and return pipe of the solar loop between storage and collector field.

Ü : Übergang ¾" auf Rohr, Innendurchmesser 10.3 mm, Länge (dieser Engstelle) 30 mm

M: Muffe (Rohr-Rohr) bzw. T-Stück, Innen 10.3 mm, Länge 70 mm

Leitungen zwischen A und B zusätzlich in 70 mm-Kunststoffrohr gegen konvektive Verluste

Rücklauf:

Vorlauf:

Horizontale Rohre sind in Orange gezeichnet

Bögen 90° wenn nicht anders beschriftet

Nicht alle Details sind eingezeichnet (Hähne, T-Stücke mit grossem Querschnitt etc.)

B

0.92 m

M

1.03 m

0.2 m

0.44 m

0.2 m

0.23 m

0.13 m

0.25 m

0.25 m

0.2 m

0.45 m

M

0.2 m

2.1m

Hallenboden

B

0.25 m

Glas: 1.00 m

0.18m

0.13 m

M

1.60 m

0.25 m

0.33 m
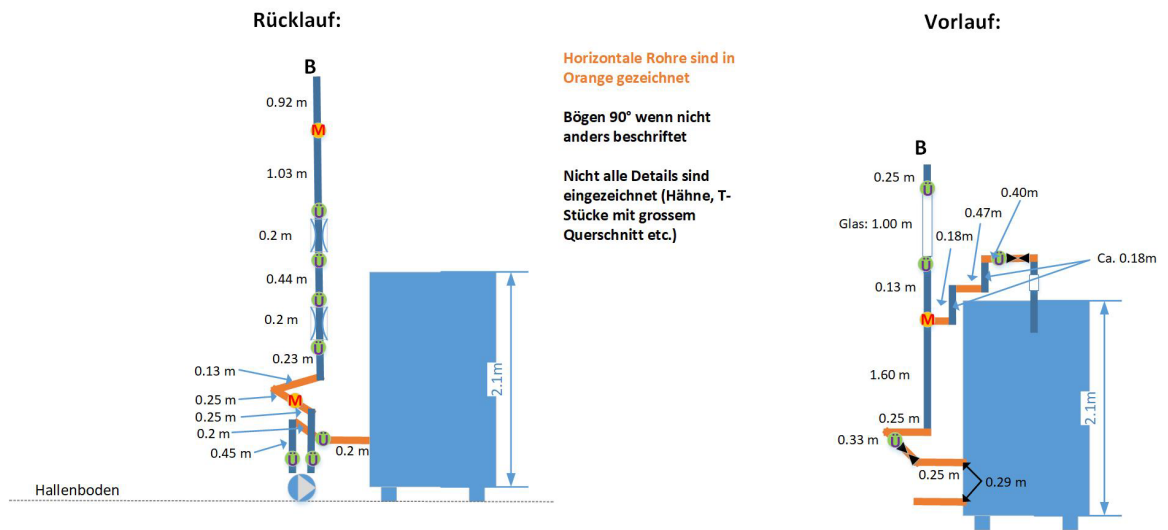
0.40m

0.47m

Ca. 0.18m

2.1m

0.25 m

0.29 m

Figure 73: Geometrical details of the solar loop return pipe (left) and flow pipe (right) at the solar DB storage.